

## **Distribution Agreement**

In presenting this thesis or dissertation as a partial fulfillment of the requirements for an advanced degree from Emory University, I hereby grant to Emory University and its agents the non-exclusive license to archive, make accessible, and display my thesis or dissertation in whole or in part in all forms of media, now or hereafter known, including display on the world wide web. I understand that I may select some access restrictions as part of the online submission of this thesis or dissertation. I retain all ownership rights to the copyright of the thesis or dissertation. I also retain the right to use in future works (such as articles or books) all or part of this thesis or dissertation.

Signature:

---

Gabrielle K. Delima

---

Date

Coinfection Dynamics and Host Restriction in Influenza A Virus Infection

By

Gabrielle K. Delima  
Doctor of Philosophy

Graduate Division of Biological and Biomedical Sciences  
Microbiology and Molecular Genetics

---

Anice C. Lowen, Ph.D  
Advisor

---

John Steel, Ph.D  
Advisor

---

Graeme Conn, Ph.D  
Committee Chair

---

Bernardo Mainou, Ph.D  
Committee Member

---

Gregory Melikian, Ph.D  
Committee Member

Accepted:

---

Kimberly Jacob Arriola, Ph.D., MPH  
Dean of the James T. Laney School of Graduate Studies

---

Date

Coinfection Dynamics and Host Restriction in Influenza A Virus Infection

By

Gabrielle K. Delima  
B.S., Delaware State University, 2015

Advisor: Anice C. Lowen, Ph.D.  
Advisor: John Steel, Ph.D.

An abstract of  
A dissertation submitted to the Faculty of the  
James T. Laney School of Graduate Studies of Emory University  
in partial fulfillment of the requirements for the degree of  
Doctor of Philosophy  
in the Graduate Division of Biological and Biomedical Sciences  
Microbiology and Molecular Genetics  
2023

## Abstract

### Coinfection Dynamics and Host Restriction in Influenza A Virus Infection

By Gabrielle K. Delima

Genetic exchange between coinfecting influenza A viruses can drive viral evolution and is particularly important in facilitating adaptation to new host species. Thus, we investigated how coinfection and host restriction impact IAV replication in novel hosts. We have previously demonstrated that IAVs benefit from virus-virus interactions during homologous coinfection, indicating an intrinsic reliance on coinfection. However, whether IAV virus-virus interactions during coinfection with a heterologous strain are similarly beneficial had not been explored. To address this, we assessed the outcomes of heterologous virus-virus interactions by evaluating the extent to which a coinfecting IAV could augment the replication of a focal IAV. We found that virus-virus interactions within cells were largely beneficial, with IAVs having the lowest intrinsic reliance on coinfection most effectively augmenting replication of a focal IAV. However, competitive virus-virus interactions were dominant during multi-cycle infection. These findings suggest that coinfecting IAVs are significantly impacted by virus-virus interactions, with differing dominant virus-virus interactions between the within-cell and within-host scales. We have previously shown that the M segments of avian IAVs support aberrantly high M2 expression in mammalian cells. The M segment of the 2009 pandemic strain, although descended from that of an avian IAV, does not show this phenotype. However, the mechanism that re-establishes optimal M gene expression, was not well understood. Thus, we undertook to elucidate the mechanism underlying differential M segment gene regulation during avian and human IAV infection of a mammalian host. We found that avian IAV circulation in swine was associated with decreased M2 expression in mammalian cells. However, introducing M segment mutations that arose during IAV swine circulation into an avian precursor did not change M2 protein expression. Introducing regions of the 2009 H1N1 pandemic IAV did decrease avian M2 protein, but not mRNA, expression. These findings suggest that re-establishing regulation of M gene expression is necessary to overcome host restriction. Together, these studies further our understanding of the impacts of coinfection dynamics and host restriction on IAV replication in novel hosts.

Coinfection Dynamics and Host Restriction in Influenza A Virus Infection

By

Gabrielle K. Delima  
B.S., Delaware State University, 2015

Advisor: Anice C. Lowen, Ph.D.  
Advisor: John Steel, Ph.D.

A dissertation submitted to the Faculty of the  
James T. Laney School of Graduate Studies of Emory University  
in partial fulfillment of the requirements for the degree of  
Doctor of Philosophy  
in the Graduate Division of Biological and Biomedical Sciences  
Microbiology and Molecular Genetics  
2023

## Acknowledgements

“ It takes a village to raise a child” is an old saying that I could not truly appreciate until now. I cannot understate the amount of support and guidance that made this achievement possible, because without the following people, I could not have come this far:

**Anice Lowen:** Thank you for mentoring me not only in techniques and hypotheses, but also in what it means to be a strong woman in science. Thank you for helping me grow both as a scientist and person.

**John Steel:** Thank you for starting me on this journey and fostering my passion for science.

**My committee:** Thank you Grame, Bernardo, and Greg for always having great advice, both scientific and professional, and supporting my growth as a scientist.

**Lowen lab:** Shamika, Kayle, Jessica, Kate, Meher, Vedhika, Nahara, Ketaki, Camden, Lucas, Dave, Young, Christina, Lisa, Courtney, Meg, Kara, Nate, Maria, and Hui. Thank you all, both current and past, for the advice, support, friendship, and laughs. I see you all as my brothers and sisters in science and I can't wait to see what you all achieve in the future.

**Dwight Lacy:** Thank you for supporting my decision to come to Emory and every step after. Thank you for loving and believing in me when times got hard, or when I got on your last nerves. You bring out the best in me, and I'm looking forward to spending the rest of our lives together.

**Marie Mombrun:** Mom, there are not enough words to properly thank you for everything that you have done. Thank you for pushing me to be my best self, for showing me what it means to work hard, and to never give up. Thank you for always being in my corner and being my greatest role model.

## Table of Contents

<b>Chapter 1: Introduction</b> .....	<b>1</b>
<b>Introduction</b> .....	<b>1</b>
<b>Influenza viruses</b> .....	<b>1</b>
<i>Fig 1. influenza A virus structure</i> .....	<i>2</i>
<b>IAV life cycle</b> .....	<b>2</b>
<i>Fig . 2 influenza A virus life cycle</i> .....	<i>4</i>
<b>IAV evolution</b> .....	<b>5</b>
<b>IAV hosts</b> .....	<b>6</b>
<b>Overcoming species barriers</b> .....	<b>6</b>
<b>Pandemic IAVs</b> .....	<b>7</b>
<b>Virus-virus interactions</b> .....	<b>8</b>
<b>Dissertation aims</b> .....	<b>9</b>
<b>References</b> .....	<b>11</b>
 <b>Chapter 2: Influenza A virus coinfection dynamics are shaped by distinct virus-virus interactions within and between cells</b> .....	<b>2</b>
<b>Abstract</b> .....	<b>24</b>
<b>Introduction</b> .....	<b>25</b>
<b>Results</b> .....	<b>27</b>
<i>Fig 1. Intrinsic reliance on multiple infection in mammalian cells is strain dependent</i> ...30	
<i>Fig 2. Coinfection with a virus with low reliance on multiple infection results in a greater increase in GFHK99 virus replication</i> .....	<i>31</i>

<i>Fig 3. The extent to which a coinfecting virus augments replication of GFHK99 is defined by its intrinsic reliance on multiple infection.....</i>	<i>32</i>
<i>Fig 4. At the level of the whole host, GFHK99 replication is diminished by coinfection.....</i>	<i>34</i>
<i>Fig 5: GFHK99 genome incorporation into progeny virions is enhanced during homologous and heterologous coinfection.....</i>	<i>36</i>
<i>Fig 6. Competitive virus-virus interactions dominate during viral propagation between cells.....</i>	<i>38</i>
<b>Discussion.....</b>	<b>39</b>
<i>Fig 7. Dominant virus-virus interactions differ at the within-cell and within-host scales.....</i>	<i>40</i>
<b>Methods.....</b>	<b>44</b>
<b>Supplemental Information.....</b>	<b>51</b>
<i>S1 Fig. Coinfection with NL09 strongly enhances GFHK99wt replication in NHBE cells.....</i>	<i>51</i>
<i>S2 Fig. At the level of the whole host, GFHK99 replication is suppressed by coinfection.....</i>	<i>53</i>
<i>S3 Fig. At the level of the whole host, GFHK99 replication is suppressed by prior IAV infection.....</i>	<i>53</i>
<i>S1 Table. Genotypes of modified viruses.....</i>	<i>54</i>
<i>S4 Fig. Quantification of defective viral genomes in virus stocks.....</i>	<i>55</i>
<i>S2 Table. Primers for the quantification of vRNA by ddPCR.....</i>	<i>56</i>
<b>References.....</b>	<b>57</b>

<b>Chapter 3: Regulation of gene expression from the influenza A virus M segment is a feature of host adaptation.....</b>	<b>64</b>
<b>Abstract.....</b>	<b>64</b>
<b>Introduction.....</b>	<b>65</b>
<b>Results.....</b>	<b>68</b>
<i>Table 1. Origin of M segments used in study.....</i>	<i>68</i>
<i>Fig. 1 High M2 protein expression of viruses carrying avian IAV M segments is seen in mammalian but not avian cells.....</i>	<i>69</i>
<i>Fig. 2 High M2 protein expression of viruses incorporating avian, but not human, M segments in mammalian cells.....</i>	<i>70</i>
<i>Fig. 3 Increased duration of avian IAV circulation in swine is associated with decreased M2 protein expression.....</i>	<i>72</i>
<i>Fig. 4 Mutations identified in M segment of swine isolates increase viral replication, but not M2 protein expression.....</i>	<i>73</i>
<i>Fig. 5 Chimeric M segments yield decreased M2 protein, but not M2 mRNA expression.....</i>	<i>75</i>
<b>Discussion.....</b>	<b>76</b>
<b>Methods.....</b>	<b>79</b>
<b>Supplemental Information.....</b>	<b>84</b>
<i>Table 2. Primers used for chimeric M segment Assembly.....</i>	<i>84</i>
<i>Table 3. Primers used for the quantification of viral mRNA by ddPCR.....</i>	<i>85</i>
<b>References.....</b>	<b>86</b>
<b>Chapter 4: Discussion.....</b>	<b>92</b>

<b>IAV virus-virus interactions.....</b>	<b>92</b>
<b>M segment gene regulation.....</b>	<b>94</b>
<b>Conclusion.....</b>	<b>95</b>
<b>References.....</b>	<b>97</b>

## 1 **Chapter 1: Introduction**

### 2 **Introduction**

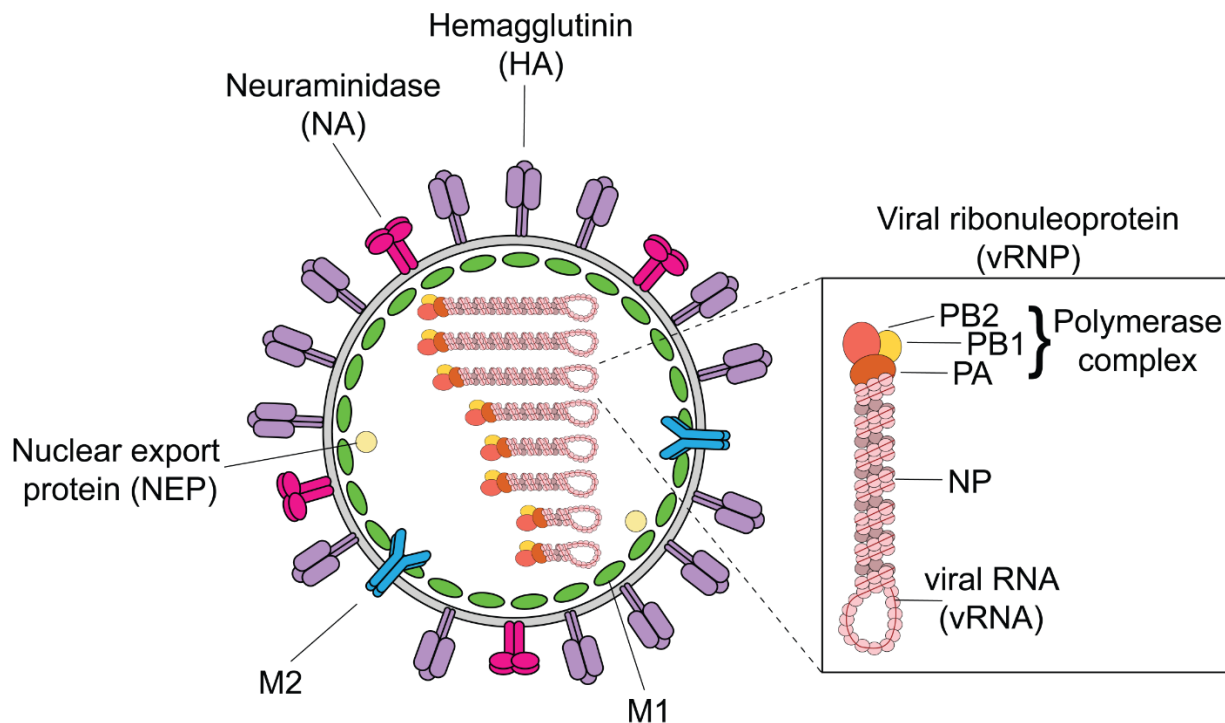
3 Influenza is a respiratory disease caused by influenza A and B viruses. In humans, influenza is  
4 seasonal as cases tend to increase in the winter months in temperate regions or rainy seasons in  
5 tropical climates (1). Each year, influenza results in an estimated 9-41 million cases, 140-  
6 710,000 hospitalizations, and 12-52,000 deaths and over \$87 billion in total economic burden the  
7 United States (2, 3). Vaccines are available to protect against seasonal influenza, however  
8 influenza strains included in the vaccine must be updated each year due to the virus' ability to  
9 evade pre-existing immunity (1, 4). Moreover, vaccines against seasonal influenza do not protect  
10 against infections caused by novel zoonotic influenza viruses. While influenza zoonoses are  
11 infrequent, novel variants that can infect, then transmit from human to human, can cause  
12 influenza pandemics which have even greater morbidity and mortality in humans than seasonal  
13 influenza (5-7) For this reason, the mechanisms behind influenza virus evolution and host  
14 adaptation continue to be an important area of research.

15

### 16 **Influenza viruses**

17 Influenza viruses belong to the family *Orthomyxoviridae* and include four types; A, B, C and D.  
18 Of these subtypes, influenza A viruses (IAVs) have the largest impact on humans but infect a  
19 wide range of avian and mammalian hosts. The IAV genome is made up of eight negative sense,  
20 single stranded RNA gene segments that encode at least 11 proteins. In the virion, each gene  
21 segment is packaged as viral ribonucleoproteins (vRNPs) bound by nucleoproteins (NP) and a  
22 polymerase complex, which comprises the polymerase basic 1 (PB1), polymerase basic 2 (PB2),  
23 and polymerase acid (PA) proteins (8-10). The vRNPs, that make up the viral core, and nuclear

24 export protein (NEP) are encased by a layer of matrix 1 (M1) proteins, which in turn is  
 25 enveloped by a lipid bilayer derived from the host cell plasma membrane. The virion envelope is  
 26 decorated with viral transmembrane proteins hemagglutinin (HA), neuraminidase (NA), matrix 2  
 27 (M2). There are 17 HA (H1-H17) and 9 NA (N1-N9) known subtypes which are used in  
 28 combination to classify IAV strains (e.g. H1N1, H3N2) (11).



29  
 30 **Fig. 1 influenza A virus structure.** This schematic illustrates the general composition and  
 31 structure of an influenza virion (8-11). (Graphic: G. Delima)

### 32 IAV life cycle

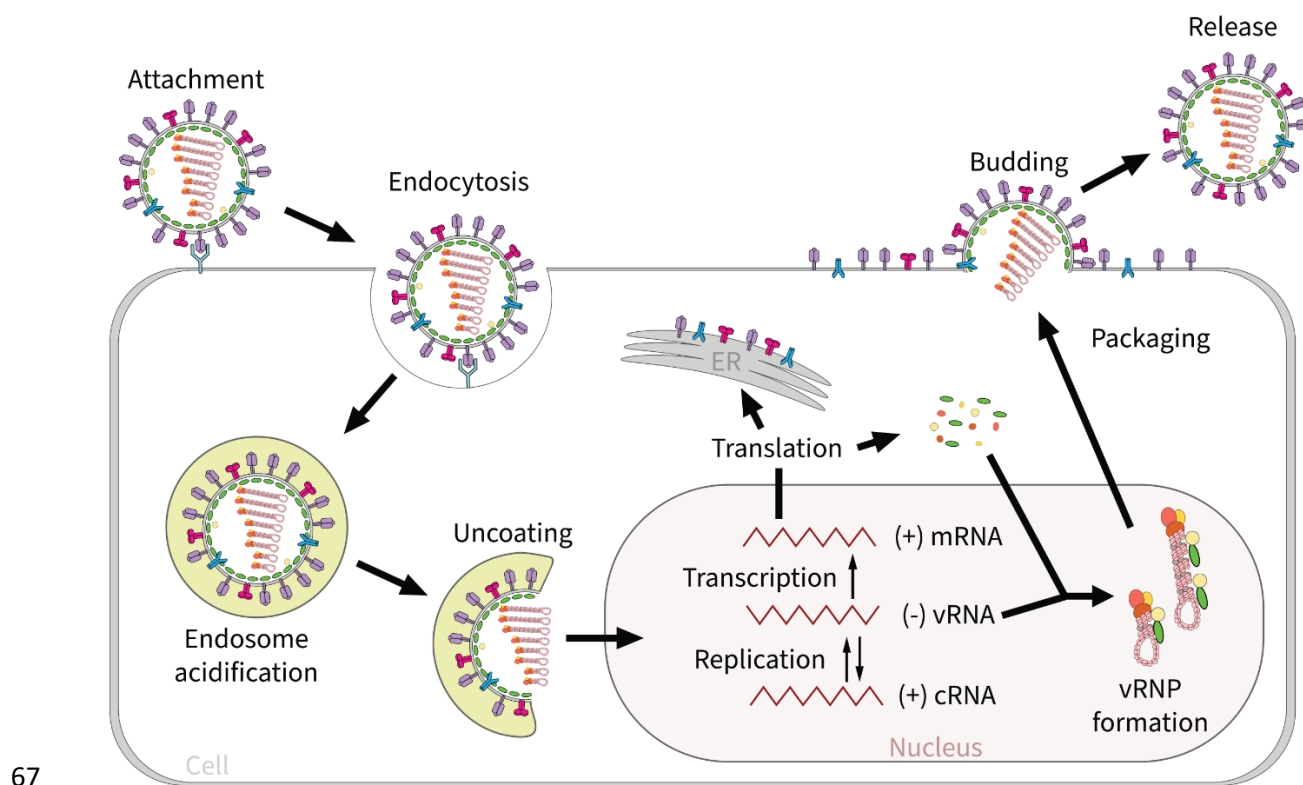
34 IAV infection begins with HA mediated attachment to terminal sialic acids on host cell  
 35 receptors, resulting in endocytosis of the virion (12). As the endosome traffics inside the  
 36 cytoplasm, the pH decreases triggering viral uncoating in two parts. One, the HA trimeric protein  
 37 undergoes a conformational change exposing a fusion peptide that inserts into the endosomal  
 38 membrane, then additional conformational changes in HA results in the formation of a pore (13,  
 39 14). Two, the tetrameric M2 proton channel activates, resulting in the acidification of the viral

40 core, which disassociates vRNPs from the M1 protein inner layer (15, 16). These two events  
41 result in vRNP release into the cellular cytoplasm where NP nuclear localization signals direct  
42 cellular importin proteins to transport vRNPs into the host cell nucleus (11, 17).

43 Once inside the nucleus, IAV replication begins. The vRNP polymerase complex, an RNA-  
44 dependent RNA polymerase, transcribes the negative sense RNA into one of two RNA species.  
45 Viral mRNA, which is used for protein synthesis, and complementary RNA, which is then used  
46 as a template to generate viral RNA (vRNA) gene segments. The IAV polymerase complex  
47 cannot generate the 5' mRNA cap needed for translation. Instead, PB2 binds to cellular mRNA  
48 caps and the endonuclease of PA cleaves the cellular mRNA 10-13 bases downstream of the 5'  
49 end, in a process known as "cap snatching" (18-20). PB1 then polymerizes extension of the  
50 capped primer along the vRNA template and "stutters" upon reaching a stretch of uradine  
51 residues at the 5' end of the vRNA which produces a poly-A tail at the 3' end of the mRNA (20-  
52 22). Notably, the viral mRNAs of certain gene segments are spliced to generate alternative  
53 transcripts. Alternative splicing of the non-structural (NS) and M segment mRNA transcripts  
54 produce the NEP and M2 proteins, respectively.

55 Regulation of gene expression from the M segment, to form M1 and M2 proteins, has important  
56 implications in IAV host adaptation and will be discussed further in chapter three. The transcript  
57 of the M segment, mRNA<sub>7</sub>, encodes M1. Alternative splicing of mRNA<sub>7</sub> forms mRNA<sub>10</sub>, which  
58 encodes M2, and mRNA<sub>11</sub>, which encodes no known protein. For mRNA<sub>7</sub>, the following model  
59 has been supported. Nuclear speckles are the site of mRNA<sub>7</sub> splicing, which is regulated by host  
60 factors (23-27). The viral NS1 protein and the host NS1 binding protein (NS1-BP) bind and  
61 transport mRNA<sub>7</sub> into nuclear speckles (28, 29). Once in the nuclear speckle, NS1 dissociates  
62 from mRNA<sub>7</sub>, and heterogenous ribonuclear protein K (hnRNP K) binds to the mRNA<sub>7</sub> intron.

63 Then hnRNP K recruits U1 small nuclear ribonuclear protein (U1 snRNP) to the mRNA<sub>10</sub> 5'  
 64 splice site, displacing NS1-BP, U1 snRNP together with the spliceosome then splices the  
 65 mRNA<sub>7</sub> to form mRNA<sub>10</sub> (28, 29). Additionally ASF/SF2, a member of the SR RNA splicing  
 66 protein family, has been described to be involved in mRNA<sub>7</sub> splicing (30).



68 **Fig. 2 influenza A virus life cycle.** Influenza virus attachment is mediated by viral HA protein  
 69 interaction with sialic acid (SA) receptors on the cell surface (12). The virion is internalized via  
 70 receptor-mediated endocytosis. The formed endosome containing the virion becomes acidified  
 71 triggering HA fusion of the viral and endosomal membranes, M2 proton channel mediated  
 72 acidification of the viral core (13-16). This uncoating of the virion results in the release of viral  
 73 ribonucleoproteins (vRNPs) into the cytoplasm and are imported into the nucleus (11, 17). In the  
 74 nucleus, vRNPs are transcribed into positive sense viral mRNA or cRNA. mRNAs are exported  
 75 from the nucleus and translated by ribosomes in the cytoplasm or endoplasmic reticulum (ER),  
 76 while cRNAs are used as a template to generate vRNAs (18, 20). vRNAs form vRNPs with viral  
 77 proteins imported into the nucleus which are exported from the nucleus toward the cell surface  
 78 (10, 38). There vRNPs of each of the eight viral gene segments are packaged into budding  
 79 virions that are released once viral assembly is complete (11, 48, 49). (Graphic: G. Delima)

80 Viral mRNAs are exported from the nucleus to be translated by cellular ribosomes. The viral  
 81 proteins that make up the envelope, HA, NA, and M2, are synthesized on ribosomes bound to the

82 endoplasmic reticulum. There they are inserted in the membrane, folded, and oligomerized  
83 before being trafficked to the Golgi apparatus for post-translational modification, and finally to  
84 the host cell plasma membrane (11). Newly synthesized NP, PB1, PB2, PA, M1, and NEP  
85 proteins are directed back into the nucleus by nuclear localization signals to engage in viral  
86 replication and vRNP formation (31-33). Nuclear export of vRNPs is mediated through viral  
87 NEP and M1 proteins and the cellular CRM1 pathway (34-37). vRNPs are then trafficked to the  
88 plasma membrane via recycling endosomes (10, 38).

89 At the plasma membrane, HA, NA, M1, and M2 mediate viral budding and release. The HA  
90 trimers and NA tetramers are targeted to lipid raft domains that lead to membrane curvature and  
91 budding (39-41). M1 proteins, which are bound to vRNPs, bind to HA, NA, and the plasma  
92 membrane, providing structural support and shape to the budding virion (42, 43). M1 also binds  
93 to the M2 tetramer which mediates virion scission from the plasma membrane (44-47). Finally,  
94 NA facilitates virion release by removing sialic acid residues from the virus envelope and cell  
95 surface, freeing the newly formed virion (11, 48, 49).

## 96 **IAV evolution**

97 IAVs evolve by two mechanisms, mutation and reassortment. The RNA-dependent RNA  
98 polymerase encoded by IAVs lacks proofreading which results in frequent mutations, at a rate of  
99 approximately  $2.5 \times 10^5$  substitutions per nucleotide per cell infection, during replication of the  
100 viral genome (50). Reassortment can occur when two or more IAVs coinfect the same cell,  
101 producing progeny that incorporate gene segments from either parental strain (51-53). While  
102 mutation and reassortment can occur readily, these processes are often deleterious, resulting in  
103 less fit progeny (50, 54-56). However, in an environment where selection is acting, rare  
104 beneficial mutations may arise leading to the emergence of progeny with enhanced fitness. Such

105 is the case with seasonal influenza, where variants that can evade pre-existing immunity,  
106 particularly HA neutralizing antibodies, become the new circulating strain (1, 57). Another  
107 context in which IAV evolution is critical for its ecology and epidemiology is adaptation of an  
108 IAV to a new host (5, 58).

### 109 **IAV hosts**

110 The natural reservoir of IAVs are waterfowl, in which nearly all of the HA and NA subtypes  
111 have been found (59-62). IAVs have spread from this reservoir and established host-specific  
112 lineages in humans, poultry, swine, and other mammals. In humans, seasonal influenza A is  
113 currently caused by human H1N1 and H3N2 IAVs (1, 63). While uncommon, human infection  
114 with IAVs that circulate in non-human hosts occur. Usually, these infections are limited to the  
115 index case, however in rare cases, sustained transmission from person to person occurs, resulting  
116 in an IAV pandemic (7, 59). Avian IAVs in poultry have become a concern due to human  
117 infection with these strains. Particularly, highly pathogenic avian influenza (HPAI) A(H5) and  
118 A(H7) viruses, bearing a multibasic cleavage site in the HA protein increasing pathogenicity in  
119 poultry, have resulted in human infections, deaths, and some instances of human to human  
120 transmission (64-66). Another host of concern for zoonotic potential is swine, as it has proven to  
121 be an intermediate host for IAVs. Significantly, the most recent IAV pandemic strain arose from  
122 reassortment in swine in 2009 (67, 68).

123

### 124 **Overcoming species barriers**

125 Species barriers impede transmission of IAVs into new hosts (5, 7, 69, 70). However, IAVs can  
126 overcome these barriers and adapt to a new host via mutation and reassortment. The HA and the  
127 polymerase complex have been well-described as important determinants of viral host range (71-

128 73). Receptor availability poses a barrier to transmission as human IAV HAs preferentially bind  
129 to sialic acid with  $\alpha$ 2,6 linkage to galactose, but avian IAV HAs prefer  $\alpha$ 2,3 linked sialic acid to  
130 mediate attachment. Humans express  $\alpha$ 2,6 sialic acid receptors in the upper respiratory tract,  
131 while  $\alpha$ 2,3 sialic acid receptors are present in the lower respiratory tract, which are more difficult  
132 to reach (74-76). However, a variety of mutations have been identified that alter receptor  
133 preference to  $\alpha$ 2,6 sialic acid (7, 77-79). Additionally, circulation in swine has been shown to  
134 mediate avian IAV adaptation to the human receptor, as swine harbor both avian and human IAV  
135 receptors (68, 80, 81). Once inside a cell, IAV polymerase activity or interactions with host  
136 factors can be diminished during infection of a new species (82-84). Nevertheless, mutations to  
137 PB2, PB1, or PA can re-establish polymerase activity in the new host (85-88). Thus, mutation  
138 has an important role in overcoming IAV barriers through host adaptation. Similarly, IAVs can  
139 rapidly overcome species barriers by acquiring gene segments pre-adapted to the host through  
140 reassortment (5, 58). This mode of host adaptation was particularly important for the emergence  
141 of several pandemic IAV strains.

142

143

#### 144 **Pandemic IAVs**

145 Pandemic IAVs pose a substantial detriment to human health. The first pandemic caused by an  
146 IAV happened in 1918, an H1N1 virus known as the “Spanish flu” and killed an estimated 50  
147 million people globally (89, 90). The 1957 H2N2 “Asian flu” virus and the 1968 H3N2 “Hong  
148 Kong flu” virus each killed approximately one million people worldwide. The most recent IAV  
149 pandemic occurred in 2009, caused by the H1N1 “Swine flu” virus, resulting in about 150-  
150 500,000 deaths. Both the 1968 H3N2 and 2009 H1N1 virus lineages continue to circulate in

151 humans as seasonal influenza strains (91). Notably, the past three IAVs pandemics share a  
152 common feature; they harbor gene segments from both human and non-human IAVs(5, 6, 67,  
153 92). Both the 1957 H2N2 and 1968 H3N2 strains were reassortants between avian IAVs and the  
154 contemporary seasonal strain (7, 84). The 2009 H1N1 strain was a reassortant between avian,  
155 swine, and human IAVs. The 2009 H1N1 strain arose from a series reassortment events in swine.  
156 In 1978, an avian H1N1 virus entered and stably circulated in European swine, establishing the  
157 Eurasian avian-like swine IAV lineage. In 1998, an H1N2 triple reassortant IAV was found in  
158 north American swine containing swine, human, and avian IAV gene segments. In the 2000s, the  
159 Eurasian avian-like swine strain and the North American triple reassortant swine strain  
160 reassorted in swine. The resulting reassortant H1N1 IAV strain would then emerge in humans  
161 causing the 2009 H1N1 IAV pandemic (68, 93, 94). These events suggest that reassortment in  
162 coinfecting hosts plays an important role in the emergence of pandemic IAVs (58).

163

#### 164 **Virus-virus interactions**

165 Virus-virus interactions occur when two or more viruses infect the same host or cell. Depending  
166 on the context, these interactions range from antagonistic to beneficial. Antagonistic interactions  
167 can take the form of competition for naïve cells, then for cellular resources within a cell during  
168 coinfection. Indirectly, an IAV that triggers antiviral responses in the host may lead to viral  
169 suppression (95). Notably, the presence of defective viral genomes (DVGs), virions  
170 incorporating gene segments with large internal deletions, can further these antagonistic effects.  
171 The defective gene segment encoded by DVGs can be replicated rapidly and packaged in place  
172 of an intact segment, suppressing the production of fully infectious virus particles, and DVGs  
173 can potentially activate antiviral responses (96-101).

174 On the other hand, coinfection is sometimes necessary for productive infection and can result in  
175 enhanced viral replication. It follows that the outcome of these interactions can vary and affect  
176 viral replication, progeny production, and diversity (102-104). For IAVs, cellular coinfection is a  
177 largely beneficial interaction between coinfecting viruses. A large portion of IAV particles  
178 initiate replication of incomplete viral genomes, requiring complementation through coinfection  
179 to initiate a productive infection (105-107). Thus, IAVs have an intrinsic reliance on coinfection,  
180 though the extent of reliance varies with virus strain and host species (108). Moreover, an IAV's  
181 reliance on coinfection may increase if there is a reduction in replicative capacity. An increase in  
182 the number of viral polymerases to replicate the genome can overcome this inefficiency. Thus,  
183 these viruses exhibit a density dependence in order to replicate (88).

184 IAV reassortment is dependent on virus-virus interactions. Within coinfecting cells, the exchange  
185 of viral gene segments and incorporation into progeny virions is highly efficient (107, 109).  
186 Within a host, reassortment dynamics vary. High virus dose and the presence of incomplete viral  
187 genomes can enhance the frequency of reassortment (107, 110, 111). However, reassortment  
188 becomes limited when infection dose is discordant or infection is asynchronous between distinct  
189 variants (109). Thus, the frequency of reassortment is strongly modulated by virus-virus  
190 interactions.

### 191 **Dissertation aims**

192 The first aim of this dissertation was to evaluate what viral traits determine the extent to which a  
193 coinfecting IAV can augment the replication of another. Specifically, we examined the impact of  
194 a coinfecting virus's intrinsic reliance on coinfection, the host species to which it adapted, and its  
195 homology to the focal virus. Using virus strains that had distinct combinations of these traits, we  
196 found that IAVs with low intrinsic reliance on coinfection could most potently augment the

197 replication of a coinfecting virus. However, during multi-cycle infection in cell culture or *in vivo*,  
198 competition between coinfecting viruses was the dominant virus-virus interaction. These  
199 findings suggest that virus-virus interactions have significant impacts on coinfecting IAV  
200 populations with dominant virus-virus interactions differing between the within-cell and within-  
201 host scales.

202 The second aim of this dissertation was to elucidate the underlying mechanism of differential M  
203 segment gene regulation that can occur when an IAV infects a new host species. To this end, we  
204 focused on the 2009 pandemic IAV M segment, which has avian origins, to identify M sequence  
205 determinants that result in aberrantly high M2 protein and mRNA expression. By examining M  
206 segments derived from the Eurasian avian-like swine lineage, we showed that avian IAV  
207 circulation in a mammalian host could re-establish M2 protein expression level to that exhibited  
208 in avian IAVs in avian hosts and mammalian IAVs in mammalian hosts but were unable to  
209 identify specific mutations that emerged in this lineage that contributed to this phenotype.  
210 Nevertheless, we found that introducing specific regions of the 2009 pandemic IAV M segment  
211 into an avian IAV precursor could reduce M2 protein expression but did not reduce M2 mRNA  
212 expression. These results suggest that the regulation of M gene expression occurs after the  
213 generation of M1 or M2 mRNAs. Together, our work supports the idea that M gene regulation  
214 has a role in IAV adaptation to new hosts.

215

216 **References Cited**

- 217 1. Petrova VN, Russell CA. 2018. The evolution of seasonal influenza viruses. *Nat Rev*  
218 *Microbiol* 16:47-60.
- 219 2. Prevention CfDCa. October 4, 2022. Disease Burden of Flu.  
220 <https://www.cdc.gov/flu/about/burden/index.html>. Accessed
- 221 3. Molinari NA, Ortega-Sanchez IR, Messonnier ML, Thompson WW, Wortley PM,  
222 Weintraub E, Bridges CB. 2007. The annual impact of seasonal influenza in the US:  
223 measuring disease burden and costs. *Vaccine* 25:5086-96.
- 224 4. Ahmed R, Oldstone MB, Palese P. 2007. Protective immunity and susceptibility to  
225 infectious diseases: lessons from the 1918 influenza pandemic. *Nat Immunol* 8:1188-93.
- 226 5. Scholtissek C. 1994. Source for influenza pandemics. *Eur J Epidemiol* 10:455-8.
- 227 6. Kilbourne ED. 2006. Influenza pandemics of the 20th century. *Emerg Infect Dis* 12:9-14.
- 228 7. Taubenberger JK, Kash JC. 2010. Influenza virus evolution, host adaptation, and  
229 pandemic formation. *Cell Host Microbe* 7:440-51.
- 230 8. Compans RW, Content J, Duesberg PH. 1972. Structure of the ribonucleoprotein of  
231 influenza virus. *J Virol* 10:795-800.
- 232 9. Murti KG, Webster RG, Jones IM. 1988. Localization of RNA polymerases on influenza  
233 viral ribonucleoproteins by immunogold labeling. *Virology* 164:562-6.
- 234 10. Einfeld AJ, Neumann G, Kawaoka Y. 2015. At the centre: influenza A virus  
235 ribonucleoproteins. *Nat Rev Microbiol* 13:28-41.
- 236 11. Bouvier NM, Palese P. 2008. The biology of influenza viruses. *Vaccine* 26 Suppl 4:D49-  
237 53.

- 238 12. Skehel JJ, Wiley DC. 2000. Receptor binding and membrane fusion in virus entry: the  
239 influenza hemagglutinin. *Annu Rev Biochem* 69:531-69.
- 240 13. Sieczkarski SB, Whittaker GR. 2005. Viral entry. *Curr Top Microbiol Immunol* 285:1-  
241 23.
- 242 14. Stegmann T. 2000. Membrane fusion mechanisms: the influenza hemagglutinin paradigm  
243 and its implications for intracellular fusion. *Traffic* 1:598-604.
- 244 15. Pinto LH, Holsinger LJ, Lamb RA. 1992. Influenza virus M2 protein has ion channel  
245 activity. *Cell* 69:517-28.
- 246 16. Wharton SA, Belshe RB, Skehel JJ, Hay AJ. 1994. Role of virion M2 protein in influenza  
247 virus uncoating: specific reduction in the rate of membrane fusion between virus and  
248 liposomes by amantadine. *J Gen Virol* 75 ( Pt 4):945-8.
- 249 17. Martin K, Helenius A. 1991. Transport of incoming influenza virus nucleocapsids into  
250 the nucleus. *J Virol* 65:232-44.
- 251 18. Krug RM. 1981. Priming of influenza viral RNA transcription by capped heterologous  
252 RNAs. *Curr Top Microbiol Immunol* 93:125-49.
- 253 19. Dias A, Bouvier D, Crépin T, McCarthy AA, Hart DJ, Baudin F, Cusack S, Ruigrok RW.  
254 2009. The cap-snatching endonuclease of influenza virus polymerase resides in the PA  
255 subunit. *Nature* 458:914-8.
- 256 20. Te Velthuis AJ, Fodor E. 2016. Influenza virus RNA polymerase: insights into the  
257 mechanisms of viral RNA synthesis. *Nat Rev Microbiol* 14:479-93.
- 258 21. Luo GX, Luytjes W, Enami M, Palese P. 1991. The polyadenylation signal of influenza  
259 virus RNA involves a stretch of uridines followed by the RNA duplex of the panhandle  
260 structure. *J Virol* 65:2861-7.

- 261 22. Li X, Palese P. 1994. Characterization of the polyadenylation signal of influenza virus  
262 RNA. *J Virol* 68:1245-9.
- 263 23. Lamb RA, Lai CJ, Choppin PW. 1981. Sequences of mRNAs derived from genome RNA  
264 segment 7 of influenza virus: colinear and interrupted mRNAs code for overlapping  
265 proteins. *Proc Natl Acad Sci U S A* 78:4170-4.
- 266 24. Valcárcel J, Portela A, Ortín J. 1991. Regulated M1 mRNA splicing in influenza virus-  
267 infected cells. *J Gen Virol* 72 ( Pt 6):1301-8.
- 268 25. Shih SR, Nemeroff ME, Krug RM. 1995. The choice of alternative 5' splice sites in  
269 influenza virus M1 mRNA is regulated by the viral polymerase complex. *Proc Natl Acad*  
270 *Sci U S A* 92:6324-8.
- 271 26. Mor A, White A, Zhang K, Thompson M, Esparza M, Muñoz-Moreno R, Koide K,  
272 Lynch KW, García-Sastre A, Fontoura BM. 2016. Influenza virus mRNA trafficking  
273 through host nuclear speckles. *Nat Microbiol* 1:16069.
- 274 27. Galganski L, Urbanek MO, Krzyzosiak WJ. 2017. Nuclear speckles: molecular  
275 organization, biological function and role in disease. *Nucleic Acids Res* 45:10350-10368.
- 276 28. Tsai PL, Chiou NT, Kuss S, García-Sastre A, Lynch KW, Fontoura BM. 2013. Cellular  
277 RNA binding proteins NS1-BP and hnRNP K regulate influenza A virus RNA splicing.  
278 *PLoS Pathog* 9:e1003460.
- 279 29. Zhang K, Shang G, Padavannil A, Wang J, Sakthivel R, Chen X, Kim M, Thompson  
280 MG, García-Sastre A, Lynch KW, Chen ZJ, Chook YM, Fontoura BMA. 2018.  
281 Structural-functional interactions of NS1-BP protein with the splicing and mRNA export  
282 machineries for viral and host gene expression. *Proc Natl Acad Sci U S A* 115:E12218-  
283 e12227.

- 284 30. Shih SR, Krug RM. 1996. Novel exploitation of a nuclear function by influenza virus: the  
285 cellular SF2/ASF splicing factor controls the amount of the essential viral M2 ion  
286 channel protein in infected cells. *Embo j* 15:5415-27.
- 287 31. Mukaigawa J, Nayak DP. 1991. Two signals mediate nuclear localization of influenza  
288 virus (A/WSN/33) polymerase basic protein 2. *J Virol* 65:245-53.
- 289 32. Nieto A, de la Luna S, Bárcena J, Portela A, Ortín J. 1994. Complex structure of the  
290 nuclear translocation signal of influenza virus polymerase PA subunit. *J Gen Virol* 75 ( Pt  
291 1):29-36.
- 292 33. York A, Hengrung N, Vreede FT, Huiskonen JT, Fodor E. 2013. Isolation and  
293 characterization of the positive-sense replicative intermediate of a negative-strand RNA  
294 virus. *Proc Natl Acad Sci U S A* 110:E4238-45.
- 295 34. Chaimayo C, Hayashi T, Underwood A, Hodges E, Takimoto T. 2017. Selective  
296 incorporation of vRNP into influenza A virions determined by its specific interaction  
297 with M1 protein. *Virology* 505:23-32.
- 298 35. Huang S, Chen J, Chen Q, Wang H, Yao Y, Chen J, Chen Z. 2013. A second CRM1-  
299 dependent nuclear export signal in the influenza A virus NS2 protein contributes to the  
300 nuclear export of viral ribonucleoproteins. *J Virol* 87:767-78.
- 301 36. Neumann G, Hughes MT, Kawaoka Y. 2000. Influenza A virus NS2 protein mediates  
302 vRNP nuclear export through NES-independent interaction with hCRM1. *Embo j*  
303 19:6751-8.
- 304 37. Paterson D, Fodor E. 2012. Emerging roles for the influenza A virus nuclear export  
305 protein (NEP). *PLoS Pathog* 8:e1003019.

- 306 38. Momose F, Sekimoto T, Ohkura T, Jo S, Kawaguchi A, Nagata K, Morikawa Y. 2011.  
307 Apical transport of influenza A virus ribonucleoprotein requires Rab11-positive recycling  
308 endosome. *PLoS One* 6:e21123.
- 309 39. Takeda M, Leser GP, Russell CJ, Lamb RA. 2003. Influenza virus hemagglutinin  
310 concentrates in lipid raft microdomains for efficient viral fusion. *Proc Natl Acad Sci U S*  
311 *A* 100:14610-7.
- 312 40. Leser GP, Lamb RA. 2005. Influenza virus assembly and budding in raft-derived  
313 microdomains: a quantitative analysis of the surface distribution of HA, NA and M2  
314 proteins. *Virology* 342:215-27.
- 315 41. Chen BJ, Leser GP, Morita E, Lamb RA. 2007. Influenza virus hemagglutinin and  
316 neuraminidase, but not the matrix protein, are required for assembly and budding of  
317 plasmid-derived virus-like particles. *J Virol* 81:7111-23.
- 318 42. Zhang J, Lamb RA. 1996. Characterization of the membrane association of the influenza  
319 virus matrix protein in living cells. *Virology* 225:255-66.
- 320 43. Ali A, Avalos RT, Ponimaskin E, Nayak DP. 2000. Influenza virus assembly: effect of  
321 influenza virus glycoproteins on the membrane association of M1 protein. *J Virol*  
322 74:8709-19.
- 323 44. Rossman JS, Jing X, Leser GP, Lamb RA. 2010. Influenza virus M2 protein mediates  
324 ESCRT-independent membrane scission. *Cell* 142:902-13.
- 325 45. Rossman JS, Lamb RA. 2011. Influenza virus assembly and budding. *Virology* 411:229-  
326 36.

- 327 46. Chen BJ, Leser GP, Jackson D, Lamb RA. 2008. The influenza virus M2 protein  
328 cytoplasmic tail interacts with the M1 protein and influences virus assembly at the site of  
329 virus budding. *J Virol* 82:10059-70.
- 330 47. McCown MF, Pekosz A. 2006. Distinct domains of the influenza A virus M2 protein  
331 cytoplasmic tail mediate binding to the M1 protein and facilitate infectious virus  
332 production. *J Virol* 80:8178-89.
- 333 48. Palese P, Tobita K, Ueda M, Compans RW. 1974. Characterization of temperature  
334 sensitive influenza virus mutants defective in neuraminidase. *Virology* 61:397-410.
- 335 49. Palese P, Compans RW. 1976. Inhibition of influenza virus replication in tissue culture  
336 by 2-deoxy-2,3-dehydro-N-trifluoroacetylneuraminic acid (FANA): mechanism of action.  
337 *J Gen Virol* 33:159-63.
- 338 50. Peck KM, Lauring AS. 2018. Complexities of Viral Mutation Rates. *J Virol* 92.
- 339 51. Lowen AC. 2017. Constraints, Drivers, and Implications of Influenza A Virus  
340 Reassortment. *Annu Rev Virol* 4:105-121.
- 341 52. Steel J, Lowen AC. 2014. Influenza A virus reassortment. *Curr Top Microbiol Immunol*  
342 385:377-401.
- 343 53. Desselberger U, Nakajima K, Alfino P, Pedersen FS, Haseltine WA, Hannoun C, Palese  
344 P. 1978. Biochemical evidence that "new" influenza virus strains in nature may arise by  
345 recombination (reassortment). *Proc Natl Acad Sci U S A* 75:3341-5.
- 346 54. Sanjuán R, Moya A, Elena SF. 2004. The distribution of fitness effects caused by single-  
347 nucleotide substitutions in an RNA virus. *Proc Natl Acad Sci U S A* 101:8396-401.

- 348 55. Phipps KL, Marshall N, Tao H, Danzy S, Onuoha N, Steel J, Lowen AC. 2017. Seasonal  
349 H3N2 and 2009 Pandemic H1N1 Influenza A Viruses Reassort Efficiently but Produce  
350 Attenuated Progeny. *J Virol* 91.
- 351 56. Villa M, Lässig M. 2017. Fitness cost of reassortment in human influenza. *PLoS Pathog*  
352 13:e1006685.
- 353 57. Smith DJ, Lapedes AS, de Jong JC, Bestebroer TM, Rimmelzwaan GF, Osterhaus AD,  
354 Fouchier RA. 2004. Mapping the antigenic and genetic evolution of influenza virus.  
355 *Science* 305:371-6.
- 356 58. Ma EJ, Hill NJ, Zabilansky J, Yuan K, Runstadler JA. 2016. Reticulate evolution is  
357 favored in influenza niche switching. *Proc Natl Acad Sci U S A* 113:5335-9.
- 358 59. Webster RG, Bean WJ, Gorman OT, Chambers TM, Kawaoka Y. 1992. Evolution and  
359 ecology of influenza A viruses. *Microbiol Rev* 56:152-79.
- 360 60. Krauss S, Walker D, Pryor SP, Niles L, Chenghong L, Hinshaw VS, Webster RG. 2004.  
361 Influenza A viruses of migrating wild aquatic birds in North America. *Vector Borne*  
362 *Zoonotic Dis* 4:177-89.
- 363 61. Olsen B, Munster VJ, Wallensten A, Waldenström J, Osterhaus AD, Fouchier RA. 2006.  
364 Global patterns of influenza a virus in wild birds. *Science* 312:384-8.
- 365 62. Vandegrift KJ, Sokolow SH, Daszak P, Kilpatrick AM. 2010. Ecology of avian influenza  
366 viruses in a changing world. *Ann N Y Acad Sci* 1195:113-28.
- 367 63. Russell CA, Jones TC, Barr IG, Cox NJ, Garten RJ, Gregory V, Gust ID, Hampson AW,  
368 Hay AJ, Hurt AC, de Jong JC, Kelso A, Klimov AI, Kageyama T, Komadina N, Lapedes  
369 AS, Lin YP, Mosterin A, Obuchi M, Odagiri T, Osterhaus AD, Rimmelzwaan GF, Shaw

- 370 MW, Skepner E, Stohr K, Tashiro M, Fouchier RA, Smith DJ. 2008. The global  
371 circulation of seasonal influenza A (H3N2) viruses. *Science* 320:340-6.
- 372 64. Suguitan AL, Jr., Matsuoka Y, Lau YF, Santos CP, Vogel L, Cheng LI, Orandle M,  
373 Subbarao K. 2012. The multibasic cleavage site of the hemagglutinin of highly  
374 pathogenic A/Vietnam/1203/2004 (H5N1) avian influenza virus acts as a virulence factor  
375 in a host-specific manner in mammals. *J Virol* 86:2706-14.
- 376 65. Yang Y, Halloran ME, Sugimoto JD, Longini IM, Jr. 2007. Detecting human-to-human  
377 transmission of avian influenza A (H5N1). *Emerg Infect Dis* 13:1348-53.
- 378 66. Guan Y, Poon LL, Cheung CY, Ellis TM, Lim W, Lipatov AS, Chan KH, Sturm-Ramirez  
379 KM, Cheung CL, Leung YH, Yuen KY, Webster RG, Peiris JS. 2004. H5N1 influenza: a  
380 protean pandemic threat. *Proc Natl Acad Sci U S A* 101:8156-61.
- 381 67. Trifonov V, Khiabani H, Greenbaum B, Rabadan R. 2009. The origin of the recent  
382 swine influenza A(H1N1) virus infecting humans. *Euro Surveill* 14.
- 383 68. Neumann G, Noda T, Kawaoka Y. 2009. Emergence and pandemic potential of swine-  
384 origin H1N1 influenza virus. *Nature* 459:931-9.
- 385 69. Sorrell EM, Schrauwen EJ, Linster M, De Graaf M, Herfst S, Fouchier RA. 2011.  
386 Predicting 'airborne' influenza viruses: (trans-) mission impossible? *Curr Opin Virol*  
387 1:635-42.
- 388 70. Matrosovich M, Tuzikov A, Bovin N, Gambaryan A, Klimov A, Castrucci MR, Donatelli  
389 I, Kawaoka Y. 2000. Early alterations of the receptor-binding properties of H1, H2, and  
390 H3 avian influenza virus hemagglutinins after their introduction into mammals. *J Virol*  
391 74:8502-12.

- 392 71. Byrd-Leotis L, Cummings RD, Steinhauer DA. 2017. The Interplay between the Host  
393 Receptor and Influenza Virus Hemagglutinin and Neuraminidase. *Int J Mol Sci* 18.
- 394 72. Galloway SE, Reed ML, Russell CJ, Steinhauer DA. 2013. Influenza HA subtypes  
395 demonstrate divergent phenotypes for cleavage activation and pH of fusion: implications  
396 for host range and adaptation. *PLoS Pathog* 9:e1003151.
- 397 73. Cauldwell AV, Long JS, Moncorgé O, Barclay WS. 2014. Viral determinants of  
398 influenza A virus host range. *J Gen Virol* 95:1193-1210.
- 399 74. Shinya K, Ebina M, Yamada S, Ono M, Kasai N, Kawaoka Y. 2006. Avian flu: influenza  
400 virus receptors in the human airway. *Nature* 440:435-6.
- 401 75. van Riel D, Munster VJ, de Wit E, Rimmelzwaan GF, Fouchier RA, Osterhaus AD,  
402 Kuiken T. 2007. Human and avian influenza viruses target different cells in the lower  
403 respiratory tract of humans and other mammals. *Am J Pathol* 171:1215-23.
- 404 76. Nicholls JM, Bourne AJ, Chen H, Guan Y, Peiris JS. 2007. Sialic acid receptor detection  
405 in the human respiratory tract: evidence for widespread distribution of potential binding  
406 sites for human and avian influenza viruses. *Respir Res* 8:73.
- 407 77. Rogers GN, Paulson JC. 1983. Receptor determinants of human and animal influenza  
408 virus isolates: differences in receptor specificity of the H3 hemagglutinin based on  
409 species of origin. *Virology* 127:361-73.
- 410 78. Belser JA, Blixt O, Chen LM, Pappas C, Maines TR, Van Hoeven N, Donis R, Busch J,  
411 McBride R, Paulson JC, Katz JM, Tumpey TM. 2008. Contemporary North American  
412 influenza H7 viruses possess human receptor specificity: Implications for virus  
413 transmissibility. *Proc Natl Acad Sci U S A* 105:7558-63.

- 414 79. Reperant LA, Kuiken T, Osterhaus AD. 2012. Adaptive pathways of zoonotic influenza  
415 viruses: from exposure to establishment in humans. *Vaccine* 30:4419-34.
- 416 80. Ito T, Couceiro JN, Kelm S, Baum LG, Krauss S, Castrucci MR, Donatelli I, Kida H,  
417 Paulson JC, Webster RG, Kawaoka Y. 1998. Molecular basis for the generation in pigs of  
418 influenza A viruses with pandemic potential. *J Virol* 72:7367-73.
- 419 81. Ma W, Kahn RE, Richt JA. 2008. The pig as a mixing vessel for influenza viruses:  
420 Human and veterinary implications. *J Mol Genet Med* 3:158-66.
- 421 82. Subbarao EK, London W, Murphy BR. 1993. A single amino acid in the PB2 gene of  
422 influenza A virus is a determinant of host range. *J Virol* 67:1761-4.
- 423 83. Gabriel G, Herwig A, Klenk HD. 2008. Interaction of polymerase subunit PB2 and NP  
424 with importin alpha1 is a determinant of host range of influenza A virus. *PLoS Pathog*  
425 4:e11.
- 426 84. Mostafa A, Abdelwhab EM, Mettenleiter TC, Pleschka S. 2018. Zoonotic Potential of  
427 Influenza A Viruses: A Comprehensive Overview. *Viruses* 10.
- 428 85. Gabriel G, Dauber B, Wolff T, Planz O, Klenk HD, Stech J. 2005. The viral polymerase  
429 mediates adaptation of an avian influenza virus to a mammalian host. *Proc Natl Acad Sci*  
430 *U S A* 102:18590-5.
- 431 86. Steel J, Lowen AC, Mubareka S, Palese P. 2009. Transmission of influenza virus in a  
432 mammalian host is increased by PB2 amino acids 627K or 627E/701N. *PLoS Pathog*  
433 5:e1000252.
- 434 87. Taubenberger JK, Reid AH, Lourens RM, Wang R, Jin G, Fanning TG. 2005.  
435 Characterization of the 1918 influenza virus polymerase genes. *Nature* 437:889-93.

- 436 88. Shartouny JR, Lee CY, Delima GK, Lowen AC. 2022. Beneficial effects of cellular  
437 coinfection resolve inefficiency in influenza A virus transcription. *PLoS Pathog*  
438 18:e1010865.
- 439 89. Pappas C, Aguilar PV, Basler CF, Solórzano A, Zeng H, Perrone LA, Palese P, García-  
440 Sastre A, Katz JM, Tumpey TM. 2008. Single gene reassortants identify a critical role for  
441 PB1, HA, and NA in the high virulence of the 1918 pandemic influenza virus. *Proc Natl*  
442 *Acad Sci U S A* 105:3064-9.
- 443 90. Belser JA, Maines TR, Tumpey TM. 2018. Importance of 1918 virus reconstruction to  
444 current assessments of pandemic risk. *Virology* 524:45-55.
- 445 91. Prevention CfDCA. August 10, 2019. Past Pandemics, *on* Centers for Disease Control  
446 and Prevention. [https://www.cdc.gov/flu/pandemic-resources/basics/past-](https://www.cdc.gov/flu/pandemic-resources/basics/past-pandemics.html)  
447 [pandemics.html](https://www.cdc.gov/flu/pandemic-resources/basics/past-pandemics.html). Accessed
- 448 92. Cox NJ, Subbarao K. 2000. Global epidemiology of influenza: past and present. *Annu*  
449 *Rev Med* 51:407-21.
- 450 93. Brockwell-Staats C, Webster RG, Webby RJ. 2009. Diversity of influenza viruses in  
451 swine and the emergence of a novel human pandemic influenza A (H1N1). *Influenza*  
452 *Other Respir Viruses* 3:207-13.
- 453 94. Mena I, Nelson MI, Quezada-Monroy F, Dutta J, Cortes-Fernández R, Lara-Puente JH,  
454 Castro-Peralta F, Cunha LF, Trovão NS, Lozano-Dubernard B, Rambaut A, van Bakel H,  
455 García-Sastre A. 2016. Origins of the 2009 H1N1 influenza pandemic in swine in  
456 Mexico. *Elife* 5.
- 457 95. García-Sastre A. 2011. Induction and evasion of type I interferon responses by influenza  
458 viruses. *Virus Res* 162:12-8.

- 459 96. Leeks A, Sanjuán R, West SA. 2019. The evolution of collective infectious units in  
460 viruses. *Virus Res* 265:94-101.
- 461 97. Nayak DP, Chambers TM, Akkina RK. 1985. Defective-interfering (DI) RNAs of  
462 influenza viruses: origin, structure, expression, and interference. *Curr Top Microbiol*  
463 *Immunol* 114:103-51.
- 464 98. Alnaji FG, Brooke CB. 2020. Influenza virus DI particles: Defective interfering or  
465 delightfully interesting? *PLoS Pathog* 16:e1008436.
- 466 99. Vignuzzi M, López CB. 2019. Defective viral genomes are key drivers of the virus-host  
467 interaction. *Nat Microbiol* 4:1075-1087.
- 468 100. Ziegler CM, Botten JW. 2020. Defective Interfering Particles of Negative-Strand RNA  
469 Viruses. *Trends Microbiol* 28:554-565.
- 470 101. Yount JS, Gitlin L, Moran TM, López CB. 2008. MDA5 participates in the detection of  
471 paramyxovirus infection and is essential for the early activation of dendritic cells in  
472 response to Sendai Virus defective interfering particles. *J Immunol* 180:4910-8.
- 473 102. DaPalma T, Doonan BP, Trager NM, Kasman LM. 2010. A systematic approach to virus-  
474 virus interactions. *Virus Res* 149:1-9.
- 475 103. Boullé M, Müller TG, Dähling S, Ganga Y, Jackson L, Mahamed D, Oom L, Lustig G,  
476 Neher RA, Sigal A. 2016. HIV Cell-to-Cell Spread Results in Earlier Onset of Viral Gene  
477 Expression by Multiple Infections per Cell. *PLoS Pathog* 12:e1005964.
- 478 104. Sanjuán R, Thoulouze MI. 2019. Erratum: Why viruses sometimes disperse in groups?  
479 *Virus Evol* 5:vez025.
- 480 105. Brooke CB. 2014. Biological activities of 'noninfectious' influenza A virus particles.  
481 *Future Virol* 9:41-51.

- 482 106. Jacobs NT, Onuoha NO, Antia A, Steel J, Antia R, Lowen AC. 2019. Incomplete  
483 influenza A virus genomes occur frequently but are readily complemented during  
484 localized viral spread. *Nat Commun* 10:3526.
- 485 107. Fonville JM, Marshall N, Tao H, Steel J, Lowen AC. 2015. Influenza Virus Reassortment  
486 Is Enhanced by Semi-infectious Particles but Can Be Suppressed by Defective Interfering  
487 Particles. *PLoS Pathog* 11:e1005204.
- 488 108. Phipps KL, Ganti K, Jacobs NT, Lee CY, Carnaccini S, White MC, Manandhar M,  
489 Pickett BE, Tan GS, Ferreri LM, Perez DR, Lowen AC. 2020. Collective interactions  
490 augment influenza A virus replication in a host-dependent manner. *Nat Microbiol*  
491 5:1158-1169.
- 492 109. Marshall N, Priyamvada L, Ende Z, Steel J, Lowen AC. 2013. Influenza virus  
493 reassortment occurs with high frequency in the absence of segment mismatch. *PLoS*  
494 *Pathog* 9:e1003421.
- 495 110. Sobel Leonard A, McClain MT, Smith GJ, Wentworth DE, Halpin RA, Lin X, Ransier A,  
496 Stockwell TB, Das SR, Gilbert AS, Lambkin-Williams R, Ginsburg GS, Woods CW,  
497 Koelle K, Illingworth CJ. 2017. The effective rate of influenza reassortment is limited  
498 during human infection. *PLoS Pathog* 13:e1006203.
- 499 111. Tao H, Steel J, Lowen AC. 2014. Intrahost dynamics of influenza virus reassortment. *J*  
500 *Virol* 88:7485-92.

501

502

503 **Chapter 2: Influenza A virus coinfection dynamics are shaped by distinct virus-virus**  
504 **interactions within and between cells**

505

506 Gabrielle K. Delima<sup>1</sup>, Ketaki Ganti<sup>1</sup>, Katie E. Holmes<sup>1</sup>, Jessica R. Shartouny<sup>1</sup> and Anice C.  
507 Lowen<sup>1,2\*</sup>

508

509 <sup>1</sup>Department of Microbiology and Immunology, Emory University School of Medicine, Atlanta,  
510 Georgia, United States of America,

511 <sup>2</sup>Emory Center of Excellence for Influenza Research and Response (Emory-CEIRR), Atlanta,  
512 Georgia, United States of America

513

514 \*Correspondence: anice.lowen@emory.edu

515

516

517 **Abstract**

518

519 When multiple viral populations propagate within the same host environment, they often shape  
520 each other's dynamics. These interactions can be positive or negative and can occur at multiple  
521 scales, from coinfection of a cell to co-circulation at a global population level. For influenza A  
522 viruses (IAVs), the delivery of multiple viral genomes to a cell substantially increases burst size.  
523 However, despite its relevance for IAV evolution through reassortment, the implications of this  
524 positive density dependence for coinfection between distinct IAVs has not been explored.  
525 Furthermore, the extent to which these interactions within the cell shape viral dynamics at the

526 level of the host remains unclear. Here we show that, within cells, coinfecting IAVs strongly  
527 augment the replication of a focal strain, irrespective of the native host of the coinfecting IAV or  
528 its homology to the focal strain. Coinfecting viruses with a low intrinsic reliance on multiple  
529 infection offer the greatest benefit. Nevertheless, virus-virus interactions at the level of the whole  
530 host are antagonistic. This antagonism is recapitulated in cell culture when the coinfecting virus  
531 is introduced several hours prior to the focal strain or under conditions conducive to multiple  
532 rounds of viral replication. Together, these data suggest that beneficial virus-virus interactions  
533 within cells are counterbalanced by competition for susceptible cells during viral propagation  
534 through a tissue. The integration of virus-virus interactions across scales is critical in defining the  
535 outcomes of viral coinfection.

536

## 537 **Introduction**

538

539 The past three influenza A virus (IAV) pandemics arose through reassortment involving human  
540 and non-human IAVs in coinfecting hosts (1-6). Due to the segmented nature of the IAV genome,  
541 when two or more IAVs coinfect the same cell, viral progeny can contain a mix of gene  
542 segments from either parental strain (7-9). Reassortment between phylogenetically distant IAVs  
543 often generates progeny less fit than the parental strains due to the unlinking of coevolved gene  
544 segments (10, 11). However, reassortment can facilitate host switching through the formation of  
545 antigenically novel strains that carry gene segments well-adapted to human infection (2, 12).  
546 Thus, coinfections involving heterologous IAVs are of constant concern.

547

548 When viruses coinfect the same host or cell, each can affect the other's replication. These virus-  
549 virus interactions range from antagonistic to beneficial, depending on the context. At the cellular  
550 scale, viruses may compete directly for limited resources within the cell or indirectly through the  
551 triggering of antiviral responses. These antagonistic effects are typically potent in the case of  
552 defective viral genomes (13). Conversely, coinfection may enhance productivity through  
553 complementation of incomplete or otherwise defective viral genomes or by increasing the  
554 availability of viral proteins needed for replication or host immune suppression (14-17). At the  
555 host scale, viruses may compete for naïve cells: in a mechanism known as superinfection  
556 exclusion, infected cells can become refractory to secondary infection. Additionally, activation  
557 of non-specific antiviral responses can further suppress viral infection within the host (18).  
558 Conversely, a focal virus may benefit indirectly from the suppression of systemic antiviral  
559 responses or induction of pro-viral processes (e.g. coughing) by a coinfecting virus. These virus-  
560 virus interactions often occur simultaneously, but which interaction is dominant may vary with  
561 context.

562

563 Our prior work focused on virus-virus interactions between homologous viruses. We previously  
564 reported that coinfection of a cell with multiple IAV particles is often required to initiate a  
565 productive infection (15). Furthermore, we determined that this reliance on multiple infection is  
566 a common feature of IAVs, but the level of reliance is both strain and host dependent (16).  
567 Density dependence of IAV replication arises due to a need for complementation of incomplete  
568 viral genomes (15) and can be heightened in the context of deleterious mutation or antiviral drug  
569 treatment (17). It follows that interactions between coinfecting IAVs impact the likelihood of  
570 productive vs abortive infection. Thus, IAV virus-virus interactions are a major factor defining

571 the outcomes of cellular infection. These outcomes include whether or not progeny are produced,  
572 their quantitative yield and their genotypes. Given that the replicative potential of a virus is  
573 strongly shaped by its interactions with other co-occurring viruses, we sought to understand the  
574 implications of virus-virus interactions in the context of coinfection between phylogenetically  
575 distinct IAVs.

576

577 Here, we investigate what viral traits define the extent to which a coinfecting IAV can augment  
578 the replication of another. Specifically, we examine the importance of a coinfecting virus'  
579 intrinsic reliance on multiple infection, the host species to which it is adapted, and its homology  
580 to the focal virus. To this end, we evaluated the outcomes of coinfection with a set of well-  
581 characterized IAV strains: influenza A/guinea fowl/Hong Kong/WF10/99 (H9N2) (GFHK99),  
582 A/mallard/Minnesota/199106/99 (H3N8) (MaMN99), A/Netherlands/602/2009 (H1N1) (NL09),  
583 and A/Panama/2007/99 (H3N2) (Pan99) viruses. Our results indicate that homology and host  
584 adaptation are not critical for defining IAV-IAV interactions within cells. Conversely, IAVs  
585 having a low intrinsic reliance on coinfection more effectively augment replication of the focal  
586 virus. While these beneficial interactions are readily detected when infection is limited to a  
587 single viral generation, under conditions that allow further propagation, antagonistic effects  
588 become predominant. Dynamics in vivo and during multiple rounds of viral infection in cell  
589 culture suggest that competition for target cells and super infection exclusion typically limit the  
590 opportunity for distinct viral populations to interact within cells.

591

## 592 **Results**

593

594 **Intrinsic reliance on multiple infection in mammalian cells is strain dependent.**

595 Previously we showed that influenza A virus replication is strongly dependent on viral density.  
596 Namely, progeny production is enhanced when population density is sufficient to ensure delivery  
597 of many viral genomes to a cell. The extent of this dependence was, however, noted to vary with  
598 virus strain. To investigate the importance of this phenotype for interactions between distinct  
599 coinfecting strains, we sought to identify a panel of viruses that vary in their reliance on multiple  
600 infection. To this end, we evaluated the sensitivity of viral RNA (vRNA) replication to  
601 multiplicity of infection (MOI) for a diverse set of IAV strains, including two of avian-origin and  
602 two of human-origin. This was done by infecting Madin Darby canine kidney (MDCK) cells  
603 with a wild type (wt) virus at a constant low dose and infecting simultaneously with increasing  
604 doses of a homologous virus, termed var. The var virus carries synonymous mutations to allow  
605 differentiation of its genome from that of the corresponding wt virus. Coinfections were limited  
606 to a single cycle of infection to ensure that results reflected processes occurring within cells. In  
607 line with previous observations, GFHK99wt virus replication is enhanced ~100-fold by co-  
608 inoculation with GFHK99var virus (Fig 1A). However, the replication of a second avian virus,  
609 MaMN99wt shows at most a 4-fold enhancement with addition of MaMN99var (Fig 1B). While  
610 peak enhancement of Pan99wt virus with the addition of Pan99var virus is ~900-fold (Fig 1C),  
611 NL09wt replication is reduced approximately 300-fold through the addition of NL09var (Fig  
612 1D). These data indicate that reliance on multiple infection is strain dependent and does not  
613 consistently correspond to the extent of viral adaptation to the host.

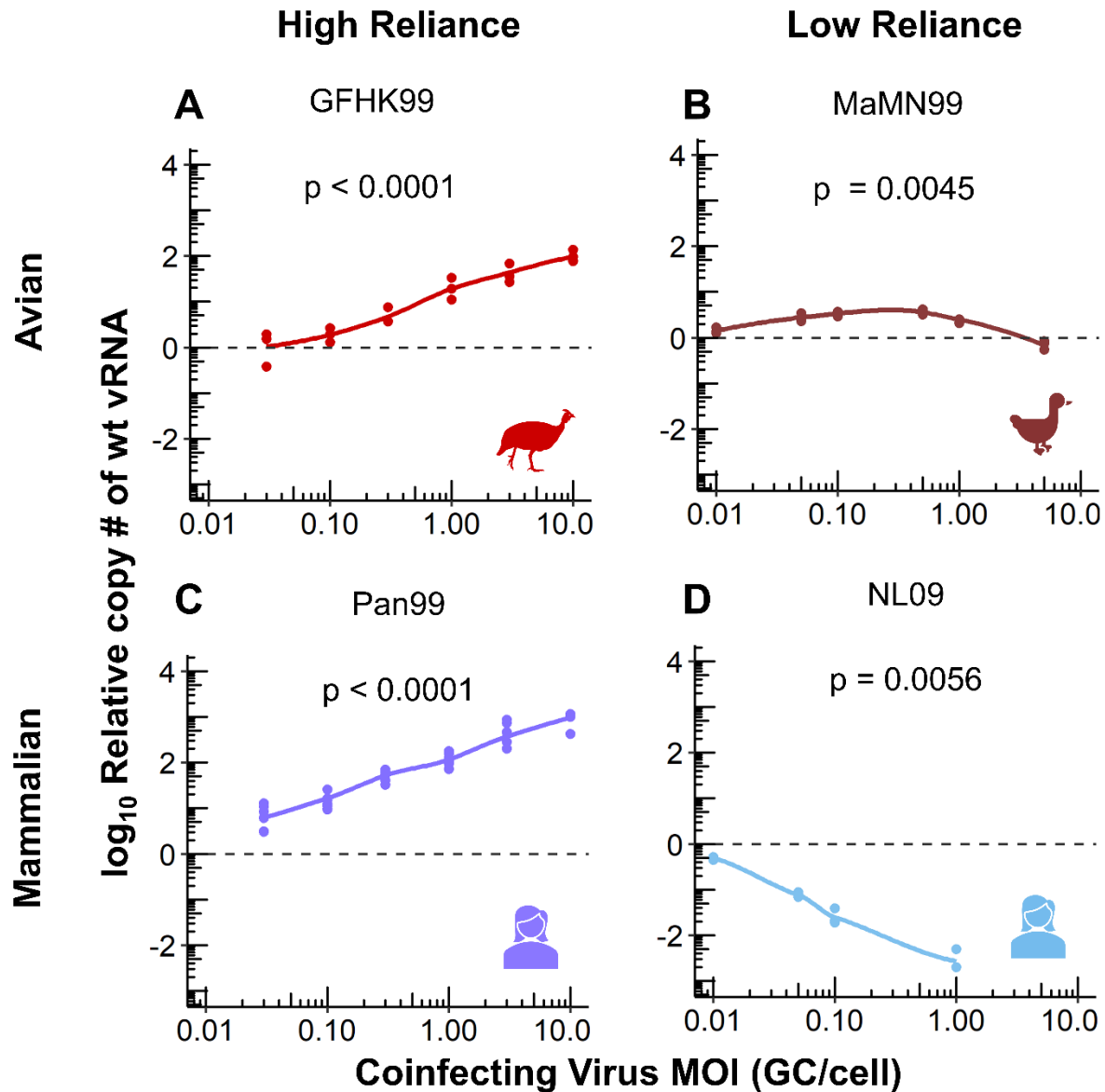
614

615 **Beneficial interactions within cells extend to heterologous virus pairings.**

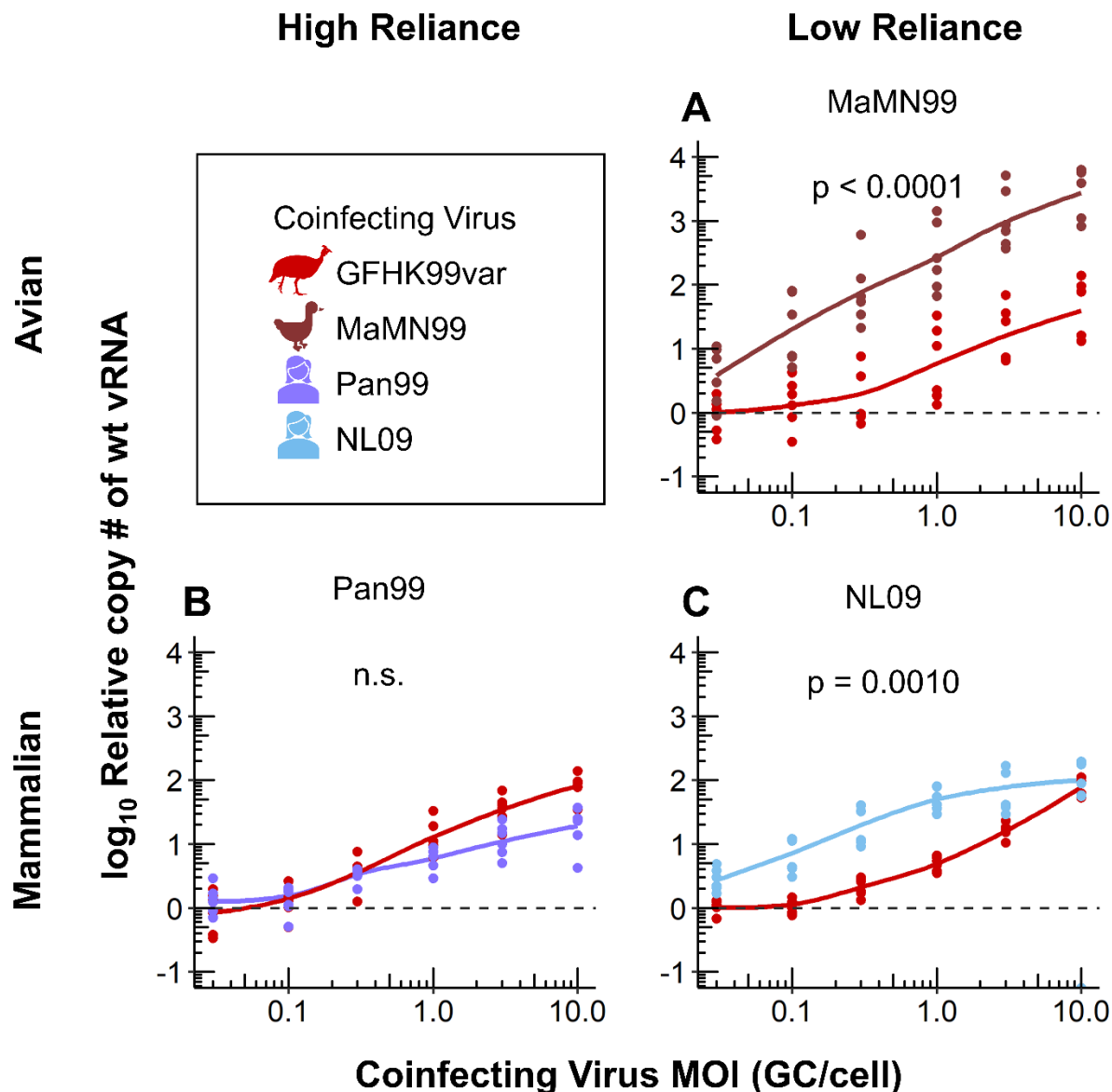
616 To date, our examination of IAV density dependence has centered on homologous interactions  
617 that would occur within a given viral population. Here, we sought to test whether the positive  
618 effects of increased density would extend to coinfection with distinct IAV strains. Although  
619 virus-virus interactions would typically be bi-directional, for the purposes of our experimental  
620 design, we measure the impact of coinfection on only one strain in the pairing, referred to here as  
621 the focal virus.

622  
623 We predicted that specific traits of a coinfecting virus, such as the strength of its intrinsic density  
624 dependence, the host to which it is adapted, or its degree of homology to the focal strain, may  
625 affect its potential to modulate the replication of the focal strain. To test these predictions, we  
626 performed a series of coinfections using GFHK99wt as the focal virus and MaMN99, NL09, or  
627 Pan99 as coinfecting viruses. We infected MDCK cells with a constant dose of GFHK99wt virus  
628 and increasing doses of GFHK99var virus (as a control) or NL09, MaMN99, or Pan99 virus,  
629 then quantified levels of GFHK99wt genomes in the cells. These coinfections were again limited  
630 to a single cycle to ensure that results reflected processes occurring within cells. The results  
631 show that GFHK99wt genome levels increase with increasing doses of every coinfecting var  
632 virus, indicating that phylogenetic relatedness within the species *influenzavirus A* is not required  
633 for beneficial interactions within the cell (Fig 2 and S1 Fig). However, the degree to which  
634 GFHK99wt virus replication was increased varied with the coinfecting strain. Compared to the  
635 control in which GFHK99var was the coinfecting virus, MaMN99 and NL09var virus  
636 coinfections resulted in significantly greater enhancement of GFHK99wt virus replication (Fig  
637 2A,C and S1 Fig) while coinfection with Pan99var virus resulted in lower enhancement (Fig 2B).  
638 These results indicate that the degree to which a coinfecting virus is adapted to the host (in this

639 case, mammalian cells) is not a major factor defining its potential to augment replication of the  
 640 focal virus. Instead, the data suggest that lower intrinsic density dependence of the coinfecting  
 641 strain, as for NL09 and MaMN99, allows a stronger benefit to be conferred on the focal virus.



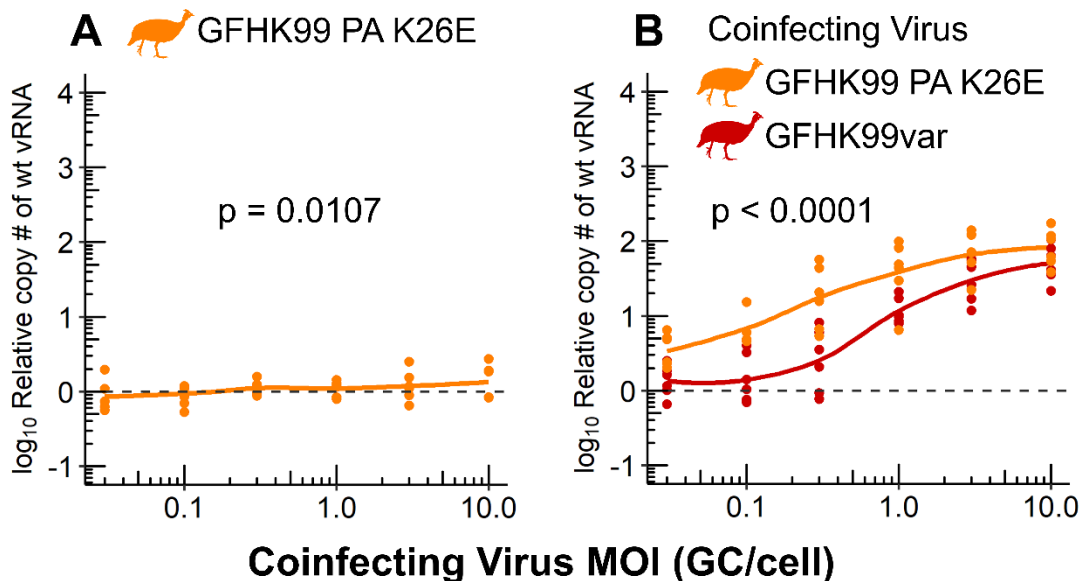
642  
 643 **Fig 1. Intrinsic reliance on multiple infection in mammalian cells is strain dependent.**  
 644 MDCK cells were coinfecting with homologous wt/var viruses of the indicated strain  
 645 backgrounds. The wt viruses had an MOI of 0.005 genome copies (GC)/cell and coinfecting var  
 646 viruses were added with increasing MOI ranging from 0.005 to 10 GC/cell. The fold change in  
 647 wt vRNA copy number, relative to wt only infection (dashed line), is plotted. Results of three to  
 648 six biological replicates derived from one to two independent experiments are plotted and solid  
 649 lines connect the means of the points shown. Each line was evaluated by linear regression to  
 650 determine if the slope was significantly non-zero. Data in panels B and D were reported in(16).



651  
 652 **Fig 2. Coinfection with a virus with low reliance on multiple infection results in a greater**  
 653 **increase in GFHK99 virus replication.** MDCK cells were coinfecting with GFHK99wt virus at  
 654 an MOI of 0.005 GC/cell and increasing doses of the homologous GFHK99var virus (red in each  
 655 panel) or a heterologous MaMN99 (A), NL09 (B), or Pan99 (C) virus. The fold change in  
 656 GFHK99wt vRNA copy number, relative to GFHK99wt-only (dashed line), is plotted. Results of  
 657 six biological replicates derived from two independent experiments are plotted and solid lines  
 658 connect the means. Significance of differences between coinfecting viruses was evaluated by  
 659 two-way ANOVA.

660  
 661 **Coinfection with a virus with low reliance on multiple infection better meets IAV need for**  
 662 **help.**

663 To more rigorously examine how the intrinsic reliance on multiple infection displayed by a  
 664 coinfecting virus modulates its impact on a focal virus, we used a mutant strain of GFHK99  
 665 virus. We previously showed that introduction of a PA K26E mutation into the GFHK99 strain  
 666 reduces reliance on multiple infection (17). We confirmed this phenotype using homologous wt  
 667 and var strains of GFHK99 PA K26E (Fig 3A) and then compared the replication of GFHK99wt  
 668 virus, the focal virus, during coinfection with either the homologous GFHK99var or the  
 669 GFHK99 PA K26E mutant virus. We found that GFHK99wt virus genome replication was  
 670 enhanced significantly more during coinfection with the low reliance GFHK99 PA K26E virus  
 671 compared to coinfection with GFHK99var virus (Fig 3B). These data reinforce the role of  
 672 intrinsic density dependence in defining the benefit conferred by a coinfecting strain.  
 673



674  
 675 **Fig 3. The extent to which a coinfecting virus augments replication of GFHK99 is defined**  
 676 **by its intrinsic reliance on multiple infection.** A) MDCK cells were coinfecting with  
 677 GFHK99wt PA K26E virus at an MOI of 0.005 GC/cell and increasing doses of a homologous  
 678 GFHK99var PA:K26E virus. The fold change in GFHK99wt PA K26E vRNA copy number,  
 679 relative to wt-only (dashed line), is plotted. Results of six biological replicates derived from two  
 680 independent experiments are plotted and solid lines connect the means. The line was evaluated  
 681 by linear regression to determine if the slope was significantly non-zero. B) MDCK cells were

682 coinfecting with GFHK99wt virus at an MOI of 0.005 GC/cell and increasing doses of  
683 GFHK99var or GFHK99var PA K26E virus. The fold change in GFHK99wt vRNA copy,  
684 relative to wt-only (dashed line), is plotted. Results of six biological replicates derived from two  
685 independent experiments are plotted and solid lines connect the means. Significance of  
686 differences between coinfecting viruses were evaluated by two-way ANOVA.

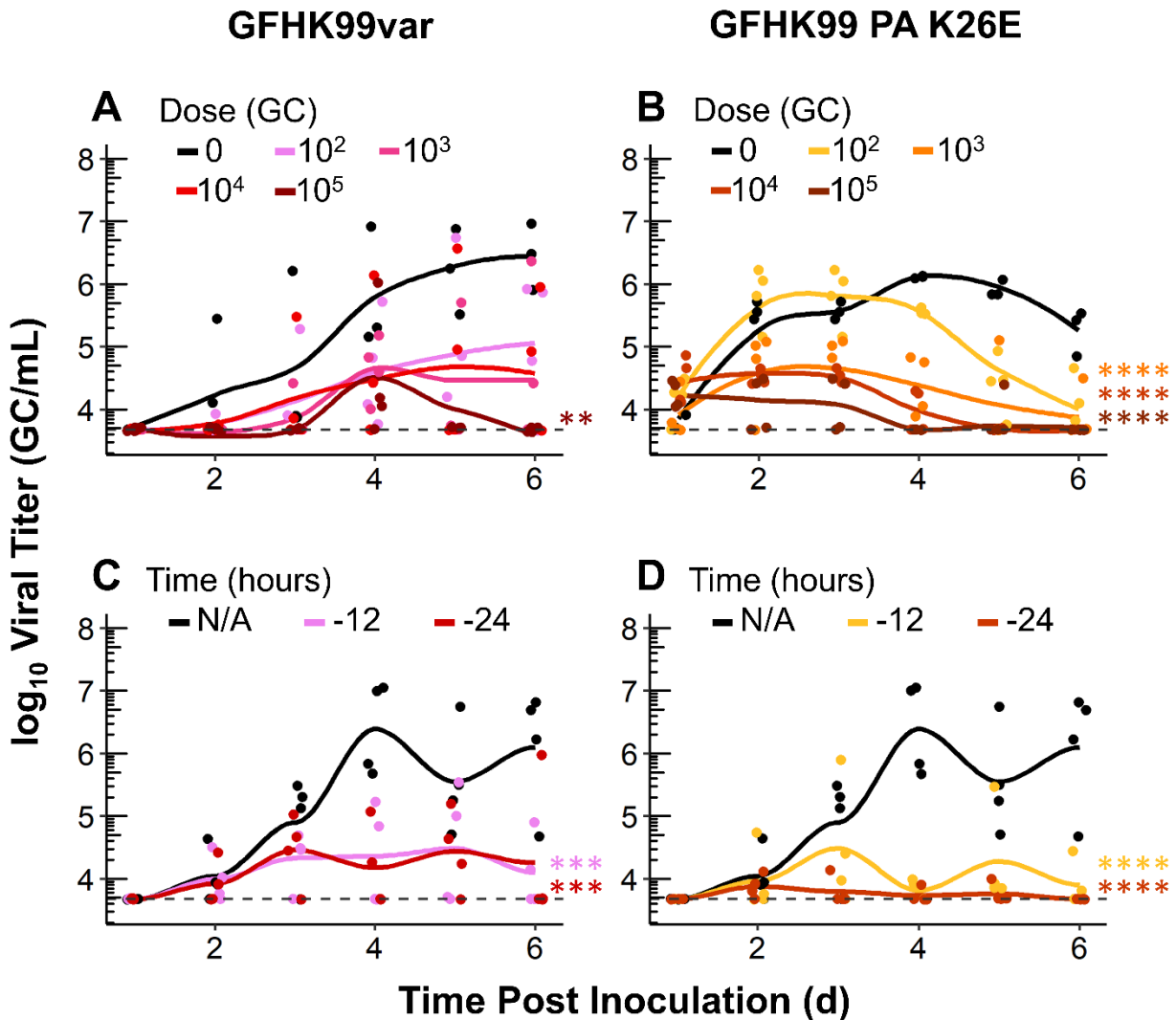
687

### 688 **Competitive virus-virus interactions predominate at the level of the whole host**

689 To test the extent to which the beneficial interaction observed in our cell culture model shapes  
690 viral dynamics in vivo, we used a guinea pig model. Mimicking the experiments in cell culture,  
691 guinea pigs were inoculated simultaneously with a low dose of GFHK99wt virus and increasing  
692 doses of GFHK99var or GFHK99 PA K26E viruses. The titer of GFHK99wt virus was assessed  
693 in daily nasal wash samples. Contrary to expectation, GFHK99wt virus replication over the  
694 course of the infection was suppressed by the coinfecting virus: relative to GFHK99wt-only  
695 controls, GFHK99wt virus vRNA levels were lower during coinfection with either GFHK99var  
696 or GFHK99 PA K26E viruses (Fig 4A,B and S2 Fig).

697 Unlike in cell culture, multiplicity of infection cannot be controlled in vivo and mixing of  
698 coinfecting viruses can be constrained by spatial structure, limiting the potential for cellular  
699 coinfection (8, 19-21). Thus, we reasoned that the failure to detect the beneficial effects of  
700 coinfection in vivo may stem from a paucity of wt-var coinfections occurring under the  
701 conditions used. Based on prior studies (22), we hypothesized that pre-inoculation with  
702 GFHK99var or GFHK99 PA K26E viruses would increase the likelihood of cellular coinfection  
703 with the focal virus by allowing their propagation in the target tissue prior to introduction of  
704 GFHK99wt virus. Thus, in a second experiment, control guinea pigs were left alone and test  
705 guinea pigs were pre-inoculated with GFHK99var or GFHK99 PA K26E virus either 12 h or 24  
706 h before inoculation with GFHK99wt virus, using equivalent doses. Analysis of nasal wash  
707 samples revealed that GFHK99wt virus was able to replicate in each of the four GFHK99wt-only

708 infected guinea pigs, reaching peak titers by day 4 (Fig 4 and S3 Fig). However, GFHK99wt  
 709 virus was not detected in at least one guinea pig in each group co-inoculated with GFHK99var  
 710 virus and two guinea pigs in each group co-inoculated with GFHK99 PA K26E virus (Fig 4 and  
 711 S3 Fig). Furthermore, in line with the previous experiment, the peak titer of GFHK99wt virus  
 712 was greatest in GFHK99wt only inoculated guinea pigs (Fig 4C,D).



713

714 **Fig 4. At the level of the whole host, GFHK99 replication is diminished by coinfection.** A-B)  
 715 Guinea pigs were coinfecting with GFHK99wt at a dose of 10<sup>3</sup> GC and increasing doses of the  
 716 GFHK99var or GFHK99 PA K26E virus. The viral titer of GFHK99wt is plotted and the limit of  
 717 detection is indicated by the dashed line. C-D) Guinea pigs were pre-inoculated with 10<sup>4</sup> GC of  
 718 either GFHK99var (C) or GFHK99 PA K26E (D) virus either 12 or 24 h prior to a dose of 10<sup>4</sup>  
 719 GC of GFHK99wt virus. Results of four guinea pigs per condition are plotted and solid lines

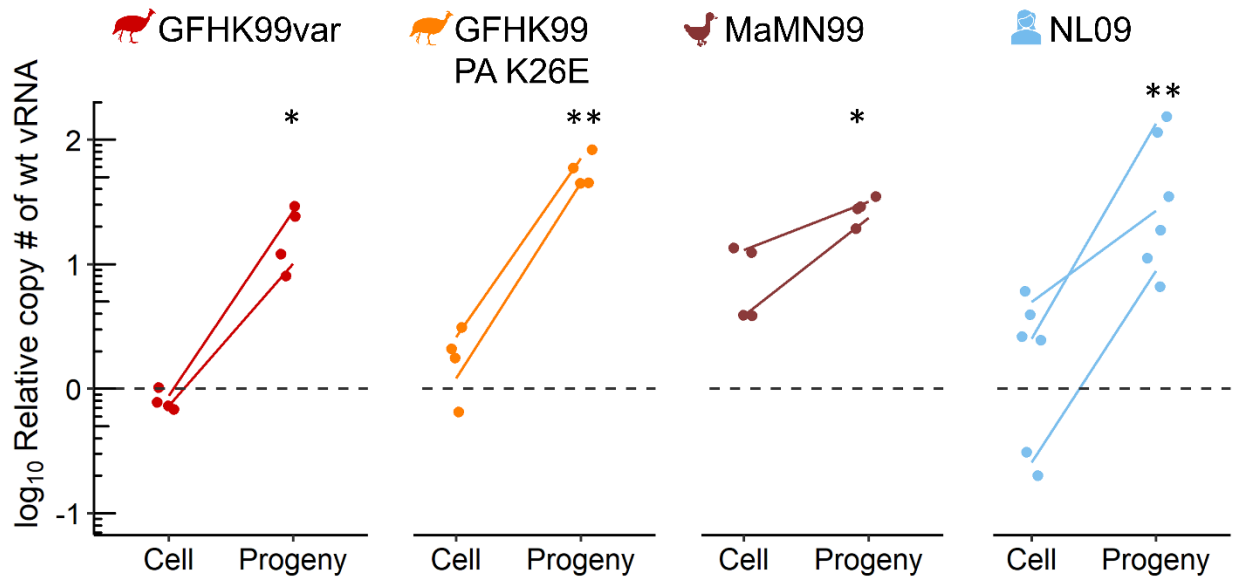
720 connect the means. Significance of differences between coinfecting viruses were evaluated by  
721 two-way ANOVA; \*\*p< 0.01, \*\*\*p< 0.001, \*\*\*\*p< 0.0001.

722  
723 Taken together, these experiments revealed that the dynamics of coinfecting viruses within an  
724 intact animal host are antagonistic. Combined with our cell culture experiments, which indicate  
725 that beneficial interactions occur within individual coinfecting cells, these data suggest that either  
726 the enhancement of focal vRNA replication within cells is not translated into increased viral  
727 release or that antagonistic interactions occurring at a higher spatial scale are predominant.

728

### 729 **Genome incorporation into progeny virions is enhanced during coinfection.**

730 To assess whether beneficial virus-virus interactions within cells results in increased virus  
731 release, we evaluated the impact of coinfection in cultured cells on the abundance of focal viral  
732 genomes in both infected cells and released progeny. Similar to the experiments outlined above,  
733 a low dose GFHK99wt virus and a high dose of a homologous var or heterologous GFHK99 PA  
734 K26E, MaMN99, or NL09 viruses were used. After 24 h, GFHK99wt virus genomes within cells  
735 and in the supernatant containing released progeny virions were quantified. Under the conditions  
736 of MOI used and at this time point, GFHK99wt virus genome replication in the cells was  
737 enhanced during coinfection with MaMN99var and NL09var viruses, but not with GFHK99var  
738 or GFHK99 PA K26E viruses (Fig 5). However, GFHK99wt virus genome incorporation into  
739 progeny virions was enhanced during coinfection with all coinfecting viruses tested. In fact,  
740 enhancement relative to the GFHK99wt only control was greater when considering GFHK99wt  
741 genomes in progeny virions than when considering their levels within cells (Fig 5). Thus, the  
742 beneficial virus-virus interactions observed within cells extend to the release of progeny virions  
743 and appear to do so with a higher than expected efficiency.



744

745 **Fig 5: GFHK99 genome incorporation into progeny virions is enhanced during homologous**  
 746 **and heterologous coinfection.** MDCK cells were coinfecting with GFHK99wt virus at an MOI  
 747 of 1 GC/cell and a homologous GFHK99var or heterologous NL09, MaMN99, or GFHK99var  
 748 PA K26E virus strains at an MOI of 8 GC/cell. The fold change in wt vRNA copy number,  
 749 relative to GFHK99wt-only controls (dashed line), in cells and progeny virions collected in the  
 750 supernatant, is plotted. Results of four to six biological replicates derived from two to three  
 751 independent experiments are plotted and solid lines connect paired means from each experiment.  
 752 Significance of differences between wt-only and coinfecting viruses were evaluated by two-way  
 753 ANOVA and sidak post-hoc analysis; \* $p < 0.015$ , \*\* $p < 0.01$ .  
 754

755 **Asynchrony of coinfection and competition for target cells contribute to suppressive virus-**  
 756 **virus interactions.**

757 The cell culture-based experiments outlined above were all performed under conditions that  
 758 limited viral replication to a single round, an approach that allows tight control of MOI and  
 759 detection of intra-cellular virus-virus interactions. Concomitantly, this strategy eliminates the  
 760 potential for coinfecting viruses to modulate each other's dynamics during spread through the  
 761 cellular population. To better understand the dynamics observed in vivo, we therefore adopted a  
 762 cell culture model in which multiple cycles of viral replication could occur, thereby allowing  
 763 virus-virus interactions at this higher spatial scale.

764

765 Thus, cells were infected at low MOIs in medium conducive to multicycle replication.

766 GFHK99wt virus was used at an MOI of 0.005 GC/cell and GFHK99var or GFHK99 PA K26E

767 virus at an MOI of 0.1 GC/cell. GFHK99wt virus replication was monitored up to 48 h post

768 infection. Consistent with minimal interaction between these relatively small viral populations

769 early in the infection, GFHK99wt virus replication was comparable with or without coinfection

770 up to 24 h post infection (Fig 6 A, B). However, by 36 h or 48 h post infection, a suppressive

771 effect of coinfection was observed (Fig 6 A, B). These data are consistent with observations in

772 guinea pigs, where GFHK99wt replication in coinfecting animals begins to show evidence of

773 suppression at 2 days post inoculation (Fig 4A, B). Together, these data suggest that, during

774 multi-cycle replication, limited availability of susceptible target cells gives rise to potent

775 competition between viruses.

776

777 To further evaluate this concept, we tested the impact of modulating the timing of coinfection on

778 the replication of a focal virus. Here, cells were pre-inoculated at varying times up to 24 h before

779 infection with GFHK99var or GFHK99 PA K26E virus at a relatively high MOI and with

780 GFHK99wt virus at low MOI. The replication of the focal virus, GFHK99wt, was then assessed.

781 This experimental design was chosen to model a situation in which most cells were infected (or

782 indirectly affected) by the coinfecting virus prior to introduction of the focal virus. Thus, the

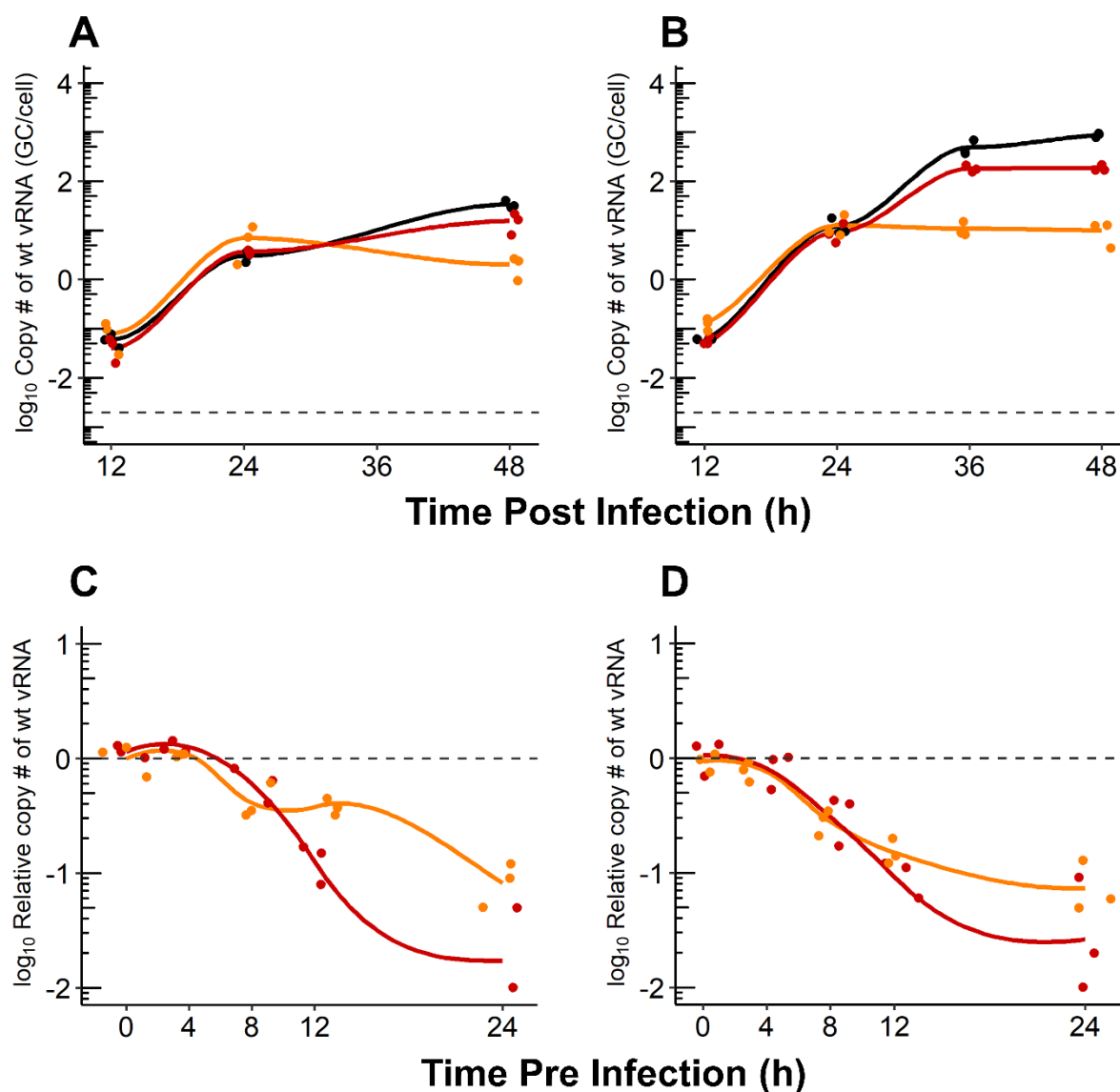
783 potential for cellular coinfection would be high only if cells remain susceptible to infection at the

784 time of GFHK99wt virus introduction. The results show little change to GFHK99wt replication

785 when the coinfecting virus was added up to 4 h before GFHK99wt virus. However, there is a

786 significant decrease in GFHK99wt replication as the interval between infections was increased

787 (Fig 6 C, D). These data indicate that the time window during which beneficial interactions  
 788 within cells can occur is narrow (between 4 h and 8 h in this system). This temporal effect is  
 789 likely to be important in shaping viral dynamics during multi-cycle replication, where the  
 790 introduction of coinfecting viruses into a cell is likely to be asynchronous.



791 Coinfecting Virus:  N/A  GFHK99var  GFHK99 PA K26E

792 **Fig 6. Competitive virus-virus interactions dominate during viral propagation between**  
 793 **cells.** A-B) MDCK cells were coinfecting, under multi-cycle conditions, with GFHK99wt virus at  
 794 an MOI of 0.005 genome copies GC/cell and GFHK99var or GFHK99 PA K26E virus at an  
 795 MOI of 0.1 GC/cell. The titer of GFHK99wt virus is plotted and the limit of detection is

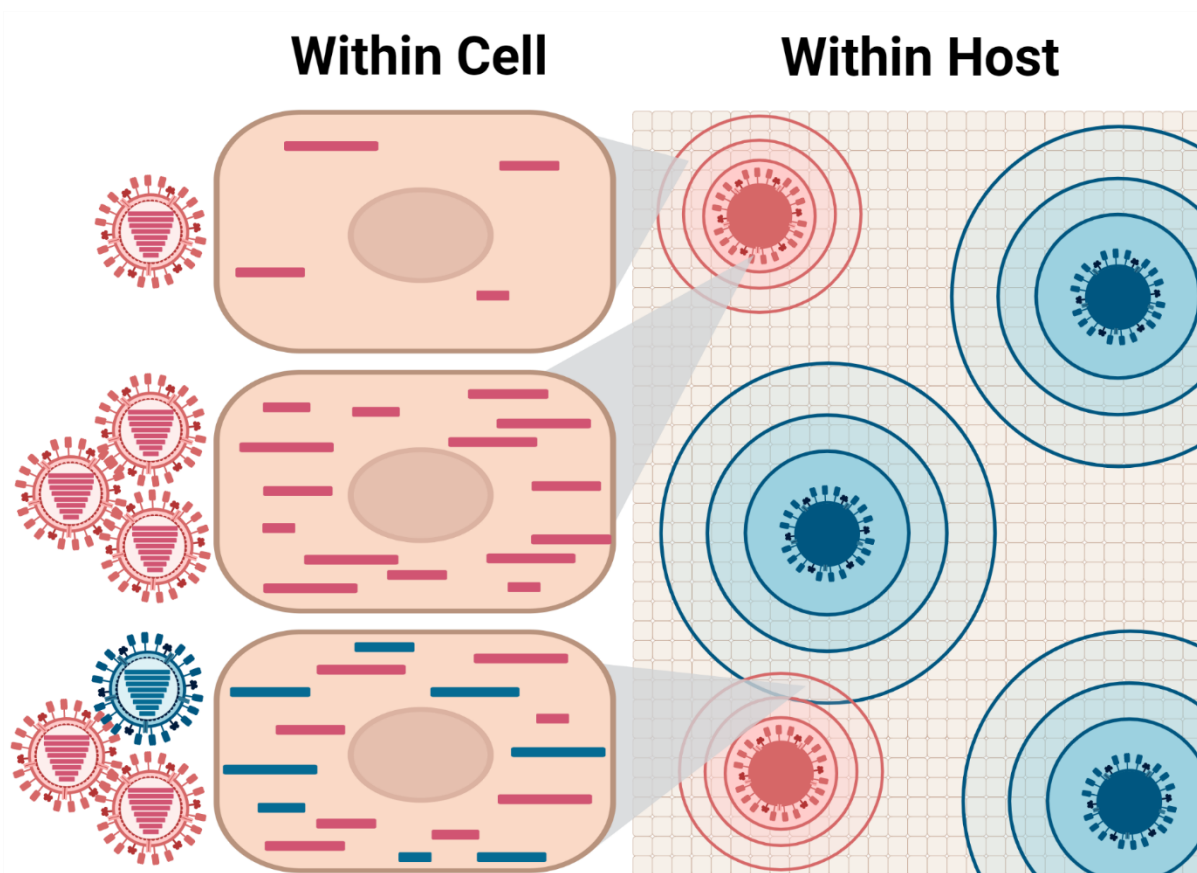
796 indicated by the dashed line. C-D) MDCK cells were pre-infected with GFHK99<sub>var</sub> or GFHK99  
797 PA K26E virus, 0–24 h prior to inoculation with GFHK99<sub>wt</sub> virus. Cells were infected, under  
798 single cycle conditions, at an MOI of 0.005 GC/cell of GFHK99<sub>wt</sub> virus and an MOI of 1 (C) or  
799 10 (D) GC/cell of GFHK99<sub>var</sub> or GFHK99 PA K26E virus. The fold change in GFHK99<sub>wt</sub>  
800 vRNA copy number, relative to GFHK99<sub>wt</sub>-only (dashed line), is plotted. Results of three  
801 biological replicates derived from one experiment are plotted and solid lines connect the means.  
802

## 803 **Discussion**

804 Our results reveal that, within cells, IAV coinfection is strongly beneficial, irrespective of the  
805 coinfecting virus's native host or its homology to the focal strain. Not all coinfecting viruses  
806 confer an equal benefit, however, and the magnitude of the benefit is defined by the coinfecting  
807 strain's intrinsic reliance on multiple infection. Despite this clearly cooperative effect within  
808 cells, virus-virus interactions at the level of the whole host are antagonistic. Examination of this  
809 effect in cell culture suggests that this negative interaction arises at least in part because  
810 coinfecting viruses access potential target cells asynchronously, leading to competition for a  
811 limited supply of susceptible cells.

812 Our data suggest a model in which dominant virus-virus interactions differ at the within-cell and  
813 within-host scales (Fig 7). Within cells, the positive density dependence of IAV replication  
814 extends to heterologous coinfections. However, between cells, the more abundant virus will  
815 typically suppress the propagation of the less abundant virus, likely both through depletion of  
816 susceptible target cells and triggering of host antiviral responses. This suppression in turn will  
817 limit potential for cellular coinfection involving distinct strains. In a natural coinfection,  
818 differences in viral abundance are likely to be the norm, resulting from differential fitness,  
819 differing initial doses or differing times of introduction into the host. Thus, while intra-cellular  
820 interactions within a single viral population are fundamentally important for efficient IAV  
821 propagation (14-16, 23), intra-cellular interactions between distinct IAVs are likely to occur  
822 more rarely and have a relatively minor effect on within-host viral dynamics. At the level of the

823 whole host, the dominant interaction between distinct viral populations appears to be  
 824 antagonistic.



825

826 **Fig 7. Dominant virus-virus interactions differ at the within-cell and within-host scales.**  
 827 Within an infected cell, coinfection with either homologous (pink) or heterologous (blue) IAVs  
 828 enhances the replication and augments the progeny production of a focal virus (pink). However,  
 829 at the within host scale, virus-virus interactions are largely antagonistic as distinct IAV  
 830 populations compete for susceptible target cells. Target cells can be rendered non-susceptible  
 831 through super infection exclusion or as a result of cellular antiviral responses triggered indirectly.  
 832 Within foci, homologous coinfection is highly likely to occur and will promote viral replication.  
 833 Mixed foci are relatively rare, however, owing to differences in initial dose, the timing of  
 834 infection or intrinsic fitness leading to discordance in viral population sizes. Created with  
 835 Biorender.com.

836 For IAVs, cellular coinfection is beneficial in large part because it allows complementation of  
 837 (very common) incomplete viral genomes, increasing the likelihood of productive infection (14,  
 838 15, 24). In addition, cellular coinfection can augment viral yield from productively infected cells

839 by increasing the efficiency of core viral processes (17). Localized viral spread yields areas of  
840 high MOI, providing ample opportunity for coinfection, complementation and enhanced  
841 replication (15, 21).

842

843 At the within-host scale, our data reveal a competitive effect wherein the virus introduced at a  
844 higher dose or an earlier time point suppresses the replication of the other. Similar dynamics  
845 have been reported previously. In particular, superinfection exclusion, in which the replication of  
846 the secondary virus diminished if it is introduced outside of a somewhat narrow time window, is  
847 well documented. The duration of the window observed here (4-8 h) is in line with previous  
848 work (20, 22, 23, 25). Competitive interactions have also been noted in the context of  
849 experiments designed to evaluate the relative fitness of two viral variants (26-30). Conversely, in  
850 our own prior work, we have frequently examined coinfection between wt and var viruses with  
851 well-matched fitness that are introduced simultaneously and at the same dose. In this scenario, wt  
852 and var gene segments are maintained at comparable frequencies throughout the course of  
853 infection (19, 22, 31-33). The juxtaposition of these disparate coinfection dynamics suggests  
854 that virus-virus interactions within a host are very sensitive to differences between coinfecting  
855 strains in their fitness, timing of infection or population size. Effectively, when co-inoculated at  
856 equivalent dose, wt and var behave as a single viral population. By contrast, when divergent  
857 strains are introduced or when homologous viruses are introduced independently, one strain will  
858 typically gain an advantage in the resultant competition for limited resources (or limited time  
859 before the immune system responds).

860

861 The same conditions that allow the beneficial effects of cellular coinfection to occur also support  
862 the replication of defective viral genomes (DVGs). DVGs differ from incomplete viral genomes  
863 in that, instead of missing entire segments, DVGs include segment(s) containing large internal  
864 deletions. These defective segments can be replicated rapidly and packaged in place of a  
865 standard segment, thereby suppressing the production of infectious progeny viruses (34-37).  
866 While we ensure low levels of DVGs in our virus stocks and their effects would therefore be  
867 minimal in assays limited to a single round of viral replication, we would expect the formation of  
868 DVGs *in vivo* (38-40). Prior studies show the presence of DVGs negatively impacts viral  
869 replication (13) and can potentially activate innate immune responses (41). Thus, delivery of  
870 multiple viral genomes to a cell may be predominantly beneficial early on during infection but  
871 may become detrimental as DVGs accumulate. In the context of heterologous coinfection, the  
872 DVGs of the more abundant coinfecting virus may furthermore drive the suppression of the less  
873 abundant strain. While we did not monitor DVG levels in the experiments reported here, these  
874 are hypotheses that can be addressed in future work.

875  
876 Due to the segmented nature of the IAV genome, cellular coinfection yields progeny containing  
877 gene segments from both parent strains. Such reassortment plays an important role in IAV  
878 evolution in many contexts but is especially prominent in IAV expansion into new host species,  
879 including humans (8, 12, 42, 43). The frequency of IAV reassortment involves virus-virus  
880 interactions at every biological scale. Exchange of viral gene segments can only occur – and is  
881 highly efficient – in coinfecting cells (22, 24). Our finding herein that the benefits of cellular  
882 coinfection are high even for poorly matched virus strains indicates that virus-virus interactions  
883 within cells will promote reassortment between IAVs of distinct lineages. However, our

884 observation that virus-virus interactions at the level of the whole host are antagonistic suggests  
885 that the potential for cellular coinfection between independently introduced and/or  
886 phylogenetically distinct strains is likely to be limited. When IAVs derived from distinct host  
887 species coinfect, the virus replicating in its native host is likely to have a fitness advantage (1, 6,  
888 44, 45). However, if the host has pre-existing immunity to the well-adapted strain, this could tip  
889 the balance in favor of the novel virus. Of course, should conditions of timing, dose and fitness  
890 combine to allow reassortment, a chimeric strain that brings together genes well-adapted to the  
891 host with genes encoding novel antigenic determinants can result. In humans, such a virus would  
892 have pandemic potential. Our data nonetheless suggest that the propagation of such a strain  
893 within the host would usually be strongly limited by the already established parental virus  
894 populations. Onward transmission, in turn, would be unlikely owing to tight transmission  
895 bottlenecks (46-48). In sum, the antagonistic nature of virus-virus interactions at the within host  
896 scale is likely a major factor contributing to the rarity of IAV pandemics.

897

898 In conclusion, while the benefits of cellular coinfection extend to heterologous strains, disparate  
899 fitness or conditions of introduction into a host will typically limit the opportunity for  
900 heterologous strains to meet within cells. The need for multiple infection is therefore more likely  
901 to be met within a single viral population. Nevertheless, IAV populations coinfecting the same  
902 host have a significant impact on each other's dynamics owing to competition for limited  
903 resources.

904

905 **Author Contributions**

906 Concept and experimental planning was performed by GD and ACL. Data was collected GD,  
907 KG and KEH and analyzed by GD with input from ACL. Key reagents and intellectual input  
908 were provided by JRS. Manuscript and figures were written, designed, and edited by GD and  
909 ACL. Research funding was acquired by ACL.

910

### 911 **Acknowledgements**

912 This work was supported by funding from NIH/NIAID under the Centers of Excellence for  
913 Influenza Research and Response contract no. 75N93021C00017 to ACL and R01 AI127799 to  
914 ACL.

915

### 916 **Declaration of Interests**

917 The authors declare no conflicts of interest.

918

### 919 **Materials and Methods**

920

### 921 **Ethics statement**

922 Experiments using guinea pigs were conducted in accordance with the Guide for the Care and  
923 Use of Laboratory Animals of the National Institutes of Health. All studies were approved by the  
924 Emory University Institutional Animal Use and Care Committee (protocol PROTO201700595)  
925 and were conducted under animal biosafety level (ABSL-2) containment. Guinea pigs were  
926 humanely euthanized following America Veterinary Medical Association approved guidelines.

927

### 928 **Cells**

929 Madin-Darby Canine Kidney (MDCK) cells, a gift of Daniel Perez at University of Georgia,  
930 were maintained in minimum essential medium (MEM; Gibco) supplemented with Normocin  
931 (InvivoGen) and 10% Fetal Bovine Serum (FBS). Human kidney 293T cells (ATCC CRL-3216)  
932 were maintained in Dulbecco's minimal essential medium (Gibco) supplemented with Normocin  
933 and 10% FBS. Normal Human Bronchial Epithelial (NHBE) cells (Lonza) were maintained in  
934 bronchial epithelial cell growth medium (BEGM) purchased from Lonza. NHBE cells from a  
935 single donor were amplified and differentiated into air-liquid interface cultures as recommended  
936 by Lonza and described in (49). All cells were cultured at 37°C and 5% CO<sub>2</sub> in a humidified  
937 incubator. Cells were tested monthly for mycoplasma contamination during use. Medium used  
938 for IAV infection in each cell line (virus medium) was prepared using the appropriate medium  
939 containing Normocin and 4.3% bovine serum albumin. Infection of NHBE cells was performed  
940 with BEGM in the basolateral chamber. Virus medium or BEGM containing ammonium chloride  
941 was prepared by adding HEPES buffer and NH<sub>4</sub>Cl at final concentrations of 50 mM and 20 mM,  
942 respectively.

943

944

## 945 **Viruses**

946 The strains influenza A/Netherlands/602/2009 (H1N1) and A/Panama/2007/99 (H3N2) are  
947 referred to herein as NL09 and Pan99, respectively. NL09 and Pan99 were handled under BSL2  
948 conditions. The strains influenza A/guinea fowl/Hong Kong/WF10/99 (H9N2) and  
949 A/mallard/Minnesota/199106/99 (H3N8) are referred to herein as GFHK99 and MaMN99,  
950 respectively. GFHK99 and MaMN99 were handled under BSL2 conditions with enhancements

951 as required by the United States Department of Agriculture. Coinfections involving human and  
952 avian IAVs were performed under BSL3 conditions.

953

954 All viruses used were generated using reverse genetics (50, 51). The reverse genetics system for  
955 GFHK99 is in the ambisense vector pDP and was a kind gift of Daniel Perez. The reverse  
956 genetics system for NL09 is in the ambisense vector pHW and was a kind gift of Ron Fouchier.  
957 The reverse genetics systems for Pan99 and MaMN99 viruses were generated in house in the  
958 pDP vector (a gift of Daniel Perez). The GFHK99 PA K26E mutant virus was described in (17)  
959 and was generated by introducing the K26E mutation to the reverse genetics plasmid encoding  
960 the PA gene segment of GFHK99 using site-directed mutagenesis. The specific mutations  
961 introduced are listed in S1 Table. Silent mutations were introduced into var viruses by site-  
962 directed mutagenesis to allow discrimination between wt and var gene segments by site-specific  
963 primers used in ddPCR. The specific mutations introduced into all var viruses are listed in S1  
964 Table.

965

966 Briefly, avian viruses were generated by transfecting 293T cells with eight reverse genetics  
967 plasmids encoding each IAV segment. After 16 h, transfected 293T cells were injected into the  
968 allantoic cavity of 11-day old chicken eggs, incubated at 37°C for 40-48 h, and allantoic fluid  
969 was recovered for use as a passage 1 working virus stock. Mammalian IAVs were generated by  
970 transfecting 293T cells with reverse genetics plasmids encoding each IAV segment. After 16 h,  
971 transfected 293T cells were then cocultured with MDCK cells at 37°C for 40-48 h. Collected  
972 supernatants were then propagated in MDCK cells from low MOI to generate a working virus  
973 stock. Every virus stock was tested for defective viral genomes (DVGs) as described previously

974 (52) (S4 Fig). We define ‘low DVG content’ as follows: the ratio of copy number for terminal  
975 and internal targets (T:I) is  $<2.0$  for each of the PB2, PB1 and PA gene segments. Any stocks not  
976 meeting this criterion were regenerated.

977

978 Viral concentrations are reported in genome copies per mL throughout this work for two reasons.  
979 First, use of a molecular assay for viral quantification allows differentiation of IAVs present in a  
980 mixture. Second, this approach ensures consistency in the limit of detection across virus strains.  
981 In this work and in prior studies, we have found that viral infectivity varies with MOI and the  
982 efficiency with which a single virus particle initiates infection varies widely across strains. As a  
983 result, titration of infectious units at limiting dilution by plaque assay or TCID<sub>50</sub> assay measures  
984 differing sub-populations for different IAV strains.

985

### 986 **Synchronized, single- and multi-cycle infections**

987 Synchronization was used to coordinate the timing of viral entry into cells and was carried out as  
988 follows: The monolayer of cells was washed 3x with cold PBS and placed on ice. Chilled virus  
989 inoculum was added to each well and kept at 4°C for 45 min with rocking to allow time for IAV  
990 attachment but not entry. After that time, the inoculum was aspirated, each well was washed 3x  
991 with cold PBS. Warmed virus medium without trypsin was added to allow entry and this time is  
992 defined as  $t=0$ . Cultures were incubated at 37°C. Single-cycle conditions were designed to  
993 prevent released progeny virus from initiating a subsequent round of infection. A single cycle of  
994 infection was imposed by replacing virus medium with virus medium containing NH<sub>4</sub>Cl and  
995 HEPES solution at final concentrations of 20 mM and 50 mM, respectively, at 3 h post-infection.  
996 In the case of NHBE cells, this medium was added to the basolateral chamber only. Addition of

997 NH<sub>4</sub>Cl and HEPES to the medium prevents the acidification of endosomes, thereby blocking  
998 infection (42). For multi-cycle infections, L-1-tosylamido-2-phenylethyl chloromethyl ketone  
999 (TPCK)-treated trypsin was added to virus medium at 0 h post-infection at a final concentration  
1000 of 1 μM, and NH<sub>4</sub>Cl and HEPES were not added. Addition of TPCK-treated trypsin allows  
1001 cleavage activation of the HA protein on released virus, which is required for infection.

1002

### 1003 **Detection of virus-virus interactions within cells**

1004 MDCK cells were seeded into 12-well plates at  $4 \times 10^5$  cells per well 24 h prior to infection.  
1005 NHBE cells were cultured at an air-liquid interface as previously described (49). Each infection  
1006 took place under synchronized, single-cycle conditions. For homologous coinfections, triplicate  
1007 wells were inoculated with wt virus at an MOI of 0.005 genome copies (GC)/cell in MDCK  
1008 cells, or 0.5 GC/cell in NHBE cells and increasing doses of a matched var virus. For  
1009 heterologous coinfections, triplicate wells were inoculated with GFHK99wt virus at an MOI of  
1010 0.005 GC/cell in MDCK cells, or 0.5 GC/cell in NHBE cells, and increasing doses of  
1011 MaMN99wt, NL09var, or Pan99wt viruses. At 12 h post infection, virus medium containing  
1012 NH<sub>4</sub>Cl and HEPES was removed, cell surfaces were washed 3x with PBS, and cells were  
1013 harvested for RNA extraction using the Qiagen RNeasy mini kit.

1014

### 1015 **Impact of intracellular virus-virus interactions on released viral progeny**

1016 MDCK cells were seeded into T75 flasks at  $5 \times 10^6$  cells per flask 24 h prior to infection. Each  
1017 infection took place under synchronized, single-cycle conditions. Duplicate flasks were  
1018 inoculated with GFHK99wt virus at an MOI of 1 GC/cell and either PBS, homologous  
1019 GFHK99var virus, or heterologous MaMN99wt, NL09var, or Pan99wt viruses at an MOI of 8

1020 GC/cell. At 24 h post infection medium (containing viral progeny) was collected separately from  
1021 cells. Cells were washed 3x with PBS and harvested using the Qiagen RNeasy mini kit and  
1022 protocol instructions. Collected medium was centrifuged (Thermofisher Sorvall ST 16R  
1023 Centrifuge) at 3000 rpm for 10 min at 4°C to remove cell debris. The resultant supernatant was  
1024 transferred into a Beckman ultracentrifuge tube and centrifuged (Beckman Coulter Optima™  
1025 XL-100K Ultracentrifuge) at 10,000 rpm for 30 min at 4°C to further clarify the sample of cell  
1026 debris. The final supernatant was then transferred into a new ultracentrifuge tube. A cushion of 5  
1027 mL 30% sucrose in NTE buffer[1 M NaCl, 0.1 M Tris, 0.01 M EDTA, pH 7.4] as injected into  
1028 the bottom of the tube and the sample was centrifuged (Beckman Coulter Optima™ XL-100K  
1029 Ultracentrifuge) at 25,000 rpm for 2 h at 4°C. The resultant viral pellet was resuspended in PBS  
1030 and RNA extracted using the Qiagen Viral RNA mini kit and protocol instructions.

1031

### 1032 **Monitoring virus-virus interactions in guinea pigs**

1033 Female Hartley strain guinea pigs weighing 300-350 g were obtained from Charles River  
1034 Laboratories (Wilmington, MA) and housed by Emory University's Department of Animal  
1035 resources. Prior to intranasal inoculation, nasal lavage, and euthanasia, guinea pigs were  
1036 anesthetized by intramuscular injection with 30 mg/kg ketamine and 4 mg/kg xylazine. Guinea  
1037 pigs were inoculated intranasally with IAV in 300 µl PBS. Daily nasal washes were performed  
1038 up to 6 d post GFHK99wt inoculation. Briefly, with the animal's nose suspended in a downward  
1039 orientation over a Petri dish, 1 mL PBS was instilled into the nares in 200 µl increments and  
1040 allowed to drop back out. Liquid was pooled into a 1.5 mL tube, aliquoted and stored at -80°C.

1041

### 1042 **Quantification of vRNA**

1043 RNA was extracted from cells and viral samples using the Qiagen RNeasy mini kit and the  
1044 Qiagen Viral RNA mini kit, respectively, using included protocol instructions. Extracted vRNA  
1045 was reverse transcribed using a 1:1 ratio of universal influenza primers (53)(S2 Table) and  
1046 Maxima RT (Thermofisher) per protocol instructions. Droplet digital PCR (ddPCR) was  
1047 performed on the resultant cDNA using the QX200™ ddPCR™ EvaGreen Supermix (Bio-Rad)  
1048 and virus specific primers targeting the NP segment (final concentration 200 nM) (S2 Table).  
1049 Copy numbers of the wt virus present in coinfecting samples were normalized to those detected in  
1050 wt only control infections.

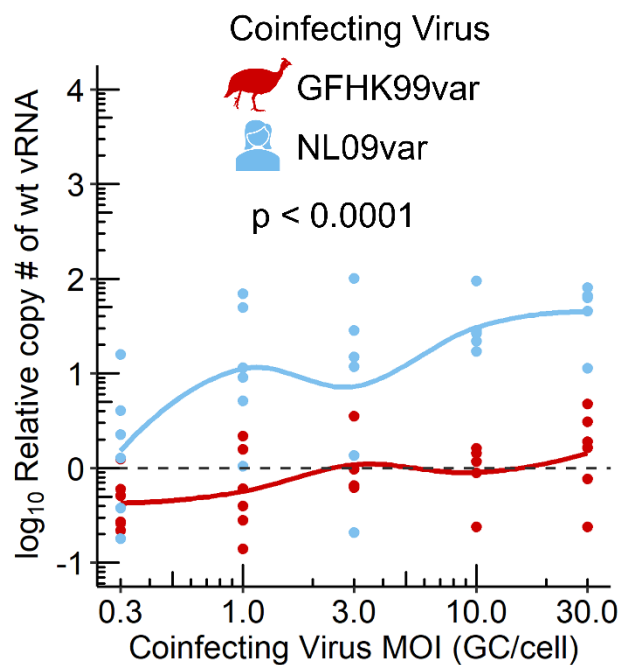
1051

1052 **Statistical analyses:**

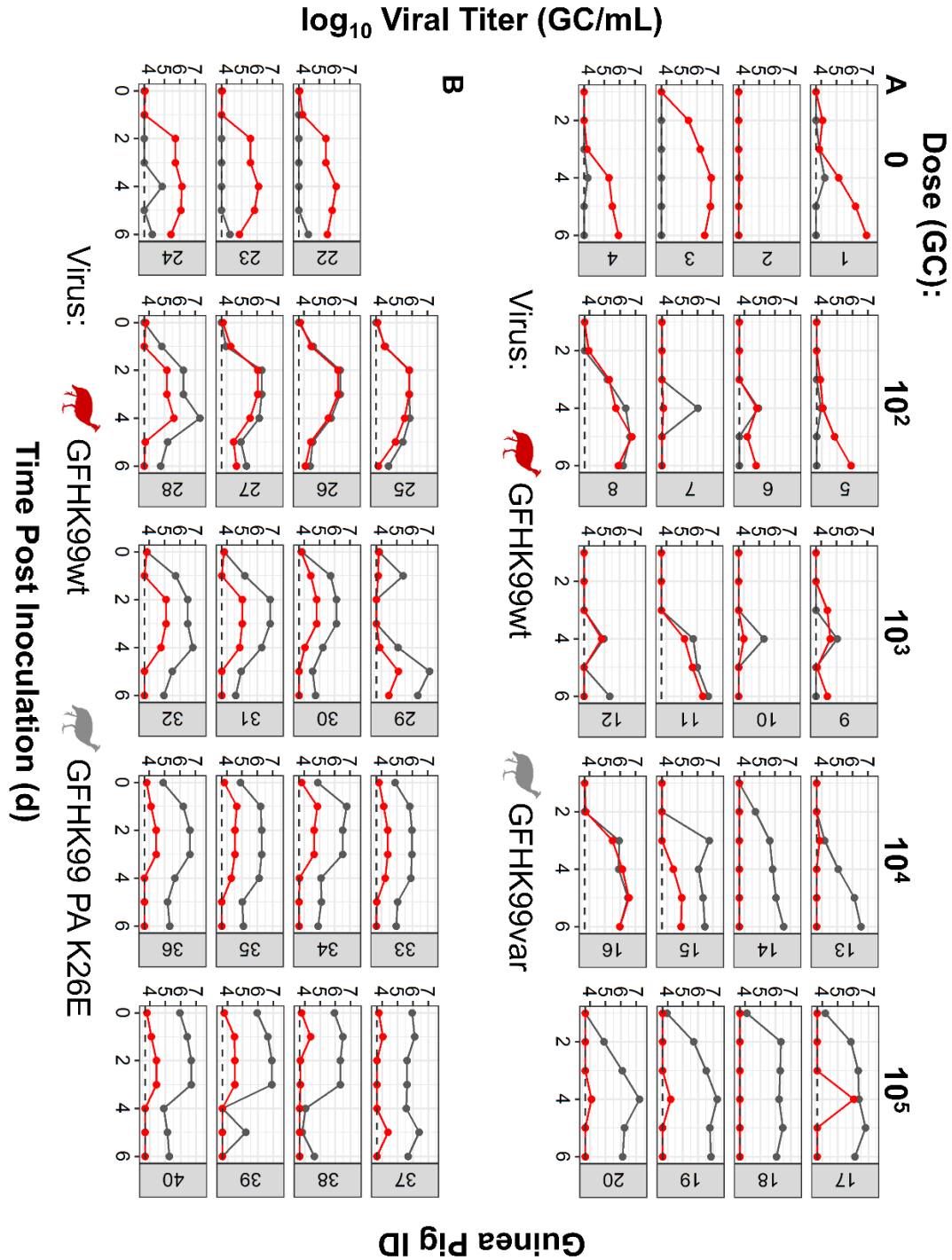
1053 All statistical analyses were performed in R (version 1.3.959). Log transformed values for  
1054 genome copy numbers and the mean of technical replicates were used for statistical analyses.

1055

## 1056 Supplemental Information

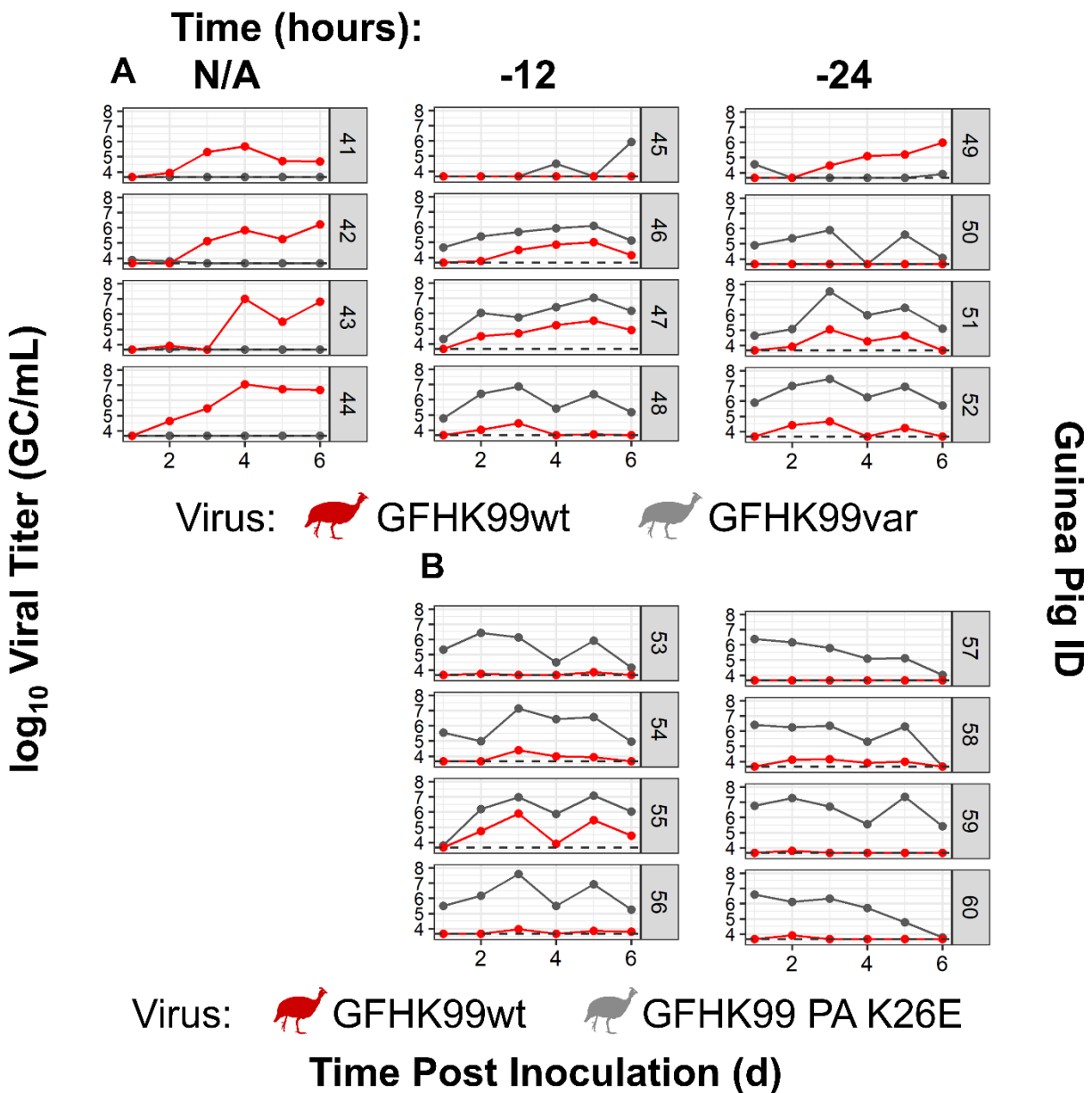


1057  
 1058 **S1 Fig. Coinfection with NL09 strongly enhances GFHK99wt replication in NHBE cells.**  
 1059 (Related to Fig 2.) NHBE cells were infected with GFHK99wt virus at an MOI of 0.5 genome  
 1060 copies (GC)/cell and increasing doses of the homologous GFHK99var virus or the heterologous  
 1061 NL09 virus. The fold change in GFHK99wt vRNA copy number, relative to GFHK99wt-only  
 1062 control (dashed line), is plotted. Results of six biological replicates derived from two  
 1063 independent experiments are plotted and solid lines connect the means. Significance of  
 1064 differences between results obtained with the differing coinfecting viruses were evaluated by  
 1065 two-way ANOVA.  
 1066



1067

1068 **S2 Fig. At the level of the whole host, GFHK99 replication is suppressed by coinfection.**  
 1069 (Related to Fig 5A). Guinea pigs were infected with GFHK99wt at a dose of 10<sup>3</sup> GC and  
 1070 increasing doses of GFHK99var (A) or GFHK99 PA K26E (B) virus. The viral titer in nasal  
 1071 washes collected from each guinea pig is plotted and the limit of is indicated by the dashed line.  
 1072 Guinea pig ID numbers are shown in grey boxes appended to each facet.



1073

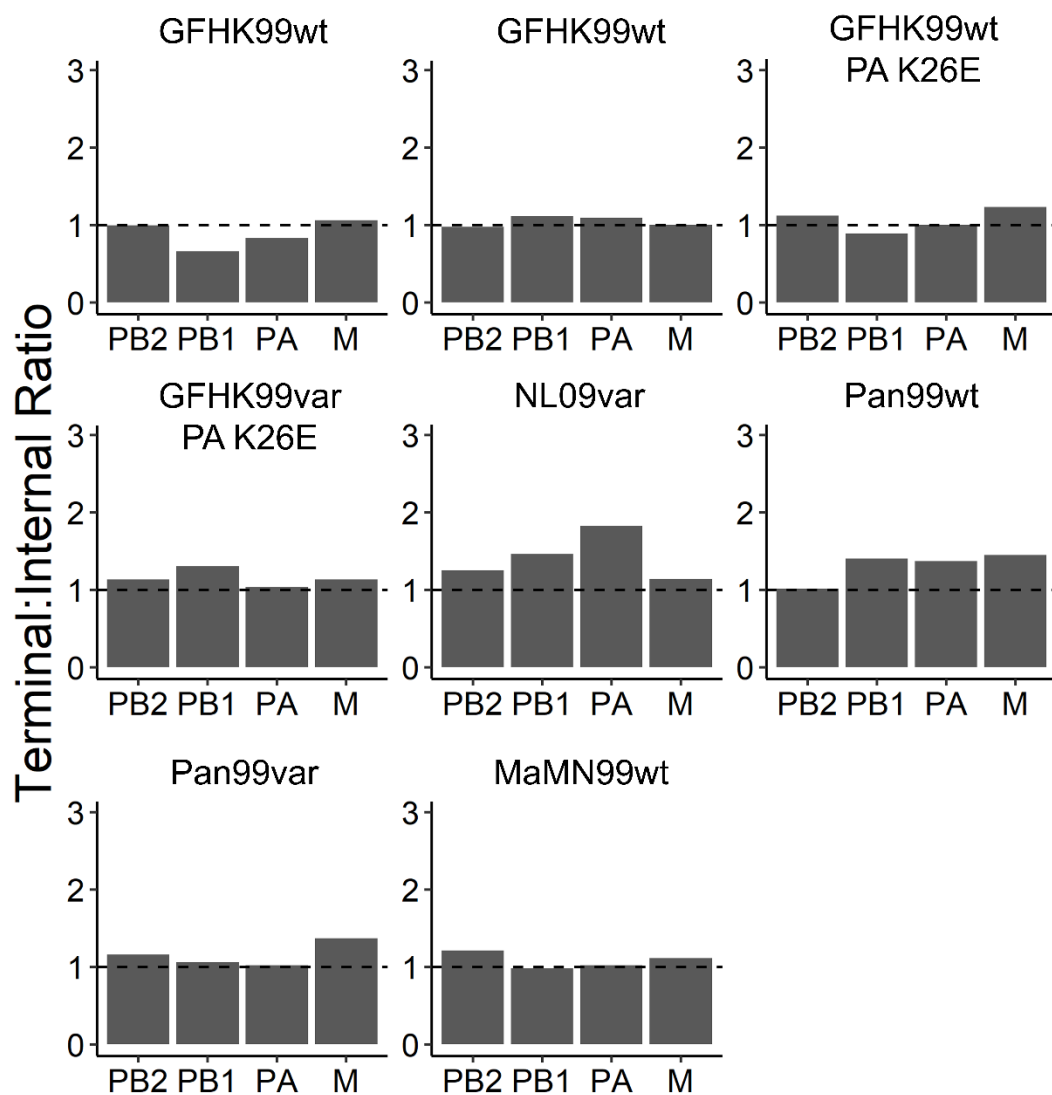
1074 **S3 Fig. At the level of the whole host, GFHK99 replication is suppressed by prior IAV**  
 1075 **infection.** (Related to Figure 4B). Guinea pigs were pre-inoculated with  $10^4$  GC of either  
 1076 GFHK99var (A) or GFHK99 PA K26E (B) virus either 12 or 24 h prior to a dose of  $10^4$  GC of  
 1077 GFHK99wt virus. The viral titer in nasal washes is plotted and the limit of detection is indicated  
 1078 by the dashed line. Guinea pig ID numbers are shown in grey boxes appended to each facet.  
 1079

1080 **S1 Table. Genotypes of modified viruses.**

	<b>PB2</b>	<b>PB1</b>	<b>PA</b>	<b>HA</b>	<b>NP</b>	<b>NA</b>	<b>M</b>	<b>NS</b>
<b>GFHK99var2</b>	A300G, A303T, T306C, G459C, T461A, T467T	T282C, T285C, A288G, A420G, T426C, C432T	A351G, C354T, C357T, T501G, C504T, C507T	A338G, A344C, A351C, A432G, T435A, C438T	A345G, G351A, A354G, A486T, C489T, A495G	A424G, T430A, G433A, A583G, G586C, G589C	G340A, A343G, A349G, G439A, C442T, A445G	C386T, G389A, A392G, A479G, G482C, A488G
<b>NL09var</b>	C273T	T288C	C360T	C305T	A351G	G336A	G295A	C341T
<b>Pan99var0</b>	A345T, C360T	A540G	G333A, A342G	T308A, C311A, C314T, A464T, C467G, T470A	C537T, T538A, C539G, C612G, G615A	C418G, T421A, A424C	G586A	A329T, A335T, C341G
<b>GFHK99wt PA K26E</b>	---	---	A100G, A102G	---	---	---	---	---
<b>GFHK99var2 PA K26E</b>	A300G, A303T, T306C, G459C, T461A, T467T	T282C, T285C, A288G, A420G, T426C, C432T	A100G, A102G, A351G, C354T, C357T, T501G, C504T, C507T	---	A345G, G351A, A354G, A486T, C489T, A495G	A424G, T430A, G433A, A583G, G586C, G589C	G340A, A343G, A349G, G439A, C442T, A445G	C386T, G389A, A392G, A479G, G482C, A488G

1081

1082



1083

1084 **S4 Fig. Quantification of defective viral genomes in virus stocks.** Levels of defective viral  
 1085 genomes (DVGs) were quantified by ddPCR using primers targeting the terminal and internal  
 1086 regions of the PB2, PB1, PA, and M gene segments. Ratios of terminal to internal copies that are  
 1087 <2.0 indicate low DVG content. Virus stocks tested are named above each facet. Two different  
 1088 stocks of GFHK99wt virus were used.

1089

1090 **S2 Table. Primers for the quantification of vRNA by ddPCR.**

<b>Universal influenza Reverse Transcription Primers</b>	
Univ.F(A)+6	GCGCGCAGCAAAAGCAGG
Univ.F(G)+6	GCGCGCAGCGAAAGCAGG
<b>GFHK99wt, GFHK99wt PA K26E Virus Primers</b>	
WF10wt NP 336 F	GAAGGAGAGACGGGAAATG
WF10wt NP 505 R	GGCTCTTGTCTCTGGTATG
<b>GFHK99var<sub>2</sub>, GFHK99var<sub>2</sub> PA K26E Virus Primers</b>	
WF10help NP 388 F	GAAGGAGGGACGGAAAGT
WF10help NP 505R	GGGCTCTTGTCCTCTGATAA
<b>NL09var Virus Primers</b>	
NL09 NP 309 F	CCCTAAGAAAACAGGAGGACCC
NL09 NP 411 R	TTGGCGCCAAACTCTCCTTA
<b>Pan99wt Virus Primers</b>	
Pan99wt NP 520 F	ATGGATCCCAGAATGTGCTC
Pan99wt NP 625 R	TCAGCTCCATTGTC
<b>Pan99var Virus Primers</b>	
Pan99var0 NP 520 F	ATGGATCCCAGAATGTGTAG
Pan99var0 NP 625 R	TCAGCTCCATAGTG
<b>MaMN99wt Virus Primers</b>	
MN99 NP 378 F	CGACAAAGAAGAGATCAGAAGGA
MN99 NP 457 R	TCATCAAATGGGTGAGACCA

1091

1092

1093

1094

1095 **References Cited**

- 1096 1. Webster RG, Bean WJ, Gorman OT, Chambers TM, Kawaoka Y. 1992. Evolution and  
1097 ecology of influenza A viruses. *Microbiol Rev* 56:152-79.
- 1098 2. Scholtissek C. 1994. Source for influenza pandemics. *Eur J Epidemiol* 10:455-8.
- 1099 3. Cox NJ, Subbarao K. 2000. Global epidemiology of influenza: past and present. *Annu*  
1100 *Rev Med* 51:407-21.
- 1101 4. Kilbourne ED. 2006. Influenza pandemics of the 20th century. *Emerg Infect Dis* 12:9-14.
- 1102 5. Trifonov V, Khiabani H, Greenbaum B, Rabadan R. 2009. The origin of the recent  
1103 swine influenza A(H1N1) virus infecting humans. *Euro Surveill* 14.
- 1104 6. Sorrell EM, Schrauwen EJ, Linster M, De Graaf M, Herfst S, Fouchier RA. 2011.  
1105 Predicting 'airborne' influenza viruses: (trans-) mission impossible? *Curr Opin Virol*  
1106 1:635-42.
- 1107 7. Steel J, Lowen AC. 2014. Influenza A virus reassortment. *Curr Top Microbiol Immunol*  
1108 385:377-401.
- 1109 8. Lowen AC. 2017. Constraints, Drivers, and Implications of Influenza A Virus  
1110 Reassortment. *Annu Rev Virol* 4:105-121.
- 1111 9. Desselberger U, Nakajima K, Alfino P, Pedersen FS, Haseltine WA, Hannoun C, Palese  
1112 P. 1978. Biochemical evidence that "new" influenza virus strains in nature may arise by  
1113 recombination (reassortment). *Proc Natl Acad Sci U S A* 75:3341-5.
- 1114 10. Phipps KL, Marshall N, Tao H, Danzy S, Onuoha N, Steel J, Lowen AC. 2017. Seasonal  
1115 H3N2 and 2009 Pandemic H1N1 Influenza A Viruses Reassort Efficiently but Produce  
1116 Attenuated Progeny. *J Virol* 91.

- 1117 11. Villa M, Lässig M. 2017. Fitness cost of reassortment in human influenza. *PLoS Pathog*  
1118 13:e1006685.
- 1119 12. Ma EJ, Hill NJ, Zabilansky J, Yuan K, Runstadler JA. 2016. Reticulate evolution is  
1120 favored in influenza niche switching. *Proc Natl Acad Sci U S A* 113:5335-9.
- 1121 13. Leeks A, Sanjuán R, West SA. 2019. The evolution of collective infectious units in  
1122 viruses. *Virus Res* 265:94-101.
- 1123 14. Brooke CB, Ince WL, Wrammert J, Ahmed R, Wilson PC, Bennink JR, Yewdell JW.  
1124 2013. Most influenza A virions fail to express at least one essential viral protein. *J Virol*  
1125 87:3155-62.
- 1126 15. Jacobs NT, Onuoha NO, Antia A, Steel J, Antia R, Lowen AC. 2019. Incomplete  
1127 influenza A virus genomes occur frequently but are readily complemented during  
1128 localized viral spread. *Nat Commun* 10:3526.
- 1129 16. Phipps KL, Ganti K, Jacobs NT, Lee CY, Carnaccini S, White MC, Manandhar M,  
1130 Pickett BE, Tan GS, Ferreri LM, Perez DR, Lowen AC. 2020. Collective interactions  
1131 augment influenza A virus replication in a host-dependent manner. *Nat Microbiol*  
1132 5:1158-1169.
- 1133 17. Shartouny JR, Lee CY, Delima GK, Lowen AC. 2022. Beneficial effects of cellular  
1134 coinfection resolve inefficiency in influenza A virus transcription. *PLoS Pathog*  
1135 18:e1010865.
- 1136 18. García-Sastre A. 2011. Induction and evasion of type I interferon responses by influenza  
1137 viruses. *Virus Res* 162:12-8.

- 1138 19. Richard M, Herfst S, Tao H, Jacobs NT, Lowen AC. 2018. Influenza A Virus  
1139 Reassortment Is Limited by Anatomical Compartmentalization following Coinfection via  
1140 Distinct Routes. *J Virol* 92.
- 1141 20. Sims A, Tornaletti LB, Jasim S, Pirillo C, Devlin R, Hirst J, Loney C, Wojtus J, Sloan E,  
1142 Thorley L, Boutell C, Roberts E, Hutchinson E. 2022. Superinfection exclusion creates  
1143 spatially distinct influenza virus populations. *bioRxiv*  
1144 doi:10.1101/2022.06.06.494939:2022.06.06.494939.
- 1145 21. Ganti K, Bagga A, Carnaccini S, Ferreri LM, Geiger G, Joaquin Caceres C, Seibert B, Li  
1146 Y, Wang L, Kwon T, Li Y, Morozov I, Ma W, Richt JA, Perez DR, Koelle K, Lowen  
1147 AC. 2022. Influenza A virus reassortment in mammals gives rise to genetically distinct  
1148 within-host subpopulations. *Nat Commun* 13:6846.
- 1149 22. Marshall N, Priyamvada L, Ende Z, Steel J, Lowen AC. 2013. Influenza virus  
1150 reassortment occurs with high frequency in the absence of segment mismatch. *PLoS*  
1151 *Pathog* 9:e1003421.
- 1152 23. Brooke CB, Ince WL, Wei J, Bennink JR, Yewdell JW. 2014. Influenza A virus  
1153 nucleoprotein selectively decreases neuraminidase gene-segment packaging while  
1154 enhancing viral fitness and transmissibility. *Proc Natl Acad Sci U S A* 111:16854-9.
- 1155 24. Fonville JM, Marshall N, Tao H, Steel J, Lowen AC. 2015. Influenza Virus Reassortment  
1156 Is Enhanced by Semi-infectious Particles but Can Be Suppressed by Defective Interfering  
1157 Particles. *PLoS Pathog* 11:e1005204.
- 1158 25. Sun J, Brooke CB. 2018. Influenza A Virus Superinfection Potential Is Regulated by  
1159 Viral Genomic Heterogeneity. *mBio* 9.

- 1160 26. Ince WL, Gueye-Mbaye A, Bennink JR, Yewdell JW. 2013. Reassortment complements  
1161 spontaneous mutation in influenza A virus NP and M1 genes to accelerate adaptation to a  
1162 new host. *J Virol* 87:4330-8.
- 1163 27. Ferreri LM, Geiger G, Seibert B, Obadan A, Rajao D, Lowen AC, Perez DR. 2022. Intra-  
1164 and inter-host evolution of H9N2 influenza A virus in Japanese quail. *Virus Evol*  
1165 8:veac001.
- 1166 28. Mhamdi Z, Carbonneau J, Venable MC, Baz M, Abed Y, Boivin G. 2021. Replication  
1167 and transmission of an influenza A(H3N2) virus harboring the polymerase acidic I38T  
1168 substitution, in guinea pigs. *J Gen Virol* 102.
- 1169 29. Lee LY, Zhou J, Koszalka P, Frise R, Farrukee R, Baba K, Miah S, Shishido T, Galiano  
1170 M, Hashimoto T, Omoto S, Uehara T, Mifsud EJ, Collinson N, Kuhlbusch K, Clinch B,  
1171 Wildum S, Barclay WS, Hurt AC. 2021. Evaluating the fitness of PA/I38T-substituted  
1172 influenza A viruses with reduced baloxavir susceptibility in a competitive mixtures ferret  
1173 model. *PLoS Pathog* 17:e1009527.
- 1174 30. Dibben O, Crowe J, Cooper S, Hill L, Schewe KE, Bright H. 2021. Defining the root  
1175 cause of reduced H1N1 live attenuated influenza vaccine effectiveness: low viral fitness  
1176 leads to inter-strain competition. *NPJ Vaccines* 6:35.
- 1177 31. Ganti K, Bagga A, DaSilva J, Shepard SS, Barnes JR, Shriner S, Koelle K, Lowen AC.  
1178 2021. Avian Influenza A Viruses Reassort and Diversify Differently in Mallards and  
1179 Mammals. *Viruses* 13.
- 1180 32. Tao H, Li L, White MC, Steel J, Lowen AC. 2015. Influenza A Virus Coinfection  
1181 through Transmission Can Support High Levels of Reassortment. *J Virol* 89:8453-61.

- 1182 33. Tao H, Steel J, Lowen AC. 2014. Intra-host dynamics of influenza virus reassortment. *J*  
1183 *Virol* 88:7485-92.
- 1184 34. Nayak DP, Chambers TM, Akkina RK. 1985. Defective-interfering (DI) RNAs of  
1185 influenza viruses: origin, structure, expression, and interference. *Curr Top Microbiol*  
1186 *Immunol* 114:103-51.
- 1187 35. Alnaji FG, Brooke CB. 2020. Influenza virus DI particles: Defective interfering or  
1188 delightfully interesting? *PLoS Pathog* 16:e1008436.
- 1189 36. Vignuzzi M, López CB. 2019. Defective viral genomes are key drivers of the virus-host  
1190 interaction. *Nat Microbiol* 4:1075-1087.
- 1191 37. Ziegler CM, Botten JW. 2020. Defective Interfering Particles of Negative-Strand RNA  
1192 Viruses. *Trends Microbiol* 28:554-565.
- 1193 38. Saira K, Lin X, DePasse JV, Halpin R, Twaddle A, Stockwell T, Angus B, Cozzi-Lepri  
1194 A, Delfino M, Dugan V, Dwyer DE, Freiberg M, Horban A, Losso M, Lynfield R,  
1195 Wentworth DN, Holmes EC, Davey R, Wentworth DE, Ghedin E. 2013. Sequence  
1196 analysis of in vivo defective interfering-like RNA of influenza A H1N1 pandemic virus. *J*  
1197 *Virol* 87:8064-74.
- 1198 39. Vasilijevic J, Zamarreño N, Oliveros JC, Rodriguez-Frandsen A, Gómez G, Rodriguez G,  
1199 Pérez-Ruiz M, Rey S, Barba I, Pozo F, Casas I, Nieto A, Falcón A. 2017. Reduced  
1200 accumulation of defective viral genomes contributes to severe outcome in influenza virus  
1201 infected patients. *PLoS Pathog* 13:e1006650.
- 1202 40. Lui WY, Yuen CK, Li C, Wong WM, Lui PY, Lin CH, Chan KH, Zhao H, Chen H, To  
1203 KKW, Zhang AJX, Yuen KY, Kok KH. 2019. SMRT sequencing revealed the diversity

- 1204 and characteristics of defective interfering RNAs in influenza A (H7N9) virus infection.  
1205 *Emerg Microbes Infect* 8:662-674.
- 1206 41. Yount JS, Gitlin L, Moran TM, López CB. 2008. MDA5 participates in the detection of  
1207 paramyxovirus infection and is essential for the early activation of dendritic cells in  
1208 response to Sendai Virus defective interfering particles. *J Immunol* 180:4910-8.
- 1209 42. Yoshimura A, Ohnishi S. 1984. Uncoating of influenza virus in endosomes. *J Virol*  
1210 51:497-504.
- 1211 43. Smith GJ, Vijaykrishna D, Bahl J, Lycett SJ, Worobey M, Pybus OG, Ma SK, Cheung  
1212 CL, Raghwani J, Bhatt S, Peiris JS, Guan Y, Rambaut A. 2009. Origins and evolutionary  
1213 genomics of the 2009 swine-origin H1N1 influenza A epidemic. *Nature* 459:1122-5.
- 1214 44. Matrosovich M, Tuzikov A, Bovin N, Gambaryan A, Klimov A, Castrucci MR, Donatelli  
1215 I, Kawaoka Y. 2000. Early alterations of the receptor-binding properties of H1, H2, and  
1216 H3 avian influenza virus hemagglutinins after their introduction into mammals. *J Virol*  
1217 74:8502-12.
- 1218 45. Taubenberger JK, Kash JC. 2010. Influenza virus evolution, host adaptation, and  
1219 pandemic formation. *Cell Host Microbe* 7:440-51.
- 1220 46. Varble A, Albrecht RA, Backes S, Crumiller M, Bouvier NM, Sachs D, García-Sastre A,  
1221 tenOever BR. 2014. Influenza A virus transmission bottlenecks are defined by infection  
1222 route and recipient host. *Cell Host Microbe* 16:691-700.
- 1223 47. Wilker PR, Dinis JM, Starrett G, Imai M, Hatta M, Nelson CW, O'Connor DH, Hughes  
1224 AL, Neumann G, Kawaoka Y, Friedrich TC. 2013. Selection on haemagglutinin imposes  
1225 a bottleneck during mammalian transmission of reassortant H5N1 influenza viruses. *Nat*  
1226 *Commun* 4:2636.

- 1227 48. McCrone JT, Woods RJ, Martin ET, Malosh RE, Monto AS, Lauring AS. 2018.  
1228 Stochastic processes constrain the within and between host evolution of influenza virus.  
1229 *Elife* 7.
- 1230 49. Danzy S, Studdard LR, Manicassamy B, Solorzano A, Marshall N, García-Sastre A, Steel  
1231 J, Lowen AC. 2014. Mutations to PB2 and NP proteins of an avian influenza virus  
1232 combine to confer efficient growth in primary human respiratory cells. *J Virol* 88:13436-  
1233 46.
- 1234 50. Hoffmann E, Neumann G, Kawaoka Y, Hobom G, Webster RG. 2000. A DNA  
1235 transfection system for generation of influenza A virus from eight plasmids. *Proc Natl*  
1236 *Acad Sci U S A* 97:6108-13.
- 1237 51. Fodor E, Devenish L, Engelhardt OG, Palese P, Brownlee GG, García-Sastre A. 1999.  
1238 Rescue of influenza A virus from recombinant DNA. *J Virol* 73:9679-82.
- 1239 52. Schwartz SL, Lowen AC. 2016. Droplet digital PCR: A novel method for detection of  
1240 influenza virus defective interfering particles. *J Virol Methods* 237:159-165.
- 1241 53. Zhou B, Donnelly ME, Scholes DT, St George K, Hatta M, Kawaoka Y, Wentworth DE.  
1242 2009. Single-reaction genomic amplification accelerates sequencing and vaccine  
1243 production for classical and Swine origin human influenza A viruses. *J Virol* 83:10309-  
1244 13.
- 1245
- 1246

1247 **Chapter 3: Regulation of gene expression from the influenza A virus M segment is a**  
1248 **feature of host adaptation**

1249 Gabrielle K. Delima<sup>1</sup>, Anice C. Lowen<sup>1,2</sup>, and John Steel<sup>3</sup>

1250

1251 <sup>1</sup> Department of Microbiology and Immunology, Emory University School of Medicine, Atlanta,  
1252 Georgia, United States of America,

1253 <sup>2</sup> Emory Center of Excellence for Influenza Research and Response (Emory-CEIRR), Atlanta,  
1254 Georgia, United States of America

1255 <sup>3</sup>Influenza Division, National Center for Immunization and Respiratory Diseases, Centers for  
1256 Disease Control and Prevention, Atlanta, Georgia, United States of America

1257

1258

1259 **Abstract**

1260 Pandemic influenza A viruses (IAVs) arise when non-human IAVs are able to overcome host  
1261 species barriers that normally hinder inter-species transmission. One way IAVs can overcome  
1262 host barriers is through accumulating mutations that confer host adaptation. In particular, swine  
1263 have shown to facilitate avian IAV adaptation to mammals and were the source of the 2009  
1264 H1N1 pandemic IAV strain. It has been shown that the M segment of this strain was important to  
1265 its pandemic potential. This M segment was derived from the Eurasian avian-like swine lineage,  
1266 which in turn was introduced into pigs directly from an avian host. Importantly, it was shown  
1267 that IAVs encoding an avian M segment have aberrantly high M2 expression during mammalian  
1268 infection that decreases viral fitness. However, the adaptive mutations that underlie differential  
1269 M gene expression between avian and human IAVs in mammals are not understood. Here we

1270 show that regulation of M segment gene expression changed progressively over time as the  
1271 Eurasian avian-like swine lineage circulated in pigs. However, introducing mutations that arose  
1272 during swine circulation into the M segment of an avian precursor did not decrease M2 gene  
1273 expression. In contrast, introducing mutations from the 2009 pandemic H1N1 IAV M segment  
1274 into an avian precursor strain resulted in decreased M2 protein, but not mRNA, expression.  
1275 Together, these data suggest that M segment gene regulation impacts viral fitness and is a key  
1276 factor in IAV host adaptation.

1277

## 1278 **Introduction**

1279 Pandemic influenza A viruses (IAV) have significant public health consequences (1). A common  
1280 feature of the past three pandemic IAVs was the inclusion in their genomes of gene segments  
1281 from both human and non-human IAVs (2-4). In the case of the 2009 IAV pandemic, the strain  
1282 emerged from swine, harboring gene segments from human, avian, and swine IAVs (4, 5). The  
1283 natural reservoir of IAV are waterfowl, but there are host specific lineages in humans, wild birds,  
1284 poultry, swine, and other mammals. However, host barriers hinder inter-species transmission (2,  
1285 6-8). For example, direct avian to human IAV transmission is uncommon, and subsequent human  
1286 to human transmission is extremely rare (8-10). Thus, an IAV strain must adapt to a new host  
1287 species to successfully replicate and spread in a new host population.

1288

1289 There are two ways an IAV can adapt to a new host. The first is by reassortment during  
1290 coinfection with two or more IAVs, where gene segments from either parental strain are  
1291 incorporated into progeny virions (11-13). The second is by mutation, which happens frequently  
1292 due to the lack of proofreading in the virus' RNA-dependent RNA polymerase (14). Though

1293 these processes are often deleterious (14-17), selection acting on rare beneficial changes can lead  
1294 to the emergence of progeny with enhanced fitness in a new host (2, 18).

1295  
1296 Swine may serve as an intermediate host for influenza A viruses as they are susceptible to  
1297 infection with diverse IAV lineages and enable mammalian host adaptation through both  
1298 mutation and reassortment. Swine harbor the preferred receptors of both avian and human IAVs  
1299 and have been shown to facilitate avian IAV adaptation to the human receptor (5, 19). Moreover,  
1300 reverse zoonosis of influenza from humans to swine occurs frequently (20). For these reasons,  
1301 swine have often been referred to as a “mixing vessel” for avian, swine, and human IAVs (19,  
1302 21, 22).

1303  
1304 The M segment of the 2009 IAV pandemic strain was important for its pandemic potential (23-  
1305 25). This segment originated from an avian H1N1 IAV that entered European swine in 1978 and  
1306 established a stable lineage, the Eurasian avian-like swine lineage. In the years preceding 2009, a  
1307 Eurasian avian-like swine virus reassorted with the North American triple reassortant swine virus  
1308 strain in swine, and the Eurasian avian-like swine M segment was maintained in the 2009  
1309 pandemic IAV (5, 26, 27). Thus, the 2009 pandemic IAV M segment, being ultimately of avian  
1310 in origin, likely acquired adaptive mutations while circulating in swine. The M segment encodes  
1311 two major proteins: M1 which gives the virion its structure and M2 which forms a pH activated  
1312 proton channel required for viral entry. The M1 and M2 proteins are expressed from the M gene  
1313 segment, where M1 (mRNA<sub>7</sub>) is made from the colinear transcript and M2 (mRNA<sub>10</sub>) is derived  
1314 from alternative splicing of the M segment transcript (28). The splicing of M1 mRNA to form

1315 M2 mRNA involves both viral and various host factors (28-35). Thus, the gene expression the M  
1316 segment is well regulated.

1317

1318 Our prior work showed the role of the IAV M segment in host transmission. An IAV with the M  
1319 segment from the 2009 pandemic strain conferred efficient transmission in a virus background  
1320 that did not transmit in guinea pigs (25). We also showed that virus strains containing avian IAV  
1321 M segments exhibited aberrantly increased M2 gene expression and decreased replication in  
1322 mammalian cells, while a strain containing the 2009 pandemic M segment displayed efficient M  
1323 gene expression and enhanced replication (36). From these data, we hypothesized that the M  
1324 segment of the 2009 IAV pandemic strain contains mutations that re-established optimal M1/M2  
1325 gene expression during mammalian infection.

1326 Here, we sought to map sequence determinants that underlie differential M1/M2 expression  
1327 between avian and human adapted IAV M segments. Specifically, we investigated differences  
1328 between the M segments of an avian precursor of the Eurasian avian-like lineage, influenza  
1329 A/dk/Schleswig/21/79 (H1N1) virus (dkSch79), and an isolate of the 2009 pandemic, influenza  
1330 A/Netherlands/602/2009 (H1N1) virus (NL09) in an isogenic background. Our results confirm  
1331 that avian IAV M segments exhibit dysregulation of M gene expression during mammalian  
1332 infection, while human IAV M segment gene expression is well regulated. Furthermore, we  
1333 show that continued IAV circulation in swine re-established low M2 protein expression in  
1334 mammalian cells. However, introduction of M mutants that arose in swine into an avian IAV  
1335 background were not sufficient to decrease M2 protein expression. Moreover, dkSch79 – NL09  
1336 M chimeric viruses exhibited varying levels of M2 protein expression, but no differences in M2

1337 mRNA expression. These data suggest that the regulation of M gene expression has a role in host  
1338 adaptation but were not able to elucidate specific adaptive mutations.

## 1339 **Results**

1340  
1341 **Avian adapted M segments confer aberrantly increased M2 gene expression in mammalian**  
1342 **cells.**

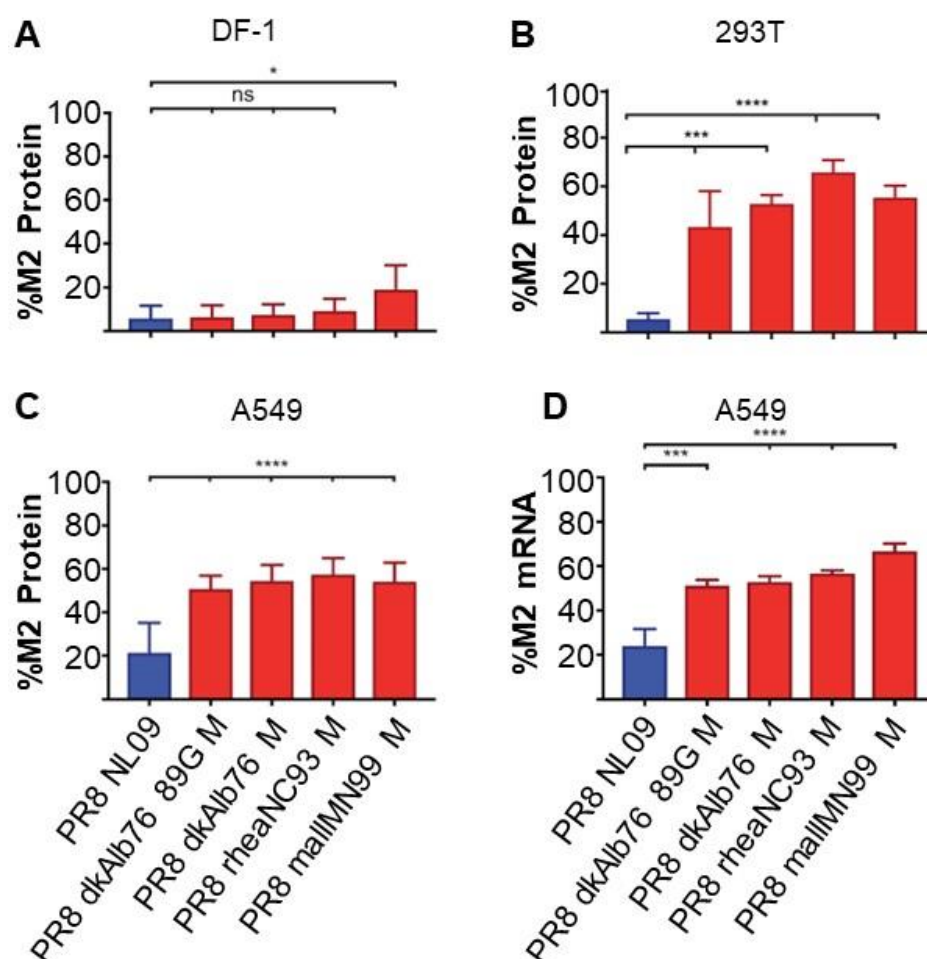
1343 We have generated recombinant viruses that contain the M segment of various avian and human  
1344 adapted IAV strains, with the remaining seven gene segments coming from A/Puerto  
1345 Rico/8/1934(H1N1) (PR8), a lab adapted IAV strain. This isogenic background ensures that any  
1346 differences observed between avian and human M segment viruses are due to the M segment  
1347 alone. The virus origin of each M segment is listed in Table 1.

1348 **Table 1. Origin of M segments used in study.**

Strain	Abbreviation
A/NL/602/2009 (H1N1)	NL09
A/duck/Alberta/35/76 (H1N1)	dkAlb76
A/rhea/North Carolina/39482/93 (H7N1)	RhNC93
A/mallard/MN/19906/99 (H3N8)	MallMN99
A/Panama/2007/99 (H3N2)	Pan99
A/Bethesda/55/2015 (H3N2)	Beth15
A/dk/Schleswig/21/79 (H1N1)	dkSch79
A/swine/Arnsberg/1/1979 (H1N1)	swArn79
A/swine/Potsdam/15/1981 (H1N1)	swPot81
A/swine/Netherlands/12/1985 (H1N1)	swNL85
A/swine/Gent/V230/1992 (H1N1)	swGen92
A/swine/Hong Kong/10022/2001 (H1N1)	swHK01
A/swine/England/010402/2003 (H1N1)	swEng03
A/swine/Spain/53207/2004 (H1N1)	Spn04

1349  
1350 Our previous work characterized differences in M segment gene expression between avian and  
1351 human adapted M segments (36). We found that IAVs containing avian or human adapted M  
1352 segments expressed similarly low levels of M2 protein in chicken fibroblast (DF-1) cells (Fig

1353 1A). However, during infection of human lung (A549) cells, human embryonic kidney (293T)  
 1354 and Madin Darby canine kidney cells (MDCK), avian M viruses expressed significantly higher  
 1355 levels of M2 protein than the PR8 NL09 M virus (Fig 1B-C). Furthermore, other human adapted  
 1356 M viruses express low levels of M2 protein during infection of A549 cells (Fig 2). These data  
 1357 indicate that, when the current or recent host origin of the M segment matches the cell type

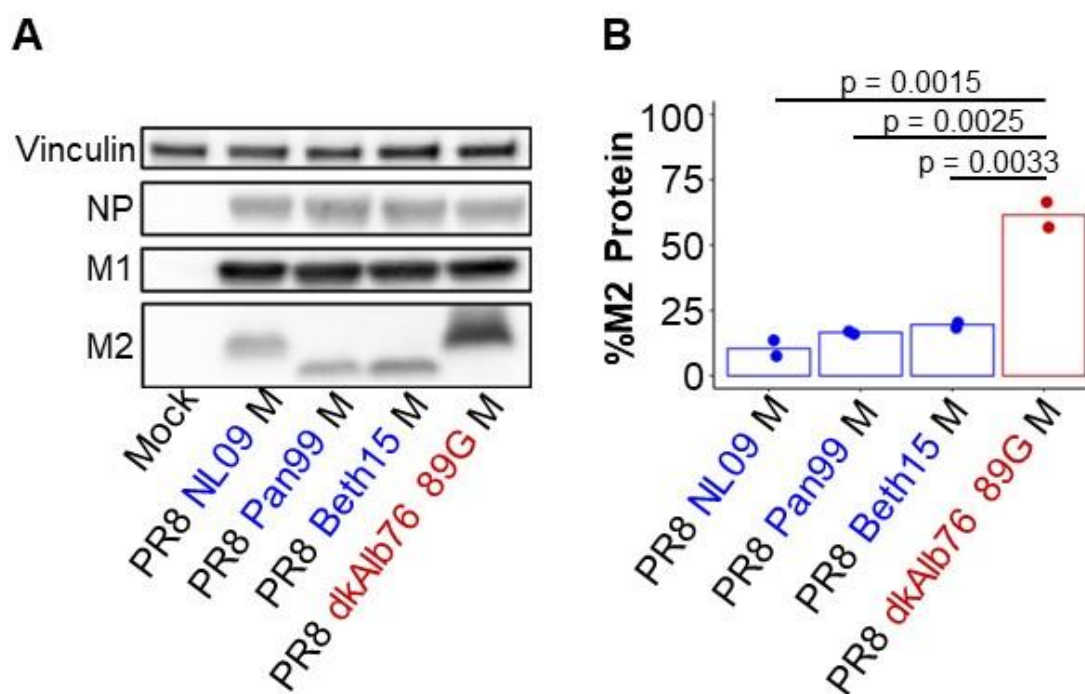


1358 **Fig. 1 High M2 protein expression of viruses carrying avian IAV M segments is seen in**  
 1359 **mammalian but not avian cells.** DF-1 (A), 293T (B), or A549 (C, D) cells were infected at an  
 1360 MOI of 5 PFU/cell with PR8 viruses encoding human (blue) or avian (red) IAV M segments.  
 1361 The percentage of M2 out of total M1 and M2 protein (A-C), or percent of M2 out of total M1,  
 1362 M2, and M3 mRNA is plotted. Results are the means of three independent experiments with  
 1363 standard deviation plotted (A-D). Significant differences between IAVs encoding human or  
 1364 avian M segments was evaluated by one-way ANOVA: \* $p < 0.05$ , \*\* $p < 0.01$ , \*\*\* $p < 0.001$ ,  
 1365 \*\*\*\* $p \leq 0.0001$ . Figure reproduced from (36).

1366 infected, the virus expresses low levels of M2 protein. However, IAVs containing avian M  
 1367 segments exhibit increased M2 protein expression during mammalian infection. Thus, aberrant  
 1368 M gene expression indicates maladaptation to the host, and adaptation to a new host would be  
 1369 expected to include re-establishing optimal M gene expression.

1370

1371



1372

1373 **Fig. 2 High M2 protein expression of viruses incorporating avian, but not human, M**  
 1374 **segments in mammalian cells.** A549 cells were mock infected or infected at an MOI of 5  
 1375 PFU/cell with PR8 viruses encoding human (blue) or avian (red) IAV M segments, as indicated  
 1376 under each panel. A) Detected proteins are labeled at the left. Vinculin and NP expression were  
 1377 measured to normalize viral protein levels and assess viral replication, respectively. B)  
 1378 Normalized band intensity of M1 and M2 proteins was quantified. The percentage of M2 out of  
 1379 total M1 and M2 protein is plotted. Results of two independent experiments, averaged from two  
 1380 technical replicates per experiment, are plotted and bars indicate the means. Significant  
 1381 differences between IAVs encoding human or avian M segments were evaluated by t-test.

1382

1383 **Avian IAV circulation in swine re-established optimal M2 protein expression in**  
1384 **mammalian cells.**

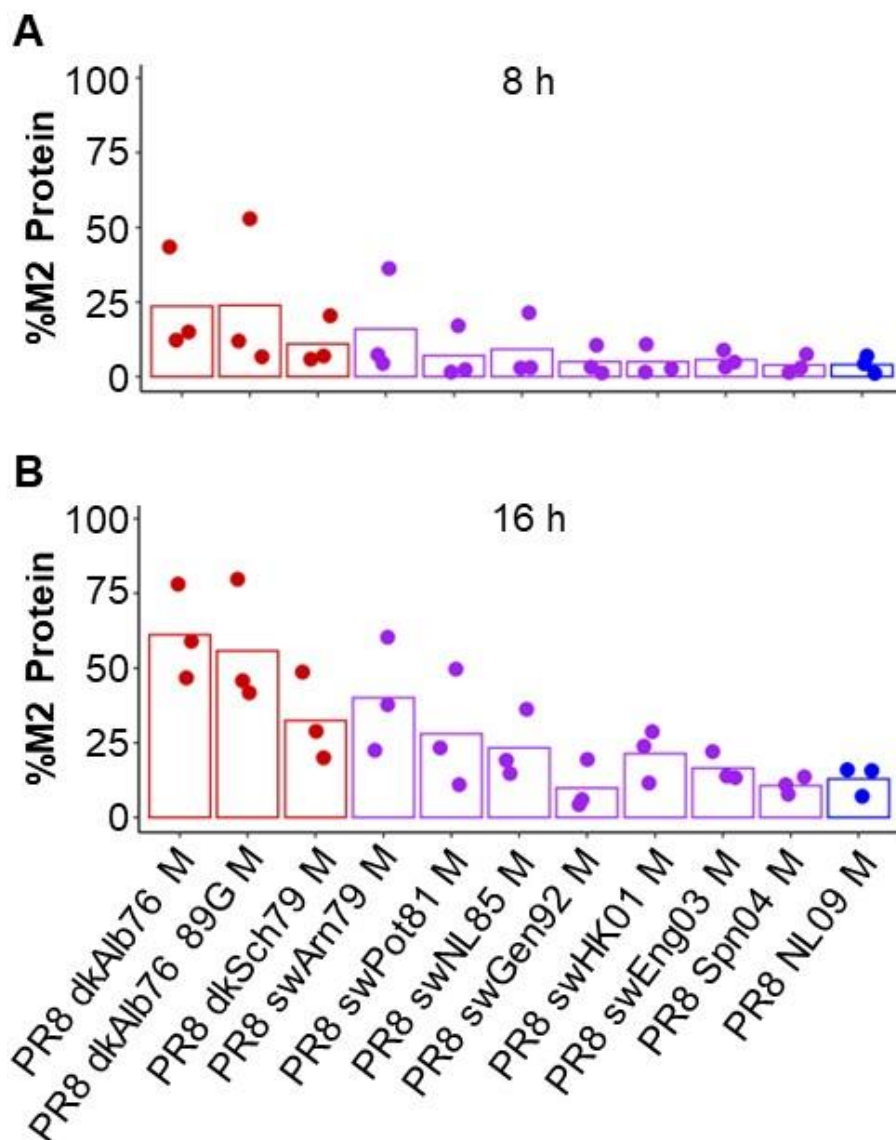
1385 The M segment of the 2009 pandemic IAV strain originates from the Eurasian avian-like swine  
1386 lineage. The Eurasian avian-like swine lineage was established by an avian IAV that stably  
1387 circulated in swine (5, 26, 27). Thus, we hypothesized that the avian origin M segment adapted  
1388 to mammalian infection over decades of circulation. To test this, we evaluated the M protein  
1389 expression by western blot. A549 cells were infected with a panel of PR8 based viruses  
1390 containing M segments from representative isolates of the Eurasian avian-like swine lineage,  
1391 including an avian precursor, dkSch79wt and a human 2009 pandemic IAV isolate, NL09. We  
1392 found that the decreasing M2 protein expression appears in early swine M segment viruses and  
1393 continues in the human PR8 NL09 M virus (Fig 3). Notably, there is a ~20% decrease in %M2  
1394 protein out of total M protein expression from the precursor avian PR8 dkSch79wt M virus to the  
1395 human PR8 NL09 M virus by 16 h (Fig 3B). These data indicate that avian IAV circulation in  
1396 mammals facilitated M segment host adaptation, resulting in decreased M2 protein expression.

1397

1398 **M segment mutations identified during swine circulation did not decrease M2 protein**  
1399 **expression.**

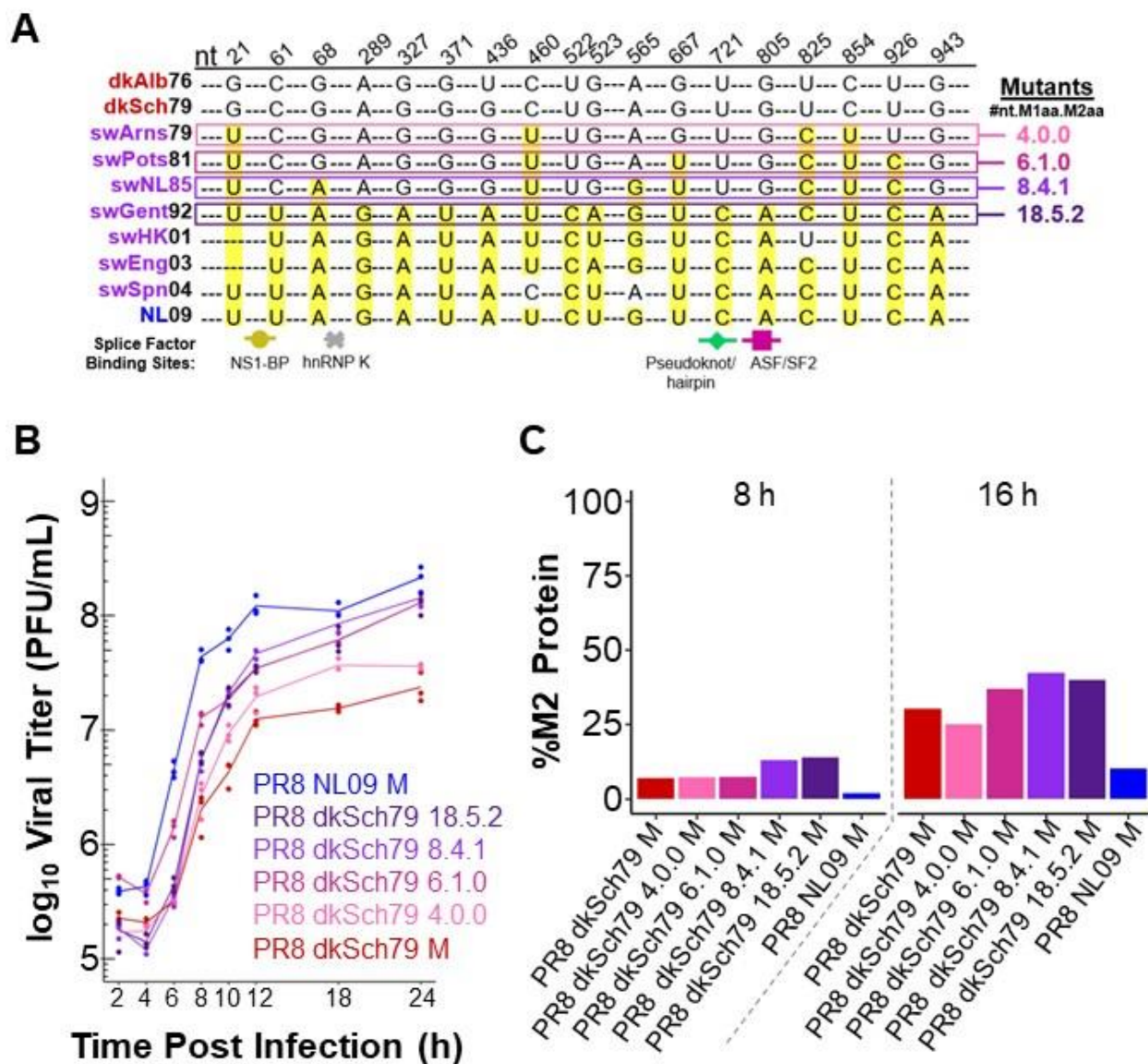
1400 Observing this trend, we then sought to identify mutations associated with decreased M2  
1401 expression by first using the M segments of Eurasian avian-like swine isolates. We first aligned  
1402 the M segment sequences of the viruses in Fig 3 and identified a total of 18 nucleotide (nt)  
1403 mutations, seven of which are non-synonymous, that arose in swine and are present in the NL09,  
1404 but not avian M segments (Fig 4A). Some of these mutations arise in or near previously  
1405 described binding regions of host factors involved in M mRNA splicing (30, 32-34). We

1406 generated a set of M segments that are progressively more similar to the NL09 M by introducing  
 1407 these mutations, as they emerged chronologically, into the dkSch79wt M segment. We rescued



1408  
 1409 **Fig. 3 Increased duration of avian IAV circulation in swine is associated with decreased M2**  
 1410 **protein expression.** A549 cells were infected at an MOI of 5 PFU/cell with PR8 viruses  
 1411 encoding avian (red), swine (purple), or human (blue) IAV M segments, as indicated under each  
 1412 panel. Cells were lysed at 8 (A) or 16 (B) h post infection. The percentage of M2 out of total M1  
 1413 and M2 proteins as detected by Western blotting is plotted. Results of three independent  
 1414 experiments, averaged from two technical replicates per experiment, are plotted and bars indicate  
 1415 the means.  
 1416

1417 these chronological mutant viruses in the PR8 dkSch79wt background. We first evaluated the  
 1418 replication of these viruses in mammalian cells by infecting A549 cells with the PR8 dkSch79 M  
 1419 mutant, PR8 dkSch79wt, and PR8 NL09 M viruses. The medium was sampled up to 24 h post  
 1420 infection to measure viral titer. The results show that the PR8 dkSch79 M mutant viruses  
 1421 replicate to higher titers than the PR8 dkSch79wt, with the PR8 dkSch79 18.5.2 and PR8  
 1422 dkSch79 8.4.1 M mutants reaching final titers comparable to the PR8 NL09 M virus (Fig 4B).



1423  
 1424 **Fig. 4 Mutations identified in M segment of swine isolates increase viral replication, but not**  
 1425 **M2 protein expression.** A) An alignment of the M segments of IAVs in Fig. 3 show 18 nt

1426 mutations that arise in swine isolates and are present in the NL09 virus. Mutations were  
1427 introduced into dkSch79 in the order they appeared during viral circulation. M segment mutants  
1428 are named to indicate the number of nt, M1 amino acid, and M2 amino acid mutations. For  
1429 example, mutant 18.5.2 has 18 nt mutations, 5 M1 amino acid mutation, and 2 M2 amino acid  
1430 mutations. B-C) A549 cells were infected at an MOI of 5 PFU/cell with PR8 viruses encoding  
1431 dkSch79, mutant dkSch79, or NL09 M segments. B) The viral titers of three biological replicates  
1432 derived from one experiment are plotted and solid lines connect the means. C). The percentage  
1433 of M2 out of total M1 and M2 proteins is plotted. The result of one experiment is plotted.  
1434

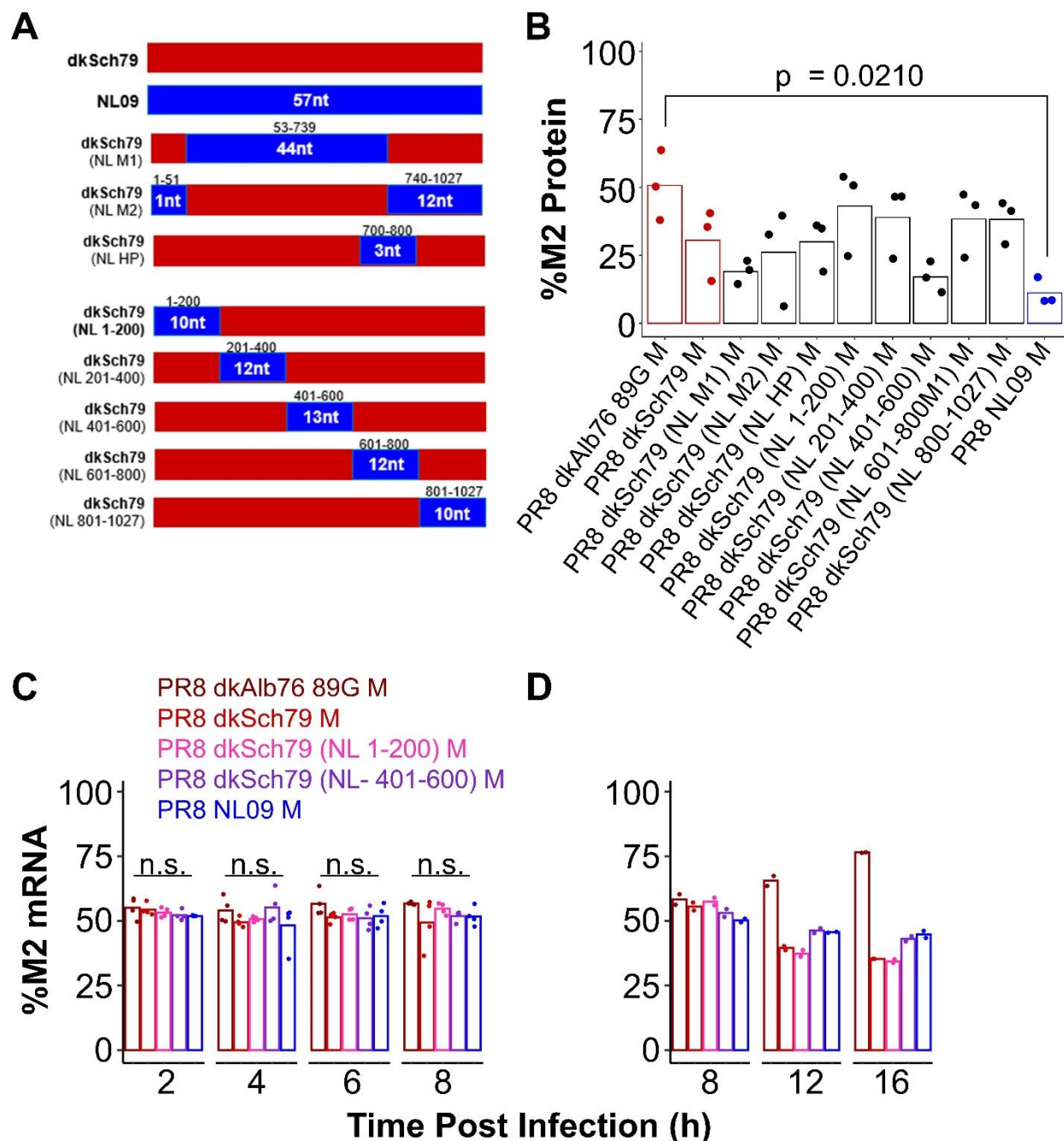
1435 We then evaluated the M protein expression of the M mutant viruses in A549 cells by western  
1436 blot. We found that the M mutant viruses did not exhibit lower %M2 protein out of total M  
1437 protein expression (Fig 4C). These data indicate that, although they supported improved viral  
1438 replication in mammalian cells, the mutations identified were not associated with decreased M2  
1439 protein expression.

1440

#### 1441 **Chimeric M segment mutants confer decreased M2 protein but not M2 mRNA expression.**

1442 The mutations identified in the Eurasian avian-like swine M panel consist of only 18 of the 57  
1443 total nt differences between the dkSch79wt and NL09 M segments. To delineate the impact of  
1444 the full set of nucleotide mutations on M gene expression, we generated a panel of chimeric M  
1445 segments in the PR8 dkSch79wt M segment background. A set of targeted chimeric segments  
1446 were made containing the NL09 M1 coding region, NL09 M2 coding region, or the NL09  
1447 sequence encoding a 3' splice site controlled by structural conformers (37, 38). Additionally, a  
1448 set of unbiased chimeric mutants were made in which approximately 200 nt of the NL09 M  
1449 sequence was introduced into each, spanning the entire M segment (Fig 5A). A549 cells were  
1450 infected with the chimeric M mutants and %M2 protein out of total M protein expression was  
1451 evaluated by western blot. Two chimeric M mutants, PR8 dkSch79 (NL M1) and PR8 dkSch79  
1452 (401-600) M viruses, showed %M2 protein, 19% and 17% respectively, comparable to those of

1453 the PR8 NL09 M virus at 11% (Fig 5B). Both viruses share the region of nt 401-600 from the  
 1454 NL09 M segment which harbors 13 nt differences from dkSch79wt M segment, indicating that  
 1455 this region contains mutations that alter M2 protein expression.



1456

1457 **Fig. 5 Chimeric M segments yield decreased M2 protein, but not M2 mRNA expression.** A)

1458 The dkSch79 and NL09 M segments differ by 57 nt. Chimeric dkSch79 M segments were

1459 generated with the sequences of the NL09 M segment (blue). A549 cells were infected at an

1460 MOI of 5 PFU/cell with PR8 viruses encoding dkAlb 89 G, dkSch79, chimeric dkSch79, or  
1461 NL09 M segments. B) The percentage of M2 protein out of total M1 and M2 protein is plotted.  
1462 Results of three independent experiments are plotted and bars indicate the means. C,D) The  
1463 percentage of M2 mRNA out of total M1 and M2 mRNA is plotted. Results of two to four  
1464 biological replicates derived from one to two independent experiments are plotted.  
1465 We then wanted to assess whether the decreased M2 protein expression associated with the 401-  
1466 600 nt region of NL09 M segment resulted from decreased M2 mRNA expression. To test this,  
1467 we infected A549 cells with avian M, PR8 dkSch79 mutant, or PR8 NL09 M viruses and  
1468 quantified the %M2 mRNA out of total M1 and M2 mRNAs. Our results indicate that the %M2  
1469 mRNA expression between the avian M, PR8 dkSch79 mutant, and PR8 NL09 M viruses were  
1470 comparable up to 8 h post infection (Fig 5C). By 16 h the PR8 dkSch79 (401-600) and PR8  
1471 NL09 M viruses trended toward higher %M2 mRNA expression than PR8 dkSch79wt M virus  
1472 (Fig 5D), counter to the %M2 protein expressed (Fig 4B). These results suggest that the  
1473 mechanism driving lower M2 protein expression occurs after M mRNA transcription or splicing.

1474

## 1475 **Discussion**

1476

1477 Our results show that optimal regulation of M1/M2 gene expression is a marker of IAV host  
1478 adaptation. IAVs containing an M segment well adapted to the host exhibit low %M2 protein out  
1479 of total M proteins expressed during infection. However, IAVs containing an M segment  
1480 maladapted to its host exhibit aberrantly high %M2 protein. Accordingly, our results demonstrate  
1481 that avian IAV circulation in swine led to a re-establishment of optimal M gene expression,  
1482 where %M2 protein expression of later Eurasian avian-like IAV isolates were lower than early  
1483 isolates. Despite this trend, introducing M segment mutations that arose during swine circulation  
1484 into an avian M IAV precursor did not decrease %M2 protein expression during mammalian cell  
1485 infection. In contrast, introducing mutations from the M segment of a 2009 pandemic IAV strain,

1486 NL09, did result in decreased %M2 protein expression. However, %M2 mRNA expression of the  
1487 avian, mutant, and NL09 M viruses were comparable. Thus, we were unable to identify M  
1488 sequences that modulate differential M gene expression. These results suggest that M gene  
1489 expression is regulated downstream of M mRNA transcription or splicing.

1490

1491 While these findings confirmed differences in avian M vs NL09 M %M2 protein expression  
1492 described in our prior work, we did not see similar differences in %M2 mRNA expression (36).  
1493 This may be due to differences in the assays used to determine %M2 mRNA expression. A  
1494 primer extension assay was used previously, while the present work used droplet digital  
1495 (ddPCR). The primer extension assay utilizes a shared primer and relies on size differences on a  
1496 gel to differentiate M1, M2, and M3 (mRNA<sub>11</sub>) mRNAs, where band intensities are used for  
1497 quantification. In contrast, the ddPCR assay utilizes primers that target either the intron of the  
1498 M1 open reading frame or the M2 splice junction, which are exclusive to each mRNA species, to  
1499 quantify absolute quantities. Differences in the specificity and sensitivity of each assay could  
1500 result in differences in the detection of each mRNA species. Moreover, M3 mRNA is another  
1501 alternative splicing product of M mRNA, but no protein corresponding to the M3 mRNA has  
1502 been identified. No differences in %M3 mRNA were observed between the various IAV M  
1503 segment viruses (36), and thus, M3 mRNA was not quantified in the experiments described  
1504 herein. While M3 mRNA expression was shown to be low, the absence of its quantification by  
1505 ddPCR could affect the %M2 mRNA calculated. Further work in this area would be needed to  
1506 clarify at what point, from transcription to post-translation modification, M gene regulation  
1507 affects the levels of M1 and M2 during infection.

1508

1509 Virus-host interactions can lead to differential M gene expression that can affect both virus and  
1510 host outcomes. During cellular infection, M segment gene expression has been shown to be time  
1511 dependent, as the ratio of M2 to M1 increases over the course of an infection (35). Importantly,  
1512 the splicing of M1 mRNA to M2 mRNA is regulated by both viral and host proteins (28-35, 39).  
1513 Differences in the binding motifs of these host proteins and viral mRNAs that have evolved in  
1514 different hosts, would likely result in dysregulation of M gene expression. Furthermore, the  
1515 accessibility of regions in the mRNA secondary structure, such as the 3' splice site can also have  
1516 an affect (37, 38). While we did not observe a change in %M2 protein or mRNA expression  
1517 corresponding to the origin of this site, another group was able to show that an avian M segment  
1518 3' splice site in a human IAV virus did reduce viral replication and increase M2 mRNA  
1519 expression (40).

1520 Differences in the M segment and gene expression can subsequently impact that host. Increased  
1521 M2 expression has been shown to affect cellular autophagy, a recycling process in which  
1522 cytoplasmic proteins and organelles are sequestered and degraded (41-43). Moreover, we have  
1523 previously shown that the increased M2 protein expression, exhibited by the avian M segment  
1524 during mammalian infection, blocked turnover of autophagosomes (36). Blocking cellular  
1525 autophagy then, in turn, disrupts the ability of the cell to maintain homeostasis and likely has  
1526 detrimental effects on the cell which may extend to the host. It follows that differences in M  
1527 segment origin can also impact IAV virulence. We have shown that the 2009 pandemic M  
1528 segment confers transmission between guinea pigs in a non-transmitting strain (25). It was also  
1529 shown that replacing just the M1 encoding region of the 2009 pandemic M with a swine M1  
1530 decreased virulence in mice (44). Moreover, replacing the M segment of a highly pathogenic

1531 avian influenza strain with that of a non-lethal, but closely related, strain reduced the mortality  
1532 rate from 100% to 25% in mallards (45).

1533

1534 In conclusion, dysregulation of M gene expression can occur when an IAV infects a new host  
1535 species. However, continued IAV circulation in the species can give rise to mutations that re-  
1536 establish optimal M gene expression. Thus, M gene expression impacts viral fitness and has a  
1537 role in IAV adaptation to new hosts.

1538

#### 1539 **Author contributions**

1540 Concept and experimental planning was performed by GD, ACL, and JS. Data was collected and  
1541 analyzed by GD with input from ACL. Key reagents and intellectual input were provided by JS.  
1542 Manuscript and figures were written, designed, and edited by GD and ACL. Research funding  
1543 was acquired by ACL and GD.

1544

#### 1545 **Acknowledgements**

1546 This work was supported by funding from NIH/NIAD under the Centers of Excellence for  
1547 influenza Research and Surveillance contract no. HHSN272201400004C to ACL and JS and  
1548 F31AI150114 to GD.

1549

#### 1550 **Declaration of interests**

1551 The authors declare no conflicts of interest

1552

#### 1553 **Materials and Methods**

**1554 Cells**

1555 Madin-Darby Canine Kidney (MDCK) cells, a gift of Peter Palese at Icahn School of Medicine  
1556 at Mount Sinai, and human lung epithelial cells (ATCC CCL-185) were maintained in minimum  
1557 essential medium (MEM; Gibco) supplemented with Normocin (InvivoGen) and 10% Fetal  
1558 Bovine Serum (FBS). Human kidney 293T cells (ATCC CRL-3216) were maintained in  
1559 Dulbecco's minimal essential medium (Gibco) supplemented with Normocin and 10% FBS. All  
1560 cells were cultured at 37°C and 5% CO<sub>2</sub> in a humidified incubator. Cells were tested monthly for  
1561 mycoplasma contamination during use. Medium used for IAV infection in each cell line (virus  
1562 medium) was prepared using the appropriate medium containing Normocin and 4.3% bovine  
1563 serum albumin. Virus medium containing ammonium chloride was prepared by adding HEPES  
1564 buffer and NH<sub>4</sub>Cl at final concentrations of 50 mM and 20 mM, respectively.

**1565 Viruses**

1566 The strains influenza A/Puerto Rico/8/1934(H1N1), A/Netherlands/602/2009 (H1N1),  
1567 A/Panama/2007/99 (H3N2), and A/Bethesda/55/2015 (H3N2) are referred to herein as PR8,  
1568 NL09, Pan99, and Beth15 respectively. PR8, NL09, Pan99, and Beth15 were handled under  
1569 BSL2 conditions. The strains influenza are A/dk/Schleswig/21/1979 (H1N1),  
1570 A/duck/Alberta/35/76 (H1N1), A/rhea/North Carolina/39482/93 (H7N1), and  
1571 A/mallard/MN/19906/99 (H3N8) are referred to herein as dkSch79, dkAlb76, RhNC93, and  
1572 MaMN99, respectively. DkSch79, dkAlb76, RhNC93, and MaMN99 were handled under BSL2  
1573 conditions with enhancements as required by the United States Department of Agriculture.

1574

1575 All viruses used were generated using reverse genetics (Hoffman 2000; Fodor 1999). The  
1576 reverse genetics system for PR8 is in the ambisense pDZ vector (a gift of Peter Palese). The

1577 reverse genetics system for NL09 is in the ambisense vector pHW and was a kind gift of Ron  
1578 Fouchier. The reverse genetics systems for Pan99, dkSch79, and MaMN99 viruses were  
1579 generated in house in the pDP vector (a gift of Daniel Perez). The dkAlb76 89G mutant virus  
1580 was described in (Calderon 2019) and was generated by introducing the S89G mutation to the  
1581 reverse genetics plasmid encoding the M gene segment in the M2 open read frame of dkAlb76  
1582 using site-directed mutagenesis. Mutant dkSch79 M viruses were generated introducing the  
1583 mutations described (Table #) to the reverse genetics plasmids encoding the M gene segment of  
1584 dkSch79 using site-directed mutagenesis. Chimeric dkSch79-NL09 M viruses were generated  
1585 using NEBuilder HiFi DNA Assembly Master mix (New England Biosciences) according to the  
1586 manufacturer's instructions using the primers in Table 1. PCR-amplified fragments encoding  
1587 regions of the M segment described in Fig. 5 from NL09 were combined with a fragment  
1588 containing the rest of dkSch79 segment in a pDP plasmid.

1589

1590 Briefly, avian viruses were generated by transfecting 293T cells with eight reverse genetics  
1591 plasmids encoding each IAV segment. After 16 h, transfected 293T cells were injected into the  
1592 allantoic cavity of 11-day old chicken eggs, incubated at 37°C for 40-48 h, and allantoic fluid  
1593 was recovered for use as a passage 1 working virus stock. Mammalian IAVs were generated by  
1594 transfecting 293T cells with reverse genetics plasmids encoding each IAV segment. After 16 h,  
1595 transfected 293T cells were then cocultured with MDCK cells at 37°C for 40-48 h. Collected  
1596 supernatants were then propagated in MDCK cells from low MOI to generate a working virus  
1597 stock.

1598

1599 **Virus infection conditions**

1600 Cells are seeded 24 h prior to infection. The monolayer was washed 3x with PBS. Virus  
1601 inoculum was added to each well at a multiplicity of infection (MOI) of 5 plaque forming units  
1602 (PFU) per cell and kept at 37°C for 45 min with rocking. After that time, the inoculum was  
1603 aspirated, each well 3x with PBS, the warmed virus medium was added. Under multi-cycle  
1604 conditions, virus medium containing L-1-tosylamido-2-phenylethyl chloromethyl ketone  
1605 (TPCK)-treated trypsin at a final concentration of 1  $\mu$ M was added. Cultures were incubated at  
1606 37°C. Each infection was performed in triplicate wells.

1607

#### 1608 **Quantification of M proteins by immunoblot**

1609 A549, MDCK, or 293T cells were seeded into 6-well plates at  $6 \times 10^5$  cells per well 24 h prior to  
1610 infection. Each infection took place under virus infection condition. At 8 or 16 h post infection,  
1611 cells were lysed with 2X Laemmli sample buffer (Bio-rad) containing 2% beta-mercaptoethanol.  
1612 Samples were boiled for 10 min at 95°C and ran on 4-20% gradient SDS-page gels, then  
1613 transferred to nitrocellulose membranes (Bio-rad) and incubated with 5% non-fat dry milk/ Tris  
1614 Buffered Saline with 1% Tween 20 (TBST) blocking buffer. Membranes were then incubated  
1615 with the following antibodies for immunoblotting: anti-vinculin monoclonal antibody (catalog  
1616 no. V9131; Sigma-Aldrich) at 1:5000 dilution, IAV nucleoprotein monoclonal antibody (HT-  
1617 103; catalog no. EMS010, Kerfast) at 1:500 dilution, and IAV matrix protein monoclonal  
1618 antibody (E10; catalog no. EMS009, Kerfast) at 1:1000 dilution. Bands were normalized to  
1619 vinculin then quantified using ImageLab software (Bio-Rad). Two technical replicates of  
1620 immunoblots for each infection were performed.

1621

#### 1622 **Quantification of viral growth**

1623 A549 cells were seeded into 6-well plates at  $6 \times 10^5$  cells per well 24 h prior to infection. Each  
1624 infection took place under multi-cycle conditions. At various time points post infection, 120  $\mu$ l  
1625 of medium was sampled from each dish and 120  $\mu$ l fresh medium was added. Samples were  
1626 stored at  $-80^\circ\text{C}$  and later titered by plaque assay on MDCK cells.

1627

### 1628 **Quantification of vRNA**

1629 RNA was extracted from cells and viral samples using the Qiagen RNeasy mini kit and the  
1630 Qiagen Viral RNA mini kit, respectively, using included protocol instructions. Extracted vRNA  
1631 was reverse transcribed using an M mRNA specific primer (Table #) and Maxima RT  
1632 (Thermofisher) per protocol instructions. Droplet digital PCR (ddPCR) was performed on the  
1633 resultant cDNA using the QX200<sup>TM</sup> ddPCR<sup>TM</sup> EvaGreen Supermix (Bio-Rad) and M1 and M2  
1634 specific primers (final concentration 200 nM) (Table 2). Copy numbers of M1 and M2 present in  
1635 samples were added to give total number of M mRNA. %M2 mRNA was calculated by dividing  
1636 the copy number of M2 mRNA by the total of M1 + M2 copy numbers.

1637

### 1638 **Statistical analyses**

1639 All statistical analyses were performed in R (version 1.3.959). The mean of technical replicates  
1640 was used for statistical analysis.

1641

1642 **Supplemental Information**

1643

1644 **Table 2. Primers used for chimeric M segment Assembly.**

<b>Primer</b>	<b>Sequence</b>
pDP 5 prime 14.32 Fwd	GGAGTACTGGTCGACCTCC
pDP 5 prime 32.14 Rev	GGAGGTCGACCAGTACTCC
Sch.pH1N1 M 39.59 Fwd	CCGAGGTCGAAACGTACGTTC
Sch.pH1N1 M 59.39 Rev	GAACGTACGTTTCGACCTCGG
Sch.pH1N1 M 206.226 Fwd	GGATTTGTGTTTCACGCTCACC
Sch.pH1N1 M 226.206 Rev	GGTGAGCGTGAACACAAATCC
Sch.pH1N1 M 389.406 Fwd	GGTGCACTTGCCAGTTGC
Sch.pH1N1 M 406.389 Rev	GCAACTGGCAAGTGCACC
Sch.pH1N1 M 592.610 Fwd	GGAACAGATGGCTGGATCG
Sch.pH1N1 M 610.592 Rev	CGATCCAGCCATCTGTTCC
Sch.pH1N1 M 689.708 Fwd	CATCCTAGCTCCAGTGCTGG
Sch.pH1N1 M 704.684 Rev	CACTGGAGCTAGGATGAGTCC
Sch.pH1N1 M 736.752 Fwd	GCAGGCCTACCAGAAGC
Sch.pH1N1 M 752.736 Rev	GCTTCTGGTAGGCCTGC
pH1N1 M 781.802 Fwd	GTGATCCTCTCGTCATTGCAGC
pH1N1 M 802.781 Rev	GCTGCAATGACGAGAGGATCAC
Sch 79 M 781.802 Fwd	GTGATCCTCTCGTTATTGCAGC
Sch 79 M 802.781 Rev	GCTGCAATAACGAGAGGATCAC
pDP 3 prime 1096.1118 Fwd	CGACTCGGAGCGAAAGATATACC
pDP 3 prime 1118.1096 Rev	GGTATATCTTTTCGCTCCGAGTCG

1645

1646 **Table 3. Primers used for the quantification of viral mRNA by ddPCR.**

<b>M Segment mRNA Reverse Transcription Primer</b>	
M mRNA RT Primer 992.1011	TTTTTTTTTTTTTTTACTCCAGCTCTATG
<b>mRNA<sub>7</sub> and mRNA<sub>10</sub> Primers</b>	
M1 Fwd 565.580	GCTGGCTAGCACTACGG
M1 Rev 708.692	CCAGCACTGGAGCTAGG
M2 Fwd 47.752	GAAACGCCTACCAGAAGC
M2 Rev. 917.900	CACTCCTTCCGTAGAAGG

1647

1648

1649 **References Cited**

- 1650 1. Belser JA, Maines TR, Tumpey TM. 2018. Importance of 1918 virus reconstruction to  
1651 current assessments of pandemic risk. *Virology* 524:45-55.
- 1652 2. Scholtissek C. 1994. Source for influenza pandemics. *Eur J Epidemiol* 10:455-8.
- 1653 3. Kilbourne ED. 2006. Influenza pandemics of the 20th century. *Emerg Infect Dis* 12:9-14.
- 1654 4. Trifonov V, Khiabani H, Greenbaum B, Rabadan R. 2009. The origin of the recent  
1655 swine influenza A(H1N1) virus infecting humans. *Euro Surveill* 14.
- 1656 5. Neumann G, Noda T, Kawaoka Y. 2009. Emergence and pandemic potential of swine-  
1657 origin H1N1 influenza virus. *Nature* 459:931-9.
- 1658 6. Sorrell EM, Schrauwen EJ, Linster M, De Graaf M, Herfst S, Fouchier RA. 2011.  
1659 Predicting 'airborne' influenza viruses: (trans-) mission impossible? *Curr Opin Virol*  
1660 1:635-42.
- 1661 7. Matrosovich M, Tuzikov A, Bovin N, Gambaryan A, Klimov A, Castrucci MR, Donatelli  
1662 I, Kawaoka Y. 2000. Early alterations of the receptor-binding properties of H1, H2, and  
1663 H3 avian influenza virus hemagglutinins after their introduction into mammals. *J Virol*  
1664 74:8502-12.
- 1665 8. Taubenberger JK, Kash JC. 2010. Influenza virus evolution, host adaptation, and  
1666 pandemic formation. *Cell Host Microbe* 7:440-51.
- 1667 9. Cauldwell AV, Long JS, Moncorgé O, Barclay WS. 2014. Viral determinants of  
1668 influenza A virus host range. *J Gen Virol* 95:1193-1210.
- 1669 10. Schrauwen EJ, Fouchier RA. 2014. Host adaptation and transmission of influenza A  
1670 viruses in mammals. *Emerg Microbes Infect* 3:e9.

- 1671 11. Lowen AC. 2017. Constraints, Drivers, and Implications of Influenza A Virus  
1672 Reassortment. *Annu Rev Virol* 4:105-121.
- 1673 12. Steel J, Lowen AC. 2014. Influenza A virus reassortment. *Curr Top Microbiol Immunol*  
1674 385:377-401.
- 1675 13. Desselberger U, Nakajima K, Alfino P, Pedersen FS, Haseltine WA, Hannoun C, Palese  
1676 P. 1978. Biochemical evidence that "new" influenza virus strains in nature may arise by  
1677 recombination (reassortment). *Proc Natl Acad Sci U S A* 75:3341-5.
- 1678 14. Peck KM, Lauring AS. 2018. Complexities of Viral Mutation Rates. *J Virol* 92.
- 1679 15. Sanjuán R, Moya A, Elena SF. 2004. The distribution of fitness effects caused by single-  
1680 nucleotide substitutions in an RNA virus. *Proc Natl Acad Sci U S A* 101:8396-401.
- 1681 16. Phipps KL, Marshall N, Tao H, Danzy S, Onuoha N, Steel J, Lowen AC. 2017. Seasonal  
1682 H3N2 and 2009 Pandemic H1N1 Influenza A Viruses Reassort Efficiently but Produce  
1683 Attenuated Progeny. *J Virol* 91.
- 1684 17. Villa M, Lässig M. 2017. Fitness cost of reassortment in human influenza. *PLoS Pathog*  
1685 13:e1006685.
- 1686 18. Ma EJ, Hill NJ, Zabilansky J, Yuan K, Runstadler JA. 2016. Reticulate evolution is  
1687 favored in influenza niche switching. *Proc Natl Acad Sci U S A* 113:5335-9.
- 1688 19. Ito T, Couceiro JN, Kelm S, Baum LG, Krauss S, Castrucci MR, Donatelli I, Kida H,  
1689 Paulson JC, Webster RG, Kawaoka Y. 1998. Molecular basis for the generation in pigs of  
1690 influenza A viruses with pandemic potential. *J Virol* 72:7367-73.
- 1691 20. Nelson MI, Vincent AL. 2015. Reverse zoonosis of influenza to swine: new perspectives  
1692 on the human-animal interface. *Trends Microbiol* 23:142-53.

- 1693 21. Ma W, Kahn RE, Richt JA. 2008. The pig as a mixing vessel for influenza viruses:  
1694 Human and veterinary implications. *J Mol Genet Med* 3:158-66.
- 1695 22. Kahn RE, Ma W, Richt JA. 2014. Swine and influenza: a challenge to one health  
1696 research. *Curr Top Microbiol Immunol* 385:205-18.
- 1697 23. Chou YY, Albrecht RA, Pica N, Lowen AC, Richt JA, García-Sastre A, Palese P, Hai R.  
1698 2011. The M segment of the 2009 new pandemic H1N1 influenza virus is critical for its  
1699 high transmission efficiency in the guinea pig model. *J Virol* 85:11235-41.
- 1700 24. Lakdawala SS, Lamirande EW, Suguitan AL, Jr., Wang W, Santos CP, Vogel L,  
1701 Matsuoka Y, Lindsley WG, Jin H, Subbarao K. 2011. Eurasian-origin gene segments  
1702 contribute to the transmissibility, aerosol release, and morphology of the 2009 pandemic  
1703 H1N1 influenza virus. *PLoS Pathog* 7:e1002443.
- 1704 25. Campbell PJ, Danzy S, Kyriakis CS, Deymier MJ, Lowen AC, Steel J. 2014. The M  
1705 segment of the 2009 pandemic influenza virus confers increased neuraminidase activity,  
1706 filamentous morphology, and efficient contact transmissibility to A/Puerto Rico/8/1934-  
1707 based reassortant viruses. *J Virol* 88:3802-14.
- 1708 26. Brockwell-Staats C, Webster RG, Webby RJ. 2009. Diversity of influenza viruses in  
1709 swine and the emergence of a novel human pandemic influenza A (H1N1). *Influenza  
1710 Other Respir Viruses* 3:207-13.
- 1711 27. Mena I, Nelson MI, Quezada-Monroy F, Dutta J, Cortes-Fernández R, Lara-Puente JH,  
1712 Castro-Peralta F, Cunha LF, Trovão NS, Lozano-Dubernard B, Rambaut A, van Bakel H,  
1713 García-Sastre A. 2016. Origins of the 2009 H1N1 influenza pandemic in swine in  
1714 Mexico. *Elife* 5.

- 1715 28. Lamb RA, Lai CJ, Choppin PW. 1981. Sequences of mRNAs derived from genome RNA  
1716 segment 7 of influenza virus: colinear and interrupted mRNAs code for overlapping  
1717 proteins. *Proc Natl Acad Sci U S A* 78:4170-4.
- 1718 29. Shih SR, Nemeroff ME, Krug RM. 1995. The choice of alternative 5' splice sites in  
1719 influenza virus M1 mRNA is regulated by the viral polymerase complex. *Proc Natl Acad*  
1720 *Sci U S A* 92:6324-8.
- 1721 30. Shih SR, Krug RM. 1996. Novel exploitation of a nuclear function by influenza virus: the  
1722 cellular SF2/ASF splicing factor controls the amount of the essential viral M2 ion  
1723 channel protein in infected cells. *Embo j* 15:5415-27.
- 1724 31. Mor A, White A, Zhang K, Thompson M, Esparza M, Muñoz-Moreno R, Koide K,  
1725 Lynch KW, García-Sastre A, Fontoura BM. 2016. Influenza virus mRNA trafficking  
1726 through host nuclear speckles. *Nat Microbiol* 1:16069.
- 1727 32. Zhang K, Shang G, Padavannil A, Wang J, Sakthivel R, Chen X, Kim M, Thompson  
1728 MG, García-Sastre A, Lynch KW, Chen ZJ, Chook YM, Fontoura BMA. 2018.  
1729 Structural-functional interactions of NS1-BP protein with the splicing and mRNA export  
1730 machineries for viral and host gene expression. *Proc Natl Acad Sci U S A* 115:E12218-  
1731 e12227.
- 1732 33. Thompson MG, Muñoz-Moreno R, Bhat P, Roytenberg R, Lindberg J, Gazzara MR,  
1733 Mallory MJ, Zhang K, García-Sastre A, Fontoura BMA, Lynch KW. 2018. Co-regulatory  
1734 activity of hnRNP K and NS1-BP in influenza and human mRNA splicing. *Nat Commun*  
1735 9:2407.

- 1736 34. Tsai PL, Chiou NT, Kuss S, García-Sastre A, Lynch KW, Fontoura BM. 2013. Cellular  
1737 RNA binding proteins NS1-BP and hnRNP K regulate influenza A virus RNA splicing.  
1738 PLoS Pathog 9:e1003460.
- 1739 35. Valcárcel J, Portela A, Ortín J. 1991. Regulated M1 mRNA splicing in influenza virus-  
1740 infected cells. J Gen Virol 72 ( Pt 6):1301-8.
- 1741 36. Calderon BM, Danzy S, Delima GK, Jacobs NT, Ganti K, Hockman MR, Conn GL,  
1742 Lowen AC, Steel J. 2019. Dysregulation of M segment gene expression contributes to  
1743 influenza A virus host restriction. PLoS Pathog 15:e1007892.
- 1744 37. Moss WN, Dela-Moss LI, Kierzek E, Kierzek R, Priore SF, Turner DH. 2012. The 3'  
1745 splice site of influenza A segment 7 mRNA can exist in two conformations: a pseudoknot  
1746 and a hairpin. PLoS One 7:e38323.
- 1747 38. Jiang T, Nogales A, Baker SF, Martinez-Sobrido L, Turner DH. 2016. Mutations  
1748 Designed by Ensemble Defect to Misfold Conserved RNA Structures of Influenza A  
1749 Segments 7 and 8 Affect Splicing and Attenuate Viral Replication in Cell Culture. PLoS  
1750 One 11:e0156906.
- 1751 39. Esparza M, Bhat P, Fontoura BM. 2022. Viral-host interactions during splicing and  
1752 nuclear export of influenza virus mRNAs. Curr Opin Virol 55:101254.
- 1753 40. Bogdanow B, Wang X, Eichelbaum K, Sadewasser A, Husic I, Paki K, Budt M,  
1754 Hergeselle M, Vetter B, Hou J, Chen W, Wiebusch L, Meyer IM, Wolff T, Selbach M.  
1755 2019. The dynamic proteome of influenza A virus infection identifies M segment splicing  
1756 as a host range determinant. Nat Commun 10:5518.
- 1757 41. Rossman JS, Lamb RA. 2009. Autophagy, apoptosis, and the influenza virus M2 protein.  
1758 Cell Host Microbe 6:299-300.

- 1759 42. Gannagé M, Dormann D, Albrecht R, Dengjel J, Torossi T, Rämer PC, Lee M, Strowig  
1760 T, Arrey F, Conenello G, Pypaert M, Andersen J, García-Sastre A, Münz C. 2009. Matrix  
1761 protein 2 of influenza A virus blocks autophagosome fusion with lysosomes. *Cell Host*  
1762 *Microbe* 6:367-80.
- 1763 43. Münz C. 2017. The Autophagic Machinery in Viral Exocytosis. *Front Microbiol* 8:269.
- 1764 44. Xie L, Xu G, Xin L, Wang Z, Wu R, Wu M, Cheng Y, Wang H, Yan Y, Ma J, Sun J.  
1765 2021. Eurasian Avian-like M1 Plays More Important Role than M2 in Pathogenicity of  
1766 2009 Pandemic H1N1 Influenza Virus in Mice. *Viruses* 13.
- 1767 45. Leyson CM, Youk S, Ferreira HL, Suarez DL, Pantin-Jackwood M. 2021. Multiple Gene  
1768 Segments Are Associated with Enhanced Virulence of Clade 2.3.4.4 H5N8 Highly  
1769 Pathogenic Avian Influenza Virus in Mallards. *J Virol* 95:e0095521.
- 1770
- 1771

1772 **Chapter 4: Discussion**

1773 **IAV Virus-virus interactions**

1774 The intrinsic properties of IAVs shape virus-virus interactions during infection. IAVs often  
1775 require coinfection to initiate a productive infection. This is due, in part, to the high frequency of  
1776 incomplete viral genomes that require complementation to initiate a productive infection (1-3).  
1777 In high MOI conditions, incomplete viral genomes can be readily complemented through  
1778 coinfection thereby increasing the likelihood of a productive infection (1, 4, 5). However, the  
1779 presence of incomplete viral genomes alone does not account for the increased reliance on  
1780 coinfection of some IAVs during infection of a new host (6). Rather, diminished viral  
1781 polymerase activity can result in reduced replicative capacity. Here, coinfection results in an  
1782 increase of viral proteins to meet the needs of viral replication (7). Furthermore, we show herein  
1783 that this need for coinfection can be met by both homologous and phylogenetically distant IAVs.  
1784 However, the benefits of positive density dependence are limited to the foci of infected cells  
1785 where local MOI is high. Beyond these foci, the relative fitness of the virus, its ability to infect  
1786 cells, replication kinetics, and progeny production, determine its ability to compete for target  
1787 cells.

1788

1789 Moreover, the immune response of the host significantly impacts the competitive landscape for  
1790 infecting IAVs. It has been well documented that adaptive immune responses to IAV impose a  
1791 strong barrier to infection and spread within host (8-11). In these studies, we did not assess the  
1792 impact of the guinea pig immune system on virus-virus interactions and importantly, these  
1793 animals were naïve, having no pre-existing immunity to IAVs. Various studies have shown prior  
1794 infection or vaccination can suppress the replication of an IAV of that strain (12-15). Under these

1795 conditions, the presence of both neutralizing and non-neutralizing antibodies would limit viral  
1796 spread within the host. In turn, the frequency of coinfection between strains within tissues would  
1797 likely decrease. To test this, guinea pigs could be inoculated with an IAV strain, then challenged  
1798 with equivalent doses of the matched wt and var IAVs of that strain. Compared to a naïve host,  
1799 the presence of reassortant viruses and change in viral population diversity could be measured as  
1800 a proxy for frequency of coinfection. If coinfection between strains is occurring, we would  
1801 expect that the presence of reassortant viruses and population diversity would increase over the  
1802 course of an infection. However, if coinfection is limited, we would expect to primarily see  
1803 parental strains and little diversity amongst the viral population.

1804 Additionally, *in vivo* coinfections were limited to pairings of homologous or mutant variants of  
1805 GFHK99 virus in this study. However, studying the outcomes of heterologous IAV coinfection,  
1806 particularly in the context of a host with pre-existing immunity, could further the understanding  
1807 of heterologous virus-virus interactions. In a naïve host, an IAV that is better adapted to the host  
1808 will likely have a fitness advantage over an IAV that is not. However, in a host that has pre-  
1809 existing immunity, the host adapted IAV may lose its fitness advantage. In this scenario, the two  
1810 coinfecting viruses differ in the factors that impact viral fitness, adaptation vs antigenic novelty.  
1811 We hypothesize that pre-existing immunity would increase the competitiveness of virus-virus  
1812 interactions, favoring IAVs that are less recognized by memory responses. To test this, guinea  
1813 pigs could be inoculated with a human IAV strain, then challenged with the same human IAV  
1814 strain and an avian IAV strain. Monitoring the replication of each virus could identify whether  
1815 host-adaptation or antigenic novelty has a greater impact on viral fitness. Importantly, the  
1816 presence of novel reassortants with enhanced replication would be monitored for. While our data

1817 suggest that cellular coinfection within a host is restricted, such conditions would favor a  
1818 reassortant that benefits from antigenic novelty and host adapted segments.

### 1819 **M segment gene regulation**

1820 IAV M gene expression is well regulated by both viral and host factors during infection. The  
1821 expression of the proteins encoded by the M segment, M1 and M2, have important roles in viral  
1822 packaging and budding. The M1 protein, in association with NEP, binds and traffics vRNPs out  
1823 of the nucleus and to the plasma membrane, where it then binds to HA and NA while forming  
1824 the structure of the budding virion (16, 17). The M2 protein completes the budding process by  
1825 mediating virion scission from the plasma membrane (18-21). It follows that newly translated  
1826 M2 proteins are needed at later stages of viral replication and budding. M2 expression has been  
1827 shown to be time dependent as its expression, relative to M1, increases over the course of an  
1828 infection (22). However, when M2 protein expression is not well regulated and is overexpressed,  
1829 this can have negative outcomes for the virus. M2 expression has been shown to block the  
1830 turnover of cellular autophagosomes, which are used to recycle cytosolic components (23-25).  
1831 Moreover, we previously showed that an avian IAV M segment confers increased M2  
1832 expression, a subsequent block in cellular autophagy, and diminished replication during infection  
1833 of mammalian, but not avian, cells (26). However, an IAV harboring the M segment of NL09  
1834 does not exhibit increased M2 expression and confers transmissibility in a non-transmitting strain  
1835 (26, 27). Together, these studies and the work herein indicate that re-establishing M gene  
1836 expression is important for host adaptation. We showed that introducing the 401-600  
1837 nucleotide(nt) region of the NL09 M segment into the dkSch79 M segment reduces M2 protein  
1838 expression. Further studies would be needed to identify which of the 13 nt mutations in this  
1839 region are responsible for reduced M2 protein expression. Interestingly, the region lies within the

1840 M1 intron and has not been previously described in modulating M gene expression. Investigating  
1841 this region could elucidate a novel mechanism of M gene regulation.

## 1842 **Conclusion**

1843 In its entirety, this work focuses on the factors and conditions that facilitate IAV replication in a  
1844 new host species. This is of particular concern to public health as IAV pandemics are caused by  
1845 IAV strains that emerge from an animal host (28-30). Chapter two illustrates that an IAV that is  
1846 not yet adapted to a host can use positive density dependence to overcome initial host barriers.  
1847 Incomplete viral genomes can be complemented, and diminished replication capacity can be  
1848 overcome through cellular coinfection. Moreover, this benefit extends to homologous and  
1849 phylogenetically distant coinfection partners. However, subsequent rounds of infection and  
1850 spread are subject to competition for target cells within a host. While IAVs that have a lower  
1851 reliance on coinfection can prove to be beneficial coinfection partners within cells, at the host  
1852 scale they can prove to be more effective competitors.

1853

1854 Our findings offer an explanation for the infrequency with which coinfection and reassortment  
1855 involving seasonal and zoonotic IAVs are detected in humans. During human coinfection with  
1856 avian and human IAVs, we would expect that human IAVs, being well-adapted, would very  
1857 likely outcompete avian IAVs. Moreover, an avian IAV would likely not benefit from cellular  
1858 coinfection with the human IAV as the heterogeneous distribution of cellular receptors would  
1859 tend to compartmentalize the viruses based on tissue tropism. Human IAVs would favor upper  
1860 respiratory replication and avian IAVs the lower respiratory tract (31-33). Moreover, evidence  
1861 suggests that within-host spread between parts of the respiratory tract is limited (34, 35). In the  
1862 event that human and avian IAVs are able to co-infect within cells, the avian IAV would likely

1863 benefit from enhanced replication and genome incorporation. Reassortant viruses would be  
1864 formed, but most reassortant progeny would be less fit than the parental viruses due to gene  
1865 segments becoming unlinked (36, 37). Onward transmission of viral progeny would likely be  
1866 dictated on two fronts. First, viral load in the infected individual and second the location of viral  
1867 replication, as progeny produced in the upper respiratory tract would be more readily shed by  
1868 mechanical transmission (e.g. coughing). Overall, these factors would likely result in the human  
1869 IAV outcompeting an avian IAV during human coinfection. Such competitive coinfection  
1870 dynamics may explain why avian-human IAV reassortants have not been detected in humans,  
1871 despite coinfection events (38-40).

1872  
1873 The key difference in the frequency of avian-human reassortants during coinfection of humans  
1874 and swine is the permissiveness of the host to both avian and human IAVs. In a non-permissive  
1875 host, replication of one of the variants would greatly be reduced and subsequently, so would the  
1876 frequency of coinfection and emergence of reassortant variants. Conversely, in a permissive host,  
1877 both variants would replicate efficiently, increasing the frequency of coinfection and reassortant  
1878 variants. These concepts underlie why hosts such as swine are a constant concern for the  
1879 emergence of pandemic IAVs. Due to their permissiveness to infection with diverse IAVs, swine  
1880 can support the formation of novel reassortants. Furthermore, as outlined in chapter three, swine  
1881 facilitate the adaptation of avian IAV segments to mammalian hosts (41, 42). Together, these  
1882 studies illustrate mechanisms that allow IAVs to infiltrate and adapt to new hosts.

1883

1884

1885 **References Cited**

- 1886 1. Brooke CB. 2014. Biological activities of 'noninfectious' influenza A virus particles.  
1887 Future Virol 9:41-51.
- 1888 2. Fonville JM, Marshall N, Tao H, Steel J, Lowen AC. 2015. Influenza Virus Reassortment  
1889 Is Enhanced by Semi-infectious Particles but Can Be Suppressed by Defective Interfering  
1890 Particles. PLoS Pathog 11:e1005204.
- 1891 3. Sanjuán R. 2017. Collective Infectious Units in Viruses. Trends Microbiol 25:402-412.
- 1892 4. Leeks A, Sanjuán R, West SA. 2019. The evolution of collective infectious units in  
1893 viruses. Virus Res 265:94-101.
- 1894 5. Jacobs NT, Onuoha NO, Antia A, Steel J, Antia R, Lowen AC. 2019. Incomplete  
1895 influenza A virus genomes occur frequently but are readily complemented during  
1896 localized viral spread. Nat Commun 10:3526.
- 1897 6. Phipps KL, Ganti K, Jacobs NT, Lee CY, Carnaccini S, White MC, Manandhar M,  
1898 Pickett BE, Tan GS, Ferreri LM, Perez DR, Lowen AC. 2020. Collective interactions  
1899 augment influenza A virus replication in a host-dependent manner. Nat Microbiol  
1900 5:1158-1169.
- 1901 7. Shartouny JR, Lee CY, Delima GK, Lowen AC. 2022. Beneficial effects of cellular  
1902 coinfection resolve inefficiency in influenza A virus transcription. PLoS Pathog  
1903 18:e1010865.
- 1904 8. Bush RM, Bender CA, Subbarao K, Cox NJ, Fitch WM. 1999. Predicting the evolution of  
1905 human influenza A. Science 286:1921-5.

- 1906 9. Smith DJ, Lapedes AS, de Jong JC, Bestebroer TM, Rimmelzwaan GF, Osterhaus AD,  
1907 Fouchier RA. 2004. Mapping the antigenic and genetic evolution of influenza virus.  
1908 Science 305:371-6.
- 1909 10. Westgeest KB, de Graaf M, Fourment M, Bestebroer TM, van Beek R, Spronken MIJ, de  
1910 Jong JC, Rimmelzwaan GF, Russell CA, Osterhaus A, Smith GJD, Smith DJ, Fouchier  
1911 RAM. 2012. Genetic evolution of the neuraminidase of influenza A (H3N2) viruses from  
1912 1968 to 2009 and its correspondence to haemagglutinin evolution. J Gen Virol 93:1996-  
1913 2007.
- 1914 11. Petrova VN, Russell CA. 2018. The evolution of seasonal influenza viruses. Nat Rev  
1915 Microbiol 16:47-60.
- 1916 12. Perrone LA, Ahmad A, Veguilla V, Lu X, Smith G, Katz JM, Pushko P, Tumpey TM.  
1917 2009. Intranasal vaccination with 1918 influenza virus-like particles protects mice and  
1918 ferrets from lethal 1918 and H5N1 influenza virus challenge. J Virol 83:5726-34.
- 1919 13. Manicassamy B, Medina RA, Hai R, Tsibane T, Stertz S, Nistal-Villán E, Palese P,  
1920 Basler CF, García-Sastre A. 2010. Protection of mice against lethal challenge with 2009  
1921 H1N1 influenza A virus by 1918-like and classical swine H1N1 based vaccines. PLoS  
1922 Pathog 6:e1000745.
- 1923 14. Yang F, Yan S, Zhu L, Wang FXC, Liu F, Cheng L, Yao H, Wu N, Lu R, Wu H. 2022.  
1924 Evaluation of panel of neutralising murine monoclonal antibodies and a humanised  
1925 bispecific antibody against influenza A(H1N1)pdm09 virus infection in a mouse model.  
1926 Antiviral Res 208:105462.

- 1927 15. Panickan S, Bhatia S, Bhat S, Bhandari N, Pateriya AK, Kalaiyarasu S, Sood R, Tripathi  
1928 M. 2022. Reverse genetics based H5N2 vaccine provides clinical protection against  
1929 H5N1, H5N8 and H9N2 avian influenza infection in chickens. *Vaccine* 40:6998-7008.
- 1930 16. Zhang J, Lamb RA. 1996. Characterization of the membrane association of the influenza  
1931 virus matrix protein in living cells. *Virology* 225:255-66.
- 1932 17. Ali A, Avalos RT, Ponimaskin E, Nayak DP. 2000. Influenza virus assembly: effect of  
1933 influenza virus glycoproteins on the membrane association of M1 protein. *J Virol*  
1934 74:8709-19.
- 1935 18. Chen BJ, Leser GP, Jackson D, Lamb RA. 2008. The influenza virus M2 protein  
1936 cytoplasmic tail interacts with the M1 protein and influences virus assembly at the site of  
1937 virus budding. *J Virol* 82:10059-70.
- 1938 19. McCown MF, Pekosz A. 2006. Distinct domains of the influenza a virus M2 protein  
1939 cytoplasmic tail mediate binding to the M1 protein and facilitate infectious virus  
1940 production. *J Virol* 80:8178-89.
- 1941 20. Rossman JS, Jing X, Leser GP, Lamb RA. 2010. Influenza virus M2 protein mediates  
1942 ESCRT-independent membrane scission. *Cell* 142:902-13.
- 1943 21. Rossman JS, Lamb RA. 2011. Influenza virus assembly and budding. *Virology* 411:229-  
1944 36.
- 1945 22. Valcárcel J, Portela A, Ortín J. 1991. Regulated M1 mRNA splicing in influenza virus-  
1946 infected cells. *J Gen Virol* 72 ( Pt 6):1301-8.
- 1947 23. Gannagé M, Dormann D, Albrecht R, Dengjel J, Torossi T, Rämer PC, Lee M, Strowig  
1948 T, Arrey F, Conenello G, Pypaert M, Andersen J, García-Sastre A, Münz C. 2009. Matrix

- 1949 protein 2 of influenza A virus blocks autophagosome fusion with lysosomes. *Cell Host*  
1950 *Microbe* 6:367-80.
- 1951 24. Münz C. 2017. The Autophagic Machinery in Viral Exocytosis. *Front Microbiol* 8:269.
- 1952 25. Rossman JS, Lamb RA. 2009. Autophagy, apoptosis, and the influenza virus M2 protein.  
1953 *Cell Host Microbe* 6:299-300.
- 1954 26. Calderon BM, Danzy S, Delima GK, Jacobs NT, Ganti K, Hockman MR, Conn GL,  
1955 Lowen AC, Steel J. 2019. Dysregulation of M segment gene expression contributes to  
1956 influenza A virus host restriction. *PLoS Pathog* 15:e1007892.
- 1957 27. Campbell PJ, Danzy S, Kyriakis CS, Deymier MJ, Lowen AC, Steel J. 2014. The M  
1958 segment of the 2009 pandemic influenza virus confers increased neuraminidase activity,  
1959 filamentous morphology, and efficient contact transmissibility to A/Puerto Rico/8/1934-  
1960 based reassortant viruses. *J Virol* 88:3802-14.
- 1961 28. Scholtissek C. 1994. Source for influenza pandemics. *Eur J Epidemiol* 10:455-8.
- 1962 29. Kilbourne ED. 2006. Influenza pandemics of the 20th century. *Emerg Infect Dis* 12:9-14.
- 1963 30. Mena I, Nelson MI, Quezada-Monroy F, Dutta J, Cortes-Fernández R, Lara-Puente JH,  
1964 Castro-Peralta F, Cunha LF, Trovão NS, Lozano-Dubernard B, Rambaut A, van Bakel H,  
1965 García-Sastre A. 2016. Origins of the 2009 H1N1 influenza pandemic in swine in  
1966 Mexico. *Elife* 5.
- 1967 31. Gallagher ME, Brooke CB, Ke R, Koelle K. 2018. Causes and Consequences of Spatial  
1968 Within-Host Viral Spread. *Viruses* 10.
- 1969 32. Lakdawala SS, Jayaraman A, Halpin RA, Lamirande EW, Shih AR, Stockwell TB, Lin  
1970 X, Simenauer A, Hanson CT, Vogel L, Paskel M, Minai M, Moore I, Orandle M, Das

- 1971 SR, Wentworth DE, Sasisekharan R, Subbarao K. 2015. The soft palate is an important  
1972 site of adaptation for transmissible influenza viruses. *Nature* 526:122-5.
- 1973 33. Shinya K, Ebina M, Yamada S, Ono M, Kasai N, Kawaoka Y. 2006. Avian flu: influenza  
1974 virus receptors in the human airway. *Nature* 440:435-6.
- 1975 34. Richard M, Herfst S, Tao H, Jacobs NT, Lowen AC. 2018. Influenza A Virus  
1976 Reassortment Is Limited by Anatomical Compartmentalization following Coinfection via  
1977 Distinct Routes. *J Virol* 92.
- 1978 35. Ganti K, Bagga A, Carnaccini S, Ferreri LM, Geiger G, Joaquin Caceres C, Seibert B, Li  
1979 Y, Wang L, Kwon T, Li Y, Morozov I, Ma W, Richt JA, Perez DR, Koelle K, Lowen  
1980 AC. 2022. Influenza A virus reassortment in mammals gives rise to genetically distinct  
1981 within-host subpopulations. *Nat Commun* 13:6846.
- 1982 36. Phipps KL, Marshall N, Tao H, Danzy S, Onuoha N, Steel J, Lowen AC. 2017. Seasonal  
1983 H3N2 and 2009 Pandemic H1N1 Influenza A Viruses Reassort Efficiently but Produce  
1984 Attenuated Progeny. *J Virol* 91.
- 1985 37. Villa M, Lässig M. 2017. Fitness cost of reassortment in human influenza. *PLoS Pathog*  
1986 13:e1006685.
- 1987 38. Zhang W, Zhu D, Tian D, Xu L, Zhu Z, Teng Z, He J, Shan S, Liu Y, Wang W, Yuan Z,  
1988 Ren T, Hu Y. 2015. Co-infection with Avian (H7N9) and Pandemic (H1N1) 2009  
1989 Influenza Viruses, China. *Emerg Infect Dis* 21:715-8.
- 1990 39. Zhu Y, Qi X, Cui L, Zhou M, Wang H. 2013. Human co-infection with novel avian  
1991 influenza A H7N9 and influenza A H3N2 viruses in Jiangsu province, China. *Lancet*  
1992 381:2134.

- 1993 40. Li J, Kou Y, Yu X, Sun Y, Zhou Y, Pu X, Jin T, Pan J, Gao GF. 2014. Human co-  
1994 infection with avian and seasonal influenza viruses, China. *Emerg Infect Dis* 20:1953-5.
- 1995 41. Ito T, Couceiro JN, Kelm S, Baum LG, Krauss S, Castrucci MR, Donatelli I, Kida H,  
1996 Paulson JC, Webster RG, Kawaoka Y. 1998. Molecular basis for the generation in pigs of  
1997 influenza A viruses with pandemic potential. *J Virol* 72:7367-73.
- 1998 42. Neumann G, Noda T, Kawaoka Y. 2009. Emergence and pandemic potential of swine-  
1999 origin H1N1 influenza virus. *Nature* 459:931-9.
- 2000